

Dissertation zur Erlangung des Doktorgrades  
der Fakultät für Chemie und Pharmazie  
der Ludwig-Maximilians-Universität München

**Investigations on Precursors and  
Polymerization Processes of Carbon Nitrides**

Nicole Elisabeth Braml

aus

Landau a. d. Isar, Deutschland

2015

### Erklärung

Diese Dissertation wurde im Sinne von § 7 der Promotionsordnung vom 18. November 2011 von Herrn Prof. Dr. Wolfgang Schnick betreut.

### Eidesstattliche Versicherung

Diese Dissertation wurde eigenständig und ohne unerlaubte Hilfe erarbeitet.

München, 26.05.2015

.....  
Nicole Elisabeth Braml

Dissertation eingereicht am	16.03.2015
1. Gutachter:	Prof. Dr. Wolfgang Schnick
2. Gutachter:	Prof. Dr. Bettina Lotsch
Mündliche Prüfung am	05.05.2015

*Für meine Familie und Freunde*



## Danksagung

Zuallererst möchte ich Herrn Prof. Dr. Wolfgang Schnick für die Aufnahme in seinem Arbeitskreis und die Möglichkeit zur Bearbeitung des interessanten Forschungsthemas danken.

Frau Prof. Dr. Bettina Lotsch danke ich sehr herzlich für die Übernahme des Zweitgutachtens und allen weiteren Hilfestellungen im Rahmen dieser Arbeit.

Ein großer Dank gilt Prof. Dr. Konstantin Karaghiosoff, Prof. Dr. Hans-Christian Böttcher, Prof. Dr. Achim Hartschuh und Prof. Dr. Dirk Johrendt für die ihre Bereitschaft, als Prüfer in meinem Rigorosum teilzunehmen.

Mein besonderer Dank gilt zudem Dr. Andreas Sattler für die hervorragende Einführung in das Thema und für alle weiterführenden Diskussionsthemen.

Linus Stegbauer danke ich für die Unterstützung und seine zahlreichen Ideen die für diese Arbeit von größter Bedeutung waren. Zudem für eine hervorragende Zeit im Labor und Reise nach Mülheim. Im Rahmen dieses Projektes möchte ich Sebastian Schaubach und den gesamten Arbeitskreis Fürstner am MPI Mülheim für die Unterstützung bedanken.

Meinen Bacheloranden und Praktikanten Annabelle Blum, Bernhard Böller, Alexander Cheperanov, Viktoria Falkowski und Michelle Klein möchte ich für ihre Arbeit und Unterstützung bedanken.

Besonderer Dank gilt auch den weiteren C/N Chemikern Dr. Barbara Jürgens, Fabian Keßler, Prof. Dr. Bettina V. Lotsch, Dr. Sophia Ringler, Dr. Andreas Satter, Katharina Schwinghammer und Dr. Eva Zeuner für ihre Ideen und Bereitschaft dieses Thema immer wieder neu zu erfinden.

Meinen Laborkollegen, Dr. Yamini Avadhut, Dajana Durach, Jonas Häusler, Christian Minke, Katrin Rudolf, Dr. Sophia Ringler und Dr. Eva Zeuner, danke ich für das freundschaftliche Miteinander im Labor sowie bei freizeitlichen Aktivitäten die auch bis heute bestehen.

Allen (ehemaligen) Arbeitskreismitgliedern, Eva-Maria Bertschler, Dr. Thomas Bräuniger, Dominik Baumann, Niklas Cordes, Dajana Durach, Jonas Häusler, Sascha Harm, Cora Hecht, Dr. Frauke Hinze, Dr. Constantin Hoch, Christine Pösl, Christian Maak, Fabian Keßler, Simon Kloß, Alexey Marchuk, Olga Lorenz, Dr. Saskia Lupart, Christian Minke, Markus Nentwig, Lukas Neudert, Robin Niklaus, Florian Pucher, Dr. Philipp Pust, Philipp Ratza, Dr. Tobias Rosenthal, Katrin Rudolf, Dr. Stefan Sedlmeier, Dr. Markus Seibald, Sebastian Schmiechen, Dr. Sebastian Schneider, Dr. Thorsten Schröder, Philipp Strobel, Frank Tambornino, Peter Wagatha und Matthias Wörsching, möchte ich für die Zusammenarbeit und große Hilfsbereitschaft danken.

Herrn Thomas Miller und Herrn Wolfgang Wünschheim möchte ich recht herzlich für die Lösung von EDV- und eine Vielzahl von weiteren Problemen, sowie die Bestellung sämtlicher Chemikalien danken.

Für weiteren technischen Support und die Durchführung zahlreicher Messungen hier am Department möchte ich danken:

- Brigitte Breitenstein für Massenspektren
- Marion Sokoll für FTIR-Spektren
- Robert Eicher, Gertraud Käser und Susanne Sauerer für Elementaranalysen
- Helmut Hartl für ICP-AAS-Analysen
- Peter Mayer und Christine Neumann für NMR-Messungen in Lösung
- Christian Minke für Festkörper-NMR-Messungen und REM/EDX-Sitzungen
- Florian Pucher und Alexey Marchuk für die Unterstützung bei Hochdrucksynthesen
- Thomas Miller, Dr. Peter Mayer und Sandra Albrecht danke ich für sämtliche Einkristallmessungen.

Allen weiteren Angehörigen der Arbeitskreise Schnick, Lotsch, Johrendt, Hoch, Müller-Buschbaum, Oeckler und Schmedt auf der Günne danke ich für das offene, freundliche Arbeitsklima und ihre Unterstützung.

Ganz herzlicher Dank ergeht an meine Studienkollegen Michael Hörmannsdorfer, Pia Köstler, Monika Lacher, Fabian Hanusch und Dr. Alexander Dippold für eine unvergessene Studienzeit inklusive diverser regenerativer Maßnahmen.

Für eine abwechslungsreiche Promotionszeit danke ich im Besonderen Jonas Häusler, Fabian Keßler, Dr. Philipp Pust, Sebastian Schmiechen, Philipp Strobel und Peter Wagatha durch unterhaltsame Mittagspausen und privaten Unternehmungen mit unerschöpflichen Gesprächsthemen.

Weiterhin möchte ich meinen Arbeitskollegen im TAZ Spiegelau für die Unterstützung und Akzeptanz gegenüber dem Endspurt meiner Promotion danken.

Mein allergrößter Dank gilt meinem Freund Bernd für seine Unterstützung und vor allem Geduld während der ganzen Studiums- und Promotionszeit. Meinen Eltern und meiner Großmutter danke ich für Ermutigungen und ihren Glauben an mich und ihre immerwährende Unterstützung dabei.



*"The person who says it cannot be done should not interrupt  
the person doing it."*

*Chinese Proverb*

---

# Table of Contents

<b>1. INTRODUCTION .....</b>	<b>4</b>
<b>2. SUMMARY .....</b>	<b>17</b>
2.1. Intermediate Phases and Salt-like Precursors for Carbon Nitrides.....	18
2.2. Alkyne-triazines on the Way to New Triazine-based Networks.....	22
2.3. Investigations into the Polymerization Process of Carbon Nitrides .....	26
<b>3. ADDUCT PHASES AND SALT-LIKE PRECURSORS FOR CARBON NITRIDES .....</b>	<b>28</b>
3.1. Formation of Melamium Adducts by Pyrolysis of Thiourea or Melamine/NH <sub>4</sub> Cl Mixtures.....	29
3.1.1. Introduction .....	30
3.1.2. Results and Discussion .....	32
3.1.3. Conclusion.....	46
3.1.4. Experimental Section .....	48
3.1.5. Bibliography .....	51
3.2. New Heptazine Based Materials with a Divalent Cation – Sr[H <sub>2</sub> C <sub>6</sub> N <sub>7</sub> O <sub>3</sub> ] <sub>2</sub> · 4 H <sub>2</sub> O and Sr[HC <sub>6</sub> N <sub>7</sub> (NCN) <sub>3</sub> ] · 7 H <sub>2</sub> O .....	54
3.2.1. Introduction .....	55
3.2.2. Results and Discussion .....	56
3.2.3. Conclusions .....	64
3.2.4. Experimental Section .....	64
3.2.5. Bibliography .....	67
<b>4. FROM ALKYNE-TRIAZINES TO NEW TRIAZINE-BASED NETWORKS .....</b>	<b>69</b>
4.1. Synthesis of Novel Triazine-based Materials by Functionalization with Alkynes .....	71
4.1.1. Introduction .....	72
4.1.2. Results and Discussion .....	75
4.1.3. Conclusion.....	87
4.1.4. Experimental Part .....	88
4.1.5. Bibliography .....	91

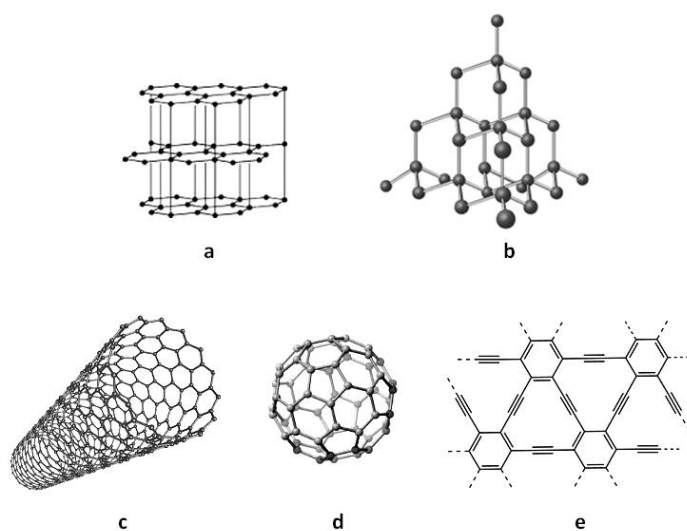
---

4.2.	Polymerization of Tris(1-propynyl)-1,3,5-triazine by Alkyne-metathesis .....	94
4.2.1.	Overview .....	94
4.2.2.	Experimental section.....	96
4.2.3.	Results and Discussion .....	98
4.2.4.	Future plans .....	100
4.2.5.	Bibliography .....	101
<b>5.</b>	<b>INVESTIGATIONS INTO THE POLYMERIZATION PROCESS OF CARBON NITRIDES</b>	<b>102</b>
5.1.	Decomposition of Melon .....	103
5.1.1.	Introduction .....	103
5.1.2.	Results and Discussion .....	104
5.1.3.	Experimental Part.....	106
5.1.4.	Conclusion .....	108
5.1.5.	Bibliography .....	110
<b>6.</b>	<b>DISCUSSION AND OUTLOOK .....</b>	<b>111</b>
6.1.	Intermediate Phases and Salt-like Precursors for Carbon Nitrides.....	111
6.2.	Alkyne-triazines on the Way to New Triazine-based Networks.....	113
6.3.	Investigations into the Polymerization Process of Carbon Nitrides.....	115
<b>7.</b>	<b>APPENDIX .....</b>	<b>119</b>
7.1.	Supporting Information .....	119
7.2.	CCDC Numbers.....	134
7.3.	List of Publications .....	135
7.4.	List of Abbreviations .....	138

## 1. Introduction

The field of materials science plays a significant role in research and modern technology and is continuously extended. Although corresponding fundamental as well as applied research is steadily growing, the interest in common main group element compounds is still strong. Particular importance has to be given to nitrogen- as well as carbon-based materials.

Main group nitrides are used in a great variety of industrial applications as most important non-oxidic ceramics.<sup>[1]</sup> One of the most notable nitridic material, silicon nitride  $\text{Si}_3\text{N}_4$ , exhibits high thermal and mechanical stability and is commonly used in engine or turbine parts.<sup>[1]</sup> Further nitrides, like AlN, GaN or InN and respective solid solution series (e.g.  $\text{In}_x\text{Ga}_{1-x}\text{N}$ ), function predominantly as wide bandgap semiconductors for blue light emitting diodes (LEDs).<sup>[2-4]</sup>



**Scheme 1.** Carbon allotropes **a** graphite **b** diamond **c** nanotubes **d** fullerene **e** graphyne.

Another extremely hard group 13 nitride, boron nitride  $\text{BN}$ ,<sup>[1]</sup> plays a significant role as abrasive. Due to its structural similarity<sup>[5]</sup> and corresponding conductivity properties it is an alternative for polymeric carbon as a high-temperature semiconductor.

The cubic modification of boron nitride is similar to diamond. Its hexagonal form corresponds to the structure of graphite which is the most stable modification of carbon.

Graphite along with diamond has been the only known allotrope of carbon for a long time. But within the last few years new carbonic compounds have gained interest, primarily regarding electronic applications.

Graphite consists of sheets containing  $sp^2$ -hybridized covalent bonded carbon atoms (see Scheme 1a).<sup>[6]</sup> Its lattice-like form of stacked aromatic six- rings makes it a good electronic conductor. It is therefore applied in electronic devices, but is also prominent as lubricant material or well known as pencil lead. The exfoliation of single graphite monolayers, named graphene, was awarded the nobel price in 2010.<sup>[7,8]</sup> Its enormous tensile strength as well as additive optical properties makes it a promising compound for a wide variety of applications. Due to its conductive properties graphene is proposed as lightweight material for electronic devices especially regarding photovoltaics or transistors.

In deviation from the two-dimensional layered assembly of graphite, diamond is built up of a three-dimensional network comprising tetrahedrally  $sp^3$ -hybridized carbon atoms (see Scheme 1b).<sup>[6]</sup> Besides from its use as jewellery, its extreme hardness leads to applications as e.g. cutting and drilling tool.

In response to the rising demand for carbon-based products new studies on carbon allotropes with postulated interesting properties were conducted in the last decades. One of the most demanding hypothetical network which combines  $sp^2$ - and  $sp^3$ -hybridized carbon atoms was postulated by *Alexandru Balaban* et al. in 1968 (Scheme 1e).<sup>[9]</sup> Herein planar sheets formed of phenyl rings connected by acetylene units were postulated based on theoretical calculations. Besides its interesting structural properties, the thus called graphyne has been predicted to exhibit semiconductor properties as well. However, graphyne has still not been successfully synthesized so far.

Excellent properties like hardness or thermal and electronic conductivity of carbon polymers have been improved by pursuing research. The isolation of an icosahedral allotrope called buckminsterfullerene,  $C_{60}$ , in 1990<sup>[10]</sup> which has already been described by *Kroto and Smalley* et al.<sup>[11]</sup> in 1985 attracted great attention and initiated new pathways on the chemistry of carbon. Just recently, fullerenes and

especially the corresponding subgroup of carbon nanotubes have begun to play an important role in nanochemistry (see Scheme 1 c and d).<sup>[12-15]</sup>

Fullerenes are built up of hollow spherical-shaped bodies of five- and six-membered carbon rings. Besides C<sub>60</sub>, the first characterized fullerene, quite a number of other fullerenes and derivatives (e.g. C<sub>70</sub>, C<sub>76</sub>, C<sub>80</sub>, C<sub>84</sub>).<sup>[13-15]</sup> were described lately. Fullerenes are nonconductive but good radical scavengers<sup>[14,15]</sup> which is why they are predominantly applied in cosmetic products.

Nanotubes, a subgroup of fullerenes, are built up of cylindric tubes of one or even more layers of graphene.<sup>[12]</sup> The current industrial production is several thousands of tons per year whereby major syntheses are carried out by chemical vapor deposition of alkenes. Industrially produced nanotubes include introduced pentagons with more complex assemblies as well. Different structures and layer thicknesses lead to specific properties, which are aimed at for specific applications. Thereby, primarily electronic properties for thin film electronics like transistors, automotive parts or batteries are targeted.

Above mentioned carbon polymers are built up of rings consisting exclusively of carbon. Molecular heterocycles for example pyrimidines as building blocks for nucleic bases connect carbon and nitrogen chemistry and are relevant in life sciences like pharmacy and synthesis of natural substances.<sup>[16]</sup> On the basis of the knowledge on carbon and nitrogen materials current research is interested in introducing nitrogen atoms in definite graphite layers. In particular, this thesis is dealing with heterocyclic compounds comprising cyclic fragments with alternating carbon and nitrogen molecules, named s-triazines or s-heptazines (see Figure 1). These materials can be classified as purely inorganic compounds due to the exclusive presence of C-N bonds.

The start of this chemistry can be traced back to the beginning of the 19<sup>th</sup> century when Justus v. Liebig mentioned the first triazine- and heptazine-based materials like melamine H<sub>6</sub>C<sub>3</sub>N<sub>6</sub>, melem H<sub>6</sub>C<sub>6</sub>N<sub>10</sub> or ameline H<sub>5</sub>C<sub>3</sub>N<sub>5</sub>O and amelide H<sub>4</sub>C<sub>3</sub>N<sub>4</sub>O<sub>2</sub> which have been synthesized by pyrolysis reactions of ammonium thiocyanate.<sup>[17-21]</sup>

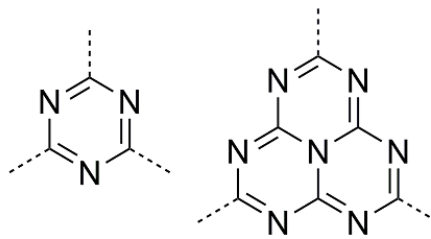


**Figure 1.** Structures of the *s*-triazine (left) and *s*-heptazine (right) core.

The first polymeric compound melon  $[\text{C}_6\text{N}_7(\text{NH}_2)(\text{NH})]_x$ , built up of heptazine fragments, was discovered by Jacob Berzelius by heating mercury thiocyanate. Due to the “snake-shaped” polymerization this reaction became a famous fairground attraction called pharaoh’s serpents. Further compounds such as potassium melonate  $\text{K}(\text{C}_6\text{N}_7)(\text{NCN})_3$  characterized by Gmelin<sup>[22]</sup> or cyameluric acid  $(\text{C}_6\text{N}_7)(\text{OH})_3$  by Henneberg<sup>[23]</sup> were milestones for C/N/H chemistry. But it took a lot of time until single crystal XRD investigations elucidated the structures of melamine or cyanuric acid unambiguously.

A tremendous progress in C/N/H chemistry was triggered by the quest for binary  $\text{sp}^3$ -hybridized carbon nitride  $\text{C}_3\text{N}_4$  (see Figure 2). *Liu* and *Cohen* postulated outstanding properties for this type of network.<sup>[24]</sup> Extreme hardness was assumed from calculations of the bulk modulus with values even higher than that of diamond. A variety of theoretical polymorphs of  $\text{sp}^3$ -hybridized  $\text{C}_3\text{N}_4$  were proposed, some of them to be mentioned are cubic  $\text{C}_3\text{N}_4$  (Willemit-II-type),  $\beta$ - $\text{C}_3\text{N}_4$  (hexagonal), pseudocubic  $\text{C}_3\text{N}_4$  (defect ZnS-type). Additionally, several graphite-type structures of  $\text{C}_3\text{N}_4$  were postulated.<sup>[25, 26]</sup>

Despite numerous attempts to synthesize crystalline 3D  $\text{C}_3\text{N}_4$  derivatives a successful pathway could not be carved out so far and there are reasonable doubts regarding the outstanding properties.<sup>[27]</sup> Nevertheless, graphitic structures of  $\text{C}_3\text{N}_4$ <sup>[28]</sup> were described and possibly lead to new conceptions which are focused on new fullerene- and nanotube-like carbon nitrides.

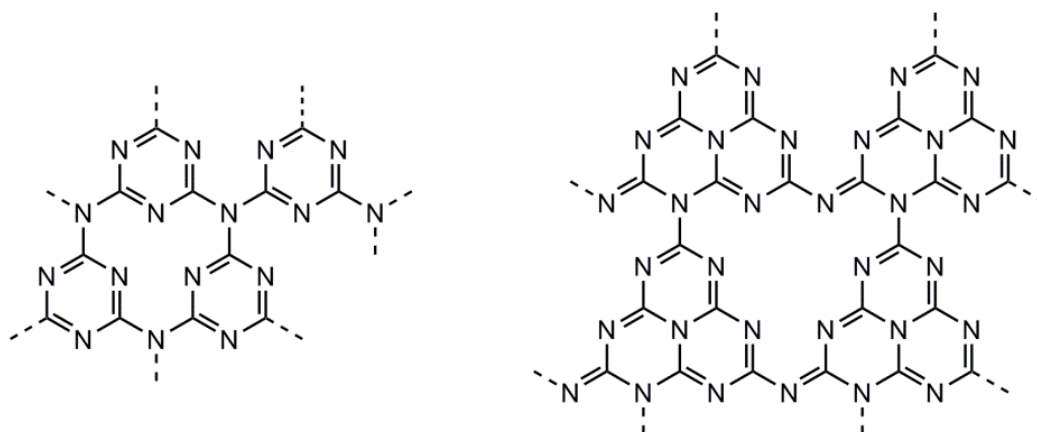


**Figure 2.** Models of possible triazine- and heptazine-based  $C_3N_4$ .

Only a few but nonetheless interesting crystalline C/N/H polymers were characterized up to now.<sup>[29-32]</sup> The first crystalline 3-dimensional carbon-nitride network synthesized by high-pressure-high-temperature (HP-HT) treatment of dicyandiamide in a laser-heated diamond-anvil cell is carbon nitride imide  $C_2N_2(NH)$ .<sup>[29]</sup> It exhibits a defect wurtzite-type structure. Moreover, two crystalline two-dimensional networks, namely poly(triazine imide) (PTI)  $[(C_3N_3)_2(NH_xLi_{1-x})_3] \cdot LiCl$ <sup>[31]</sup> built up of *s*-triazines and poly(heptazine imide) (PHI)  $[C_{12}N_{14}(NH)_3] \cdot 2 (C_3N_3)(NH_2)_3$ <sup>[30]</sup> (see Scheme 3) exhibiting condensed heptazines, were synthesized by reactions in salt melts or at moderate high-pressure conditions. Both comprising ring systems are interconnected via imide bridges. The most prominent and first described polymeric compound, melon  $[C_6N_7(NH_2)(NH)]_x$ , which was obtained during thermal treatment of dicyandiamide consists of one-dimensional chains of *s*-heptazine rings also interconnected by imide groups.<sup>[32]</sup> All polymers could be structurally elucidated by NMR and electron microscopy methods. Increasing attention has been paid on these C/N/H polymers due to innovative applications. Especially melon, mostly described in literature as an inaccurately defined structure called “g- $C_3N_4$ ”, is suitable for a variety of applications. Most outstanding are catalytic properties. Carbon nitrides as catalysts for Friedel-Crafts-reactions or  $CO_2$  activation and especially photocatalytic water splitting have gained increasing attention in recent literature.<sup>[33-35]</sup>

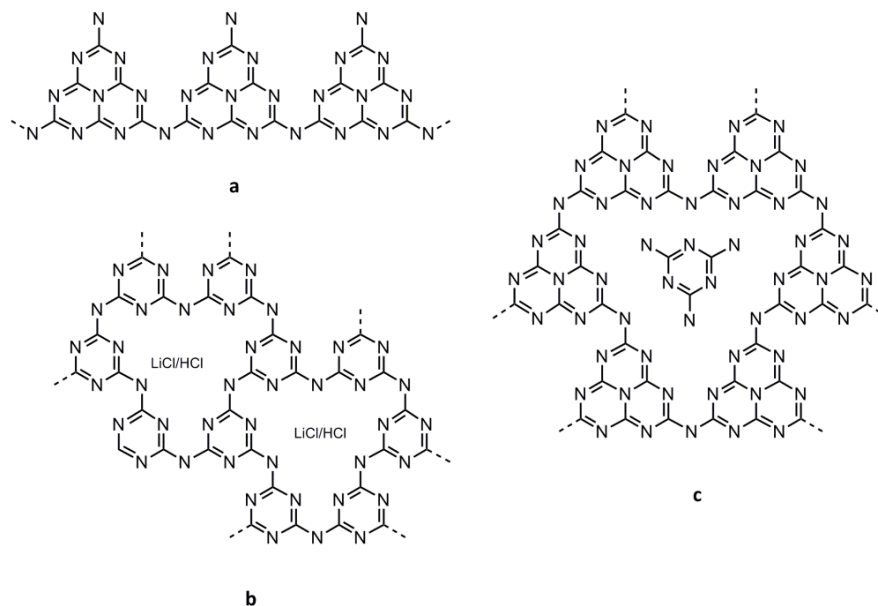
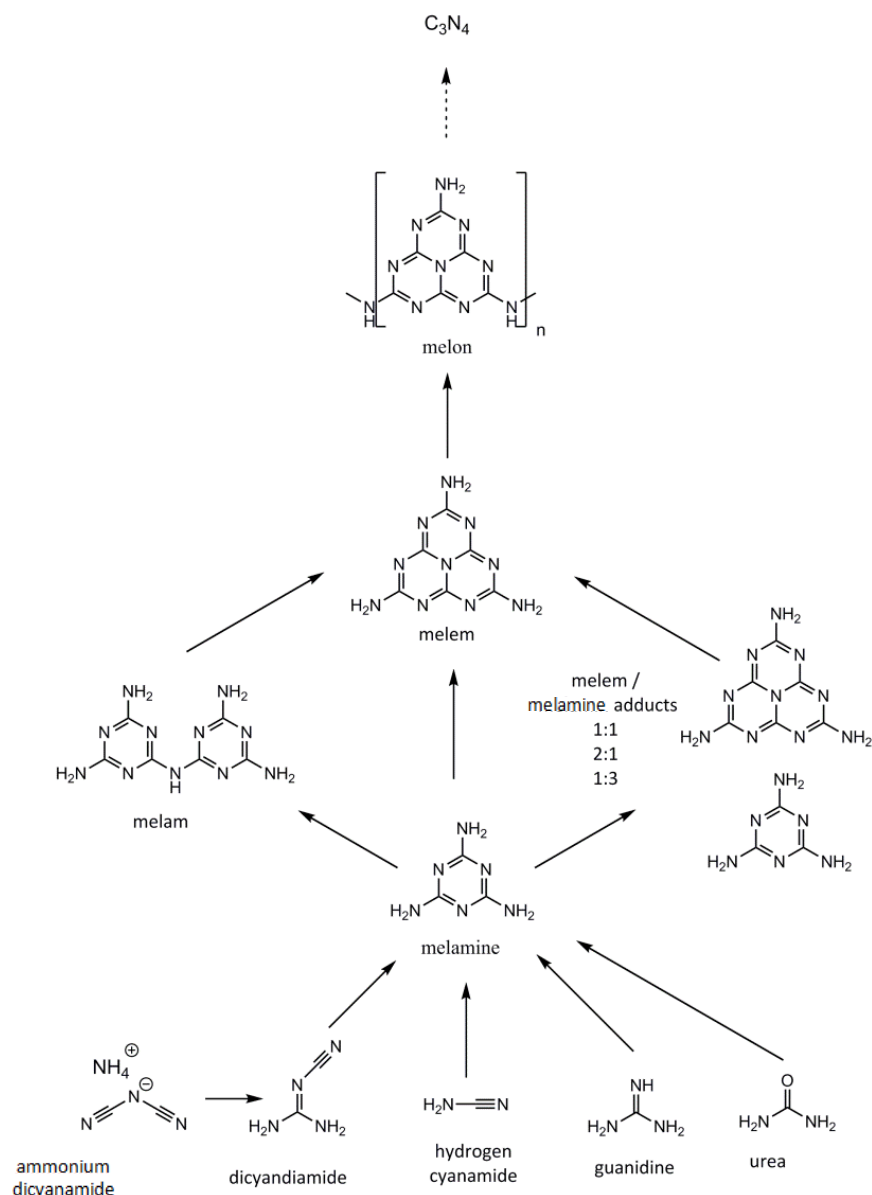


**Figure 3.** Structure models of melon **a** PTI **b** and PHI **c**.

Recent works are dealing with poly(triazine imide) (PTI) as non-metallic photocatalyst for water splitting.<sup>[36]</sup> Especially, doping with heterocycles increases the band gap for a higher catalytic efficiency.

With the focus on  $C_3N_4$  the polymerisation process of carbon nitrides was studied precisely. Therefore the knowledge of molecular structures acting as precursors for further 2-dimensional and 3-dimensional networks is steadily increasing.<sup>[37,38]</sup> Corresponding precursors can be divided into three groups: acyclic compounds, triazine- and heptazine-based compounds.

Starting materials for condensation are non-cyclic compounds like cyanamides, dicyandiamide or guanidines and urea (see Scheme 2). Thermal treatment leads to condensed cyclic compounds like melamine, melam<sup>[39]</sup> and melem.<sup>[40]</sup> Melamine and its dimer melam exhibit the triazine  $C_3N_3$  core, melem instead is built up of the heptazine  $C_6N_7$  core. During thermal reactions adduct phases of melamine and melem (melamine:melem 1:1, 2:1, 1:3) could be obtained and structurally elucidated.<sup>[41]</sup> The final known deammonation product is the 1D polymer named melon.<sup>[31]</sup> Hypothetically, hydrogen-free  $C_3N_4$  is predicted as further condensation product.



**Scheme 2.** Condensation scheme for carbon nitrides.

The range of new heptazine- and triazine-based precursors was extended by predominantly salt-like compounds like cyamelurates  $M(C_6N_7)(O)_3$ , tricyanomelatonates  $M(C_6N_7)(NCN)_3$  or tricyanomelaminates  $M(C_3N_3)(NCN)_3$  (see Figure 4). Especially metathesis reactions and studies on their thermal behavior owing to possible polymerization reactions has been conducted just recently.<sup>[42-45]</sup>

Aside from precursors for condensation processes new functionalized triazines with further remarkable properties aroused interest.<sup>[46-49]</sup> Some specific examples are shown in Figure 5. Functionalized triazines were mostly obtained by cyanuric

chloride  $C_3N_3Cl_3$  **a** as starting material and the synthesis conditions deviate mostly from common thermal reactions.<sup>[46]</sup> Important examples are briefly presented below.

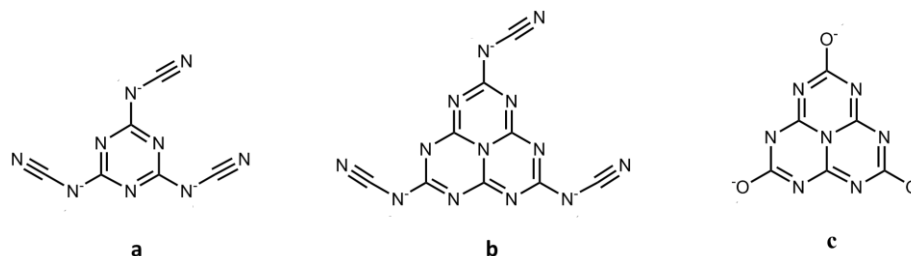


**Figure 4.** **a** Tricyanomelaminates **b** Tricyanomelonates **c** Cyamelurate.

1,3,5-triethynyl-2,4,6-triazine  $C_3N_3(C_2H_3)_3$  **b** derived by organic cross-coupling reactions exhibits interesting structural properties due to its similarity to graphene and is additionally a potential building block for COFs.<sup>[48]</sup> 1,3,5-triazine-2,4,6-carboxylate  $C_3N_3(COOH)_3$  **c** is prepared by injection of gaseous  $CO_2$  into aqueous solution of **a**.<sup>[49]</sup> Intriguing structural properties concerning supramolecular arrangement of  $C_3N_3(COOH)_3$  (see Figure 5 c) with heterocycles via hydrogen-bonding was discussed in literature just recently.<sup>[50-52]</sup> Initial aim of the synthesis of 1,3,5-hydrazino-2,4,6-triazine  $(C_3N_3)(N_2H_2)_3$  **d**,<sup>[47]</sup> synthesized by nucleophilic substitution with hydrazine, was the modification of s-triazine-based herbicides. Especially complexation with metals was in the focus of interest.

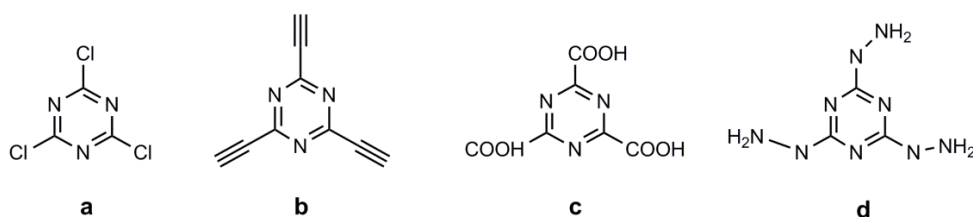


**Figure 5.** **a** Cyanuric chloride **b** 1,3,5-triethynyl-2,4,6-triazine **c** triazine-tricarboxylate **d** 1,3,5-hydrazino-2,4,6-triazine.<sup>[45-47, 51]</sup>

Recently, new related triazine-based compounds and their alternative synthesis routes for polymerization gained our interest. Especially, organometallic cross coupling syntheses with cyanuric chloride and alkyne derivatives were studied. New

materials which are suitable for use as building blocks or further material properties are of interest aside from their precursor properties.

Nevertheless, condensation routes and their precursors must not remain in the sidelines. Especially, new reaction conditions which lead to a better understanding of the condensation processes are of interest. Likewise new precursors are still of interest and play an important role in this study.

### **Goals of this study**

Carbon nitride chemistry has been studied for more than a century. Nevertheless there are a lot of unresolved questions. The suitable precursor or reaction condition for hypothetical 3D  $C_3N_4$  has not been found yet. In recent times C/N chemistry was primarily focused on pyrolysis or condensation processes which are not entirely elucidated thus far.

Therefore, further attempts regarding new polymerization routes are of essential significance. New functionalization and polymerisation processes are capable of yielding new potential precursors and polymeric compounds. Especially, syntheses applying organometallic compounds for functionalization of triazines with compatible alternative polymerization routes are of interest.

Additionally, detailed investigations focusing on decomposition could lead to a deeper insight into the polymerization of C/N/H materials. Besides common thermal solid-state reactions new work techniques shift to our attention.

As a third point of interest, precursors with foreign atoms synthesized by thermal treatment or pyrolysis are in the focus of this thesis.

**Bibliography**

- [1] W. Schnick, *Angew. Chem.* **1993**, *105*, 846; *Angew. Chem. Int. Ed.* **1993**, *32*, 806.
- [2] W. Schnick, *Phys. Status Solidi RRL* **2009**, *248*, 493.
- [3] H. A. Höpfe, *Angew. Chem.* **2009**, *121*, 3626.
- [4] M. Zeuner, S. Pagano, W. Schnick, *Angew. Chem.* **2011**, *123*, 7898; *Angew. Chem. Int. Ed.* **2011**, *50*, 7754.
- [5] N. Ooi, A. Rairkar, L. Lindsley, J. B. Adams, *J. Phys.: Condens. Matter*, **2006**, *18*, 97.
- [6] A. Krüger, *Neue Kohlenstoffmaterialien: Eine Einführung*, T. G. Teubner Verlag, GWV Fachverlage GmbH, Wiesbaden, **2007**.
- [7] A. K. Geim, K. S. Novoselov, *Nat. Mater.* **2007**, *6*, 183.
- [8] K. S. Novoselov, A. K. Geim, S. V. Morozov, D. Jiang, Y. Zhang, S. V. Dubonos, I. V. Grigorieva, A. A. Firsov, *Science* **2004**, *306*, 666.
- [9] A. T. Balaban, C. C. Rentia, E. Ciupitu, *Rev. Roum. Chim.* **1968**, *13*, 231.
- [10] W. Krätschmer, L. D. Lamb, K. Fostiropoulos, D. R. Huffman, *Nature*, **1990**, *347*, 354.
- [11] H. W. Kroto, J. R. Heath, S. C. O'Brien, R. F. Curl, R. E. Smalley, *Nature*, **1985**, *318*, 162.
- [12] M. F. L. De Volder, S. H. Tawfick, R. H. Baughman, A. J. Hart, *Science*, **2013**, *339*, 535.
- [13] T. Taylor, *J. Chem. Soc., Perkin Trans. 2*, **1993**, 813.
- [14] F. Langa, F. J. Nierengarten, *Fullerens Principles and Applications*, RSC Nanoscience and Nanotechnology, The Royal Society of Chemistry, Cambridge, **2007**; A. Hirsch, M. Brettreich, F. Wudl, *Fullerens, Chemistry and Reactions*, Wiley-VCH, **2004**.
- [15] U. H. F. Bunz, Y. Rubin, Y. Tobe, *Chem. Soc. Rev.* **1999**, *28*, 107.

- [16] L. D. Quin, J. A. Tyrell, *Fundamentals of heterocyclic chemistry*; John Wiley & Sons: Hoboken, New Jersey, **2010**.
- [17] J. Liebig, *Ann. Chem. Pharm.* **1834**, *10*, 1.
- [18] J. Liebig, *Ann. Chem. Pharm.* **1844**, *50*, 337.
- [19] J. Liebig, *Ann. Chem. Pharm.* **1845**, *53*, 330.
- [20] J. Liebig, *Ann. Chem. Pharm.* **1847**, *61*, 262.
- [21] J. Liebig, *Ann. Chem. Pharm.* **1855**, *95*, 257.
- [22] L. Gmelin, *Ann. Pharm.* **1835**, *15*, 252.
- [23] W. Henneberg, *Ann. Chem. Pharm.* **1850**, *73*, 228.
- [24] a) A. Y. Liu, M. L. Cohen, *Science* **1989**, *245*, 841; b) A. Y. Liu, M. L. Cohen, *Phys. Rev. B* **1990**, *41*, 10727; c) A. Y. Liu, R. M. Wentzcovitch, *Phys. Rev. B* **1994**, *50*, 10362.
- [25] D. M. Teter, R. J. Hemley, *Science* **1996**, *271*, 53.
- [26] C.-M. Sung, M. Sung, *Mater. Chem. Phys.* **1996**, *43*, 1.
- [27] E. Kroke, *Angew. Chem. Int. Ed.* **2014**, *53*, 2.
- [28] G. Algara-Siller, N. Severin, S. Y. Chong, T. Björkman, R. G. Palgrave, A. Laybourn, M. Antonietti, Y. Z. Khimyak, A. V. Krasheninnikov, J. P. Rabe, U. Kaiser, A. I. Cooper, A. Thomas, M. J. Bojdys, *Angew. Chem.* **2014**, *126*, 7580; *Angew. Chem. Int. Ed.* **2014**, *53*, 7450.
- [29] E. Horvath-Bordon, E. Kroke, I. Svoboda, H. Fueß, R. Riedel, S. Neeraj, A. K. Cheetham, *Dalton Trans.* **2004**, 3900.
- [30] M. Döblinger, B. V. Lotsch, J. Wack, J. Thun, J. Senker, W. Schnick, *Chem. Commun.* **2009**, 1541.
- [31] E. Wirnhier, M. Döblinger, D. Gunzelmann, J. Senker, B. V. Lotsch, W. Schnick, *Chem. Eur. J.* **2011**, *17*, 3213.
- [32] B. V. Lotsch, M. Döblinger, J. Sehnert, L. Seyfarth, J. Senker, O. Oeckler, W. Schnick, *Chem. Eur. J.* **2007**, *13*, 4969.

- [33] X. Wang, K. Maeda, A. Thomas, K. Takanahe, G. Xin, J. M. Carlsson, K. Domen, M. Antonietti, *Nat. Mater.* **2009**, *8*, 76.
- [34] A. Thomas, A. Fischer, F. Goettmann, M. Antonietti, J.-O. Müller, R. Schlögl, J. M. Carlsson, *J. Mater. Chem.* **2008**, *18*, 4893.
- [35] F. Goettmann, A. Thomas, M. Antonietti, *Angew. Chem.* **2007**, *119*, 2773; *Angew. Chem. Int. Ed.* **2007**, *46*, 2717.
- [36] K. Schwinghammer, B. Tuffy, M.B. Mesch, E. Wirnhier, C. Martineau, F. Taulelle, W. Schnick, J. Senker, B.V. Lotsch, *Angew. Chem.* **2013**, *125*, 2495; *Angew. Chem. Int. Ed.* **2013**, *52*, 2435.
- [37] E. Kroke, M. Schwarz, *Coord. Chem. Rev.* **2004**, *248*, 493.
- [38] G. Goglio, D. Foy, G. Demazeau, *Mater. Sci. Eng. R* **2008**, *58*, 195.
- [39] B. V. Lotsch, W. Schnick, *Chem. Eur. J.* **2007**, *13*, 4956.
- [40] B. Jürgens, E. Irran, J. Senker, P. Kroll, H. Müller, W. Schnick, *J. Am. Chem. Soc.* **2003**, *125*, 10288.
- [41] A. Sattler, W. Schnick, *Eur. J. Inorg. Chem.* **2009**, 4972.
- [42] B.V. Lotsch, W. Schnick, *Chem. Mater.* **2006**, *18*, 1891.
- [43] S. J. Makowski, W. Schnick, *Z. Anorg. Allg. Chem.* **2009**, *635*, 2197.
- [44] S. J. Makowski, D. Gunzelmann, J. Senker, W. Schnick, *Z. Anorg. Allg. Chem.* **2009**, *635*, 2434.
- [45] A. Sattler, M. R. Budde, W. Schnick, *Z. Anorg. Allg. Chem.* **2009**, *635*, 1933.
- [46] S. Tragl, K. Gibson, H.-J. Meyer, *Z. Anorg. Allg. Chem.* **2004**, *630*, 2373; b) S. Tragl, K. Gibson, J. Glaser, G. Heydenrych, G. Frenking, V. Duppel, A. Simon, H.-J. Meyer, *Z. Anorg. Allg. Chem.* **2008**, *634*, 2754.
- [47] D. S. Brown, J. D. Lee, P. R. Russell, *Acta Cryst.* **1976**, *B32*, 2101.
- [48] M. Ohkita, M. Kawano, T. Suzuki, T. Tsuji, *Chem. Commun.* **2002**, 3054.

- [49] C. Grundmann, E. Kober, *J. Org. Chem.* **1956**, *21*, 1392; b, J.-R. Galán-Mascarós, J.-M. Clemente-Juan, K. R. Dunbar, *J. Chem. Soc., Dalton Trans.* **2002**, *13*, 2710.
- [50] S. J. Makowski, M. Lacher, C. Lermer, W. Schnick, *J. Mol. Struct.* **2012**, *1013*, 19.
- [51] S. J. Makowski, P. Köstler, W. Schnick, *Chem. Eur. J.* **2012**, *18*, 3248.
- [52] S. J. Makowski, E. Calta, M. Lacher, W. Schnick, *Z. Anorg. Allg. Chem.* **2011**, *638*, 88.

## 2. Summary

This thesis is focused on new precursors as well as intermediate phases of polymeric carbon nitride-type materials. Additionally, common and new polymerization processes were studied and finally lead to new suitable synthesis routes.

New *s*-heptazine-based materials of divalent metals like cyamelurates  $M^{II}H(C_6N_7)(O)_3$  or tricyanomelonnates  $M^{II}H(C_6N_7)(NCN)_3$  as well as melem adduct phases as potential precursors for highly condensed carbon-nitride materials were identified. Additionally, special regard has been paid to the functionalization of triazines with alkynes as building blocks for new networked materials and as precursors for new polycondensation reactions. Corresponding syntheses were conducted by organic cross coupling reactions. The resulting compounds were structurally characterized and a first triazine based polymer connected with mesitylen units could be investigated through thermal treatment. Furthermore, alkyne-metathesis reactions led to first oligomeric triazines connected by acetylene units.

A deeper understanding of condensation processes could be achieved by deprotonation reactions. The decomposition of the highly condensed material melon was studied and therefore the reversibility of the formation reactions from cyanamide to melamine, melem and melon could be demonstrated.

## 2.1. Intermediate Phases and Salt-like Precursors for Carbon Nitrides

Carbon nitride chemistry is characterized by studying new precursor compounds which are capable of forming new networked materials. In this chapter new adduct phases as intermediates in the pyrolysis of thiourea or thermal treatment of melamine/ $\text{NH}_4\text{Cl}$  mixtures were characterized. Additionally, new heptazine-based salt-like structures with divalent metals were identified by metathesis reactions.

### 2.1.1. Formation of Melamium Adducts by Pyrolysis of Thiourea or Melamine/ $\text{NH}_4\text{Cl}$ Mixtures.

(*Chem. Eur. J.* **2012**, *18*, 1811)

To achieve new precursors or polymeric compounds with enhanced catalytic properties the introduction of heteroatoms into carbon nitrides was investigated. Therefore pyrolysis of thiourea and condensation reactions of melamine/ $\text{NH}_4\text{Cl}$  mixtures were studied and the results were outlined in the main part of this thesis.

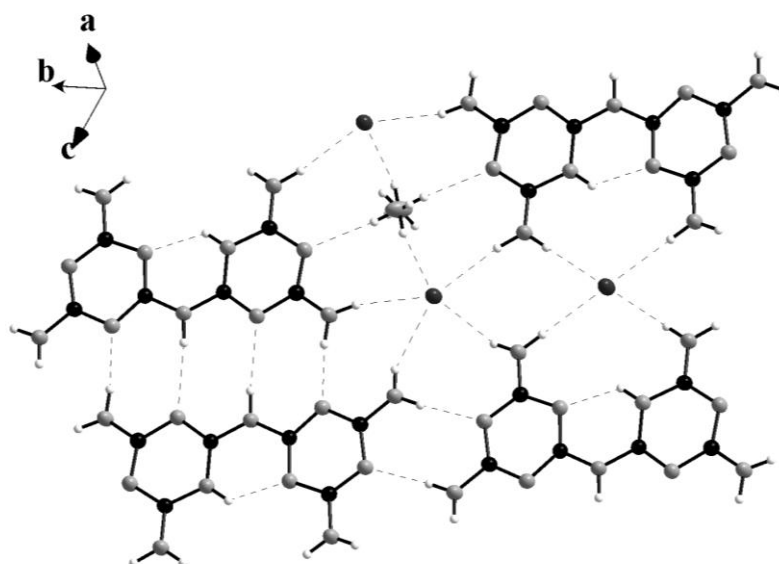


**Figure 1.** Hydrogen-bonding motifs of  $\text{C}_6\text{N}_{11}\text{H}_{10}\text{Cl} \cdot 0.5 \text{NH}_4\text{Cl}$ .

Through thermal treatment of  $\text{NH}_4\text{Cl}$  and melamine in closed ampoules a melamium/ $\text{NH}_4\text{Cl}$  adduct phase was formed instead of melem. The crystal structure was solved and refined from single-crystal diffraction data as follows:  $\text{C}_6\text{N}_{11}\text{H}_{10}\text{Cl} \cdot 0.5 \text{NH}_4\text{Cl}$ :  $P \bar{1}$  (no. 2),  $Z = 2$ ,  $a = 6.7785(14)$ ,  $b = 7.7528(16)$ ,  $c = 12.182(2) \text{ \AA}$ ,  $\alpha = 91.92(3)$ ,  $\beta = 91.61(3)$ ,  $\gamma = 112.26(3)^\circ$ ,  $V = 591.6(2) \text{ \AA}^3$ .

Thereby, structural characteristics were investigated in detail. Intra-annular hydrogen-bonding motifs stabilize a layer-like structure. Additionally, intra-molecular hydrogen-bonds connecting melamium units as well as ammonium chloride fragments were identified (see Figure 1), whereby an unequivocal proton localization at the  $\text{C}_6\text{N}_{11}\text{H}_{10}^+$  - ion plays a significant role.

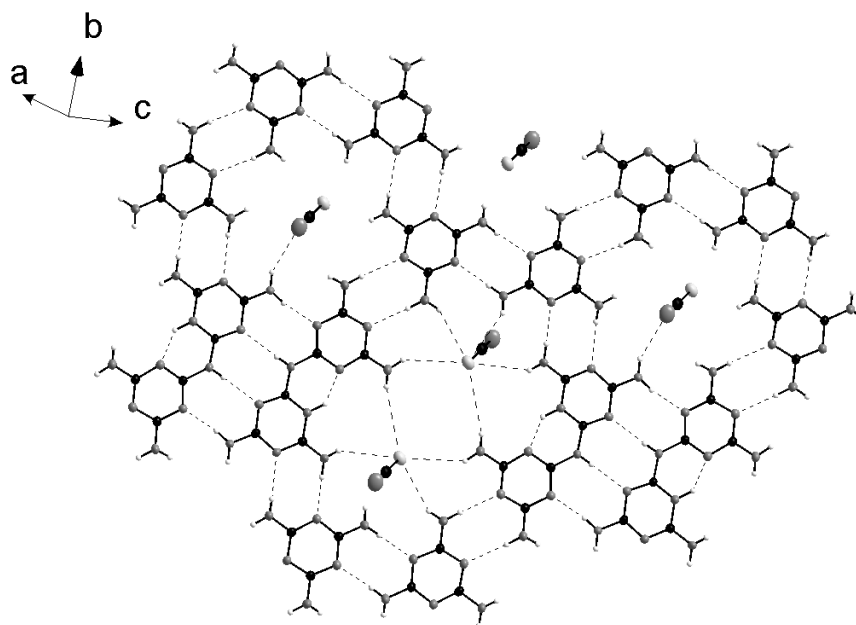


**Figure 2.** Hydrogen-bonding motifs of  $\text{C}_6\text{N}_{11}\text{H}_{10}\text{SCN} \cdot 2 \text{C}_3\text{N}_3(\text{NH}_2)_3$ .

During pyrolysis of thiourea the melamium thiocyanate-melamine adduct  $\text{C}_6\text{N}_{11}\text{H}_{10}\text{SCN} \cdot 2 \text{C}_3\text{N}_3(\text{NH}_2)_3$  could be isolated (see Figure 2). One further melaminium thiocyanate-melamine adduct of formula  $\text{HC}_3\text{N}_3(\text{NH}_2)_3\text{SCN} \cdot 2 \text{C}_3\text{N}_3(\text{NH}_2)_3$  represents an intermediary reaction product. The crystal structures of the compounds were solved by single-crystal XRD ( $\text{HC}_3\text{N}_3(\text{NH}_2)_3\text{SCN} \cdot 2 \text{C}_3\text{N}_3(\text{NH}_2)_3$ :  $P \bar{1}$  (no. 2),  $Z = 2$ ,  $a = 7.9766(16)$ ,  $b = 10.551(2)$ ,  $c = 11.353(2) \text{ \AA}$ ,  $\alpha = 86.67(3)$ ,  $\beta = 74.86(3)$ ,  $\gamma = 86.04(3)^\circ$ ,  $V = 919.3(3) \text{ \AA}^3$ ;  $\text{C}_6\text{N}_{11}\text{H}_{10}\text{SCN} \cdot 2 \text{C}_3\text{N}_3(\text{NH}_2)_3$ :  $P \bar{1}$  (no. 2),

$Z = 2$ ,  $a = 7.8625(16)$ ,  $b = 10.237(2)$ ,  $c = 14.519(3)$  Å,  $\alpha = 98.94(3)$ ,  $\beta = 103.23(3)$ ,  $\gamma = 93.33(3)^\circ$ ,  $V = 1118.4(4)$  Å<sup>3</sup>) and confirmed by NMR, FTIR-spectroscopy and mass-spectrometry.

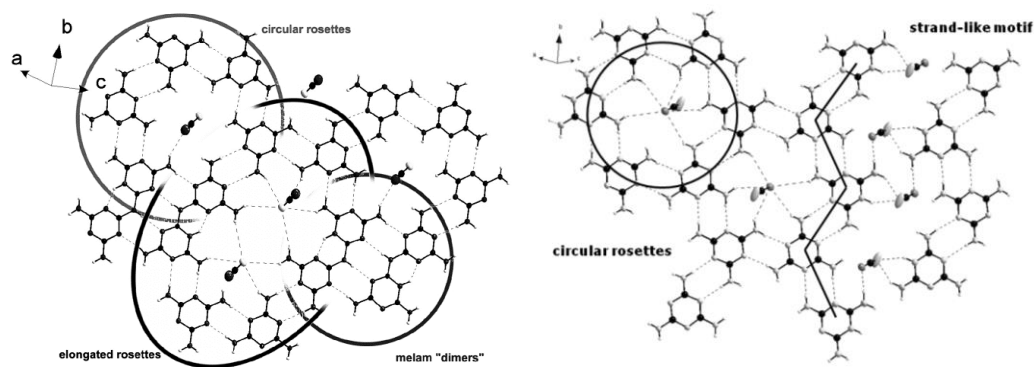


**Figure 3.** Strand-like and circular motifs of  $C_6N_{11}H_{10}SCN \cdot 2 C_3N_3(NH_2)_3$  and  $C_6N_{11}H_{10}SCN \cdot 2 C_3N_3(NH_2)_3$ .

Intriguing structural characteristics were identified in form of melaminium and melaminium rosette- or strand-like motifs within incorporated thiocyno units connected by hydrogen-bondings (see Figure 3).

### 2.1.2. New Heptazine Based Materials with a Divalent Cation – $Sr[H_2C_6N_7O_3]_2 \cdot 4 H_2O$ and $Sr[HC_6N_7(NCN)_3] \cdot 7 H_2O$

(*Z. Anorg. Allg. Chem.* **2013**, *639*, 275)

In order to expand the diversity of *s*-heptazine derivatives which are potential precursors for the synthesis of polymeric carbon nitrides a first diprotonated divalent cyamelurate  $Sr[H_2C_6N_7O_3]_2 \cdot 4 H_2O$  (*Fdd2*,  $a = 1194.0(17)$ ,  $b = 6358.14(97)$ ,  $c = 602.73(89)$  pm,  $Z = 8$ ,  $GOF = 1.034$ ,  $R_p = 0.033$ ,  $wR_p = 0.043$ ,  $R_B = 0.84$ ) has been prepared by metathesis of potassium cyamelurate with  $SrCl_2$  in aqueous solution.

The crystal structure was studied by single-crystal X-ray diffraction and Rietveld refinement and was confirmed by FTIR-spectroscopy and elemental analysis additionally. An as yet unknown stacking order for *s*-heptazine based materials arranged in distorted zig-zag strands could be found (see Figure 4).

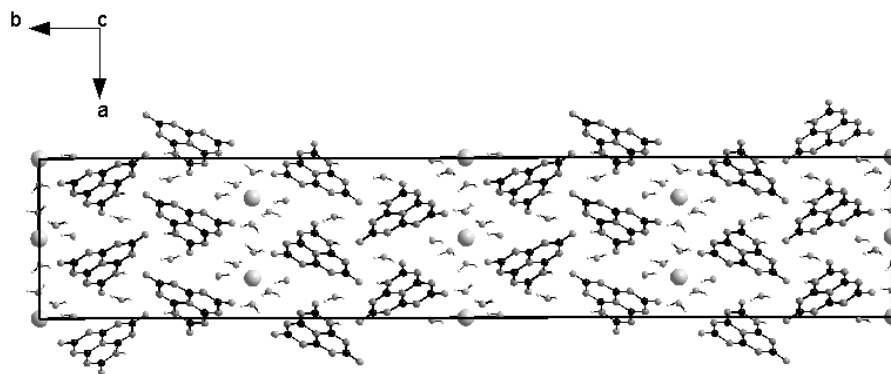


**Figure 4.** Zig-zag strands of  $\text{Sr}[\text{H}_2\text{C}_6\text{N}_7\text{O}_3]_2 \cdot 4 \text{H}_2\text{O}$ .

DTA-TG measurements indicates a relatively low thermal stability for  $\text{Sr}[\text{HC}_6\text{N}_7(\text{NCN})_3] \cdot 4 \text{H}_2\text{O}$  which can be attributed to protonation of the heptazine ring.

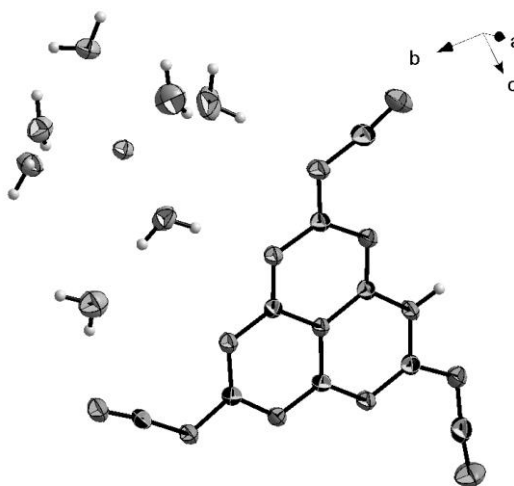


**Figure 5.** Asymmetric unit of  $\text{Sr}[\text{HC}_6\text{N}_7(\text{NCN})_3] \cdot 7 \text{H}_2\text{O}$ .

Additionally, a new monoprotonated divalent melonate  $\text{Sr}[\text{HC}_6\text{N}_7(\text{NCN})_3] \cdot 7 \text{H}_2\text{O}$  ( $P \bar{1}$ ,  $a = 660.76(13)$ ,  $b = 1080.7(2)$ ,  $c = 1353.8(3)$  pm,  $\alpha = 101.67(3)$ ,  $\beta = 101.40(3)$ ,  $\gamma = 94.60(3)^\circ$ ,  $Z = 2$ ,  $R_1 = 0.032$ ,  $wR_2 = 0.072$ ) prepared by metathesis reaction of potassium melonate and  $\text{SrCl}_2$  was characterized.

Strontium melonate heptahydrate (see Figure 5) crystallizes in a layer-like structure stabilized by inter- as well as innerlayer hydrogen-bonding motifs characteristic for heptazine based compounds.

## 2.2. Alkyne-triazines on the Way to New Triazine-based Networks

New types of precursors which induce different approaches for synthesis of new carbon nitride polymers found interest. First a new functionalization route for triazines was established and a new corresponding polymer could already be characterized through thermal treatment. Furthermore, a hydrogen-free polymer through metathesis reaction is targeted and first oligomers have been prepared.

### 2.2.1. Synthesis of Novel Triazine-based Materials by Functionalization with Alkynes

(*Chem. Eur. J.* **2015**, *21*, 7866)

In order to obtain new carbon nitride materials which are suitable precursors for polymeric compounds or as building blocks for networks the triazine based material cyanuric chloride  $C_3N_3Cl_3$  was functionalized with alkynes by organic cross coupling reactions.

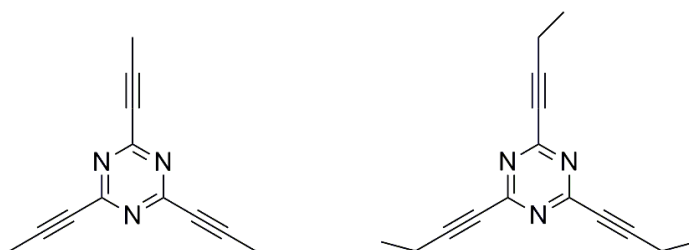


**Figure 6.** Formula units of tris(1-propynyl)-1,3,5-triazine (1) and tris(1-butynyl)-1,3,5-triazine (2).

The preparation of tris(1-propynyl)-1,3,5-triazine (1) ( $a = 1500.06(14)$ ,  $b = 991.48(10)$ ,  $c = 754.42(6)$ ,  $Z = 4$ ,  $V = 1122.03(18) \text{ \AA}^3$ ) and tris(1-butynyl)-1,3,5-triazine (2) ( $a = 10.6836(12)$ ,  $b = 12.0868(12)$ ,  $c = 15.9938(16)$ ,  $\alpha = 86.67(3)$ ,  $\beta = 86.890(4)$ ,  $\gamma = 86.890(4)^\circ$ ,  $Z = 6$ ,  $V = 1997.7(4) \text{ \AA}^3$ ) were performed by a Negishi-like coupling of cyanuric chloride  $C_3N_3Cl_3$  with butynyl zinc or propynyl zinc (see Figure 6).

Both structures were characterized by single crystal X-ray diffractometry and were additionally confirmed by NMR and FTIR-spectroscopy.

In the crystal structures *s*-triazine units are interconnected by hydrogen bonds forming zig-zag strands for tris(1-propynyl)-1,3,5-triazine while tris(1-butynyl)-1,3,5-triazine is built up of parallel layers (see Figure 7).

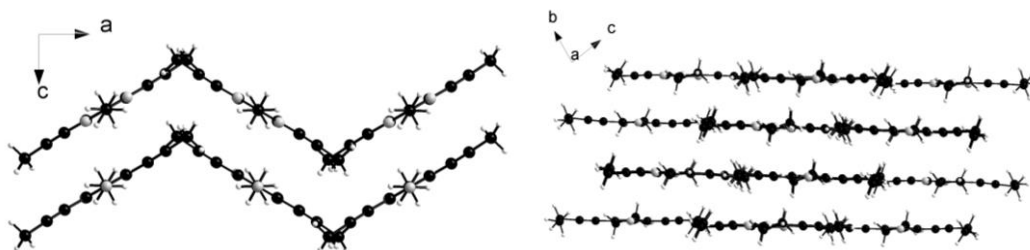


**Figure 7.** Layer-like structures of (1) and (2).

Significant van-der-Waals interactions which are responsible for stability were identified. Thereby triazines are shifted such that carbon atoms of the triazine rings and triple bonds are located upon each other. Finally, thermal investigations indicate that tris(1-propynyl)-1,3,5-triazine is best suitable for further polymerization reactions.

Corresponding to DTA-TG data tris(1-propynyl)-1,3,5-triazine (TPT) was pyrolyzed and a new disordered network, poly-TPT, could be synthesized. Initial alkyne groups undergo a thermal-induced Reppe-like 2+2+2 cyclization leading to mesitylene structures (see Figure 8) as linkers.

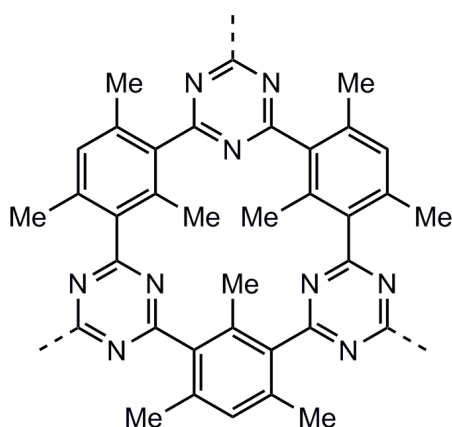


**Figure 8.** Tentative structure of poly-TPT.

The new polymer contains a high surface area and is therefore a potentially interesting compound for applications e.g. as catalyst.

### 2.2.2. Alkyne-metathesis Reactions for (1-propynyl)-1,3,5-triazine (1)

Alkyne-metathesis was conducted with tris(1-propynyl)-1,3,5-triazine (1) aiming at polymeric compounds like  $(C_6N_3)_n$  (see Figure 9). Such porous polymers with appropriate pore size distribution for catalytic application are of special interest for material science.

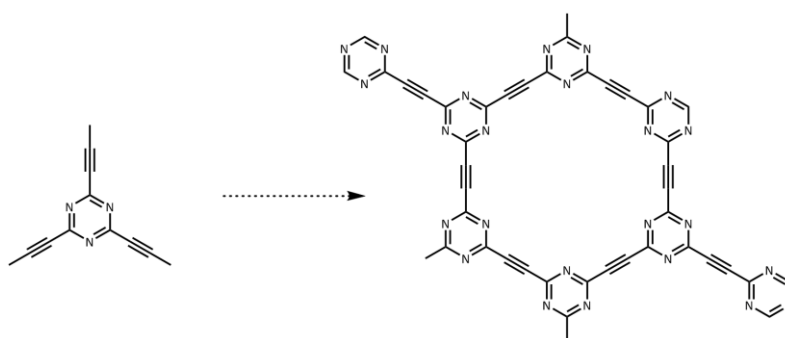


**Figure 9.** Reaction pathway for alkyne-metathesis of tris(1-propynyl)-1,3,5-triazine (1).

A variety of commonly used and new molybdenum alkylidene catalysts were used for this purpose (see Figure 10). Different parameters like temperature, duration as well as polar and nonpolar solvents were tested.

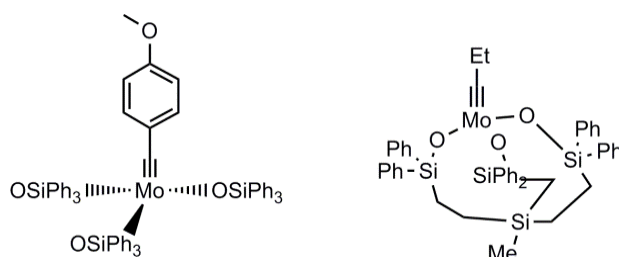


**Figure 10.** Suitable catalysts for alkyne-metathesis.

The reaction processes were continuously monitored by GC-MS and a complete conversion of tris(1-propynyl)-1,3,5-triazine could be observed. Additionally, gas evolution and precipitation of a black solid indicated a successful occurrence of polycondensation.

Finally, the product was analyzed by mass-spectrometry and FTIR-spectroscopy which demonstrated oligomeric compounds. FTIR vibrations show triazine as well as alkyne vibrations, while mass-spectrometry represents seven to 15 unit oligomers (see Figure 11). Further metathesis reactions to extend the polymerization process are still in progress.

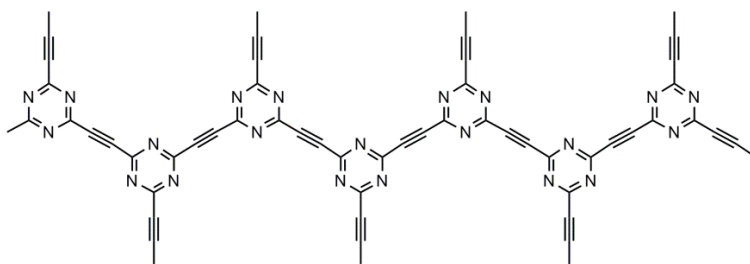


**Figure 11.** Seven unit oligomeric structure of (1).

## 2.3. Investigations into the Polymerization Process of Carbon Nitriles

In chapter 5 the decomposition of carbon nitride-type materials was investigated to obtain a better understanding of thermal reaction processes. Especially, the reversibility of the formation mechanism of melon has been paid attention to.

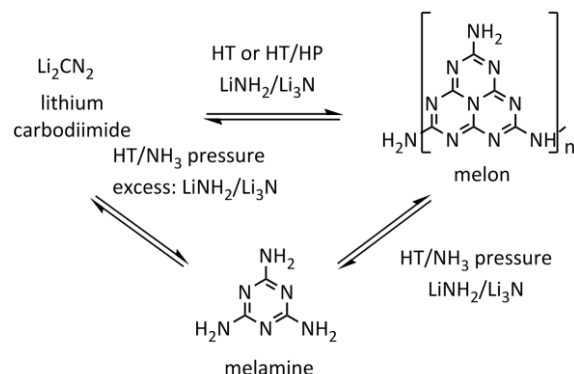


**Figure 12.** Decomposition scheme of melon.

Decomposition of melon was initiated with bases by use of thermal treatment and high pressure techniques. All reactions were based on the knowledge of the polymerization process from carbodiimides to melon which can be divided into two parts.

First addition reactions of carbodiimide lead to melamine, while melamine condenses to melon and melon under release of ammonia.

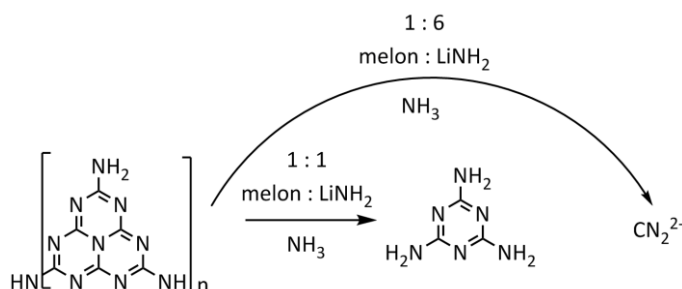


**Figure 13.** Ammonothermal decomposition of melon.

As a result, decomposition by thermal treatment in ampoules or other extreme conditions, like high pressure, leads to the formation of carbodiimides. Increasing ammonia pressure in autoclave reactions leads to melamine and the triazine ring

remains intact (Figure 12 and 13). Only an excess of bases or exceeding reaction times induce an entire decomposition of melamine to cyanamides.

Therefore the decomposition to stable compounds has been investigated and it could be shown that decomposition processes can be influenced by defined reactions parameters.

### 3. Adduct Phases and Salt-like Precursors for Carbon Nitrides

Polymerization processes are the most important issue in CN chemistry. New precursors as well as intermediate compounds which are suitable as precursors for condensation reactions are of great interest. Especially *s*-triazine- and *s*-heptazine based materials were investigated for this propose. In this thesis novel divalent heptazine-based structures, namely cyamelurates  $MH(C_6N_7)(O)_3$  or tricyanomelonates  $MH(C_6N_7)(NCN)_3$ , prepared by metathesis reactions were structurally elucidated.

Additionally, new melaminium and melamium adduct phases were described by pyrolysis of thiourea or condensation reactions of melamine and  $NH_4Cl$  mixtures. They represent new intermediate phases and possible precursor compounds including foreign atoms. In this chapter detailed synthesis conditions as well as structural investigations like crystal structures or thermal behavior are presented.

### 3.1. Formation of Melamium Adducts by Pyrolysis of Thiourea or Melamine/NH<sub>4</sub>Cl Mixtures.

Nicole E. Braml, Andreas Sattler, and Wolfgang Schnick

published in: *Chem. Eur. J.* **2012**, *18*, 1811.

DOI: 10.1002/chem.201101885

Copyright © 2014 WILEY-VCH

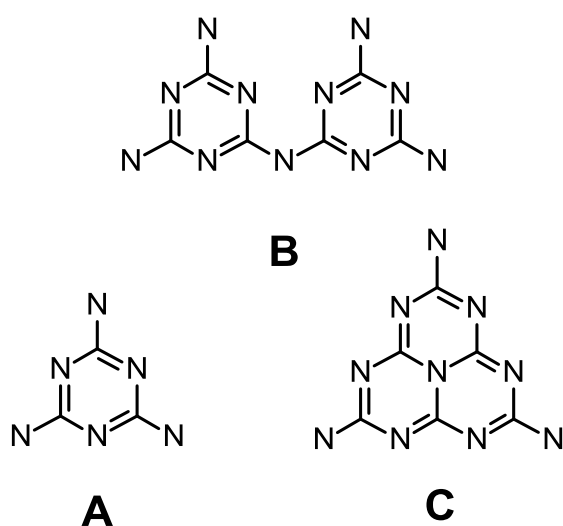
<http://onlinelibrary.wiley.com/doi/10.1002/chem.201101885/abstract>

**Keywords:** carbon nitrides · precursor · crystal-structure · solid-state NMR

**Abstract.** Pyrolysis of prominent precursor compounds for synthesis of carbon nitride type materials (e.g. melamine, thiourea) have been studied in detail. Molecular adducts containing mono-protonated melamium  $C_6N_{11}H_{10}^+$  and melaminium  $HC_3N_3(NH_2)_3^+$  ions, respectively, have been identified as intermediates. The adduct  $C_6N_{11}H_{10}Cl \cdot 0.5 NH_4Cl$  was obtained by the reaction of melamine  $C_3N_3(NH_2)_3$  with  $NH_4Cl$  at 450 °C. During pyrolysis of thiourea, guanidinium thiocyanate was initially formed and subsequently the melamium thiocyanate melamine adduct  $C_6N_{11}H_{10}SCN \cdot 2 C_3N_3(NH_2)_3$  was isolated at 300 °C. A second melaminium thiocyanate melamine adduct with the formula  $HC_3N_3(NH_2)_3SCN \cdot 2 C_3N_3(NH_2)_3$  represents an intermediary reaction product that is best accessible at low pressures. The crystal structures of the compounds were solved by single-crystal XRD. Unequivocal proton localization at the  $C_6N_{11}H_{10}^+$  ion was established. A typical intramolecular and interannular hydrogen bridge and other characteristic H-hydrogen-bonding motifs were identified. Additionally, the adducts were investigated by solid-state NMR spectroscopy. Our study provides detailed insight into the thermal condensation of thiourea by identifying and characterizing key intermediates involved in the condensation process leading to carbon nitride-type materials. Furthermore, factors promoting the formation of melamium adduct phases over meleam are discussed.

### 3.1.1. Introduction

Carbon nitrides are an important class of functional materials and they represent structurally interesting compounds. The quest for the still elusive binary nitride  $C_3N_4$ <sup>[1]</sup> has brought up a number of applications for carbon nitride-type materials.<sup>[2, 3]</sup> The envisaged use of hypothetical  $sp^3$ -hybridized  $C_3N_4$  as an ultra-hard material, potentially even exceeding the hardness of diamond, was largely responsible for the initial interest in carbon nitrides.<sup>[4, 5]</sup> More recently, employment of carbon nitride-type materials as metal free catalysts has been proposed.<sup>[6, 7]</sup>



**Scheme 1.** Molecular structures of melamine (A), melam (B) and melem (C).

Melamine  $C_3N_6H_6 \equiv C_3N_3(NH_2)_3$  (see Scheme 1 A) and other C/N/H compounds like dicyandiamide  $C_2N_4H_4$  are prominent examples for suitable molecular precursors. Indeed, several highly condensed polymeric compounds (e.g. melon<sup>[11]</sup> or poly(heptazine imide) have been prepared starting from melamine.<sup>[12]</sup> Besides the above-mentioned bulk chemicals melamine and dicyandiamide, a variety of other precursor compounds capable of forming carbon nitride-type materials upon thermal treatment has been described. Examples comprise molecular single-source precursors, such as cyanogen isocyanate<sup>[13]</sup> or triazido-*s*-heptazine<sup>[14]</sup> as well as reactive mixtures (e.g.  $C_3N_3Cl_3$  or  $C_6N_7Cl_3$  in combination with nitride sources).<sup>[15]</sup>

Other possible applications of C/N building blocks and polymeric networks as “organic semiconductors”<sup>[8]</sup> or covalent organic frameworks (COFs)<sup>[9, 10]</sup> have been discussed in the literature. Many carbon nitrides are accessible by precursor pyrolysis, making an in-depth understanding of the respective thermal condensation processes crucial for rational design of syntheses for C/N materials.

The reactivity of precursors is also notably affected by alterations of the reaction conditions and by using salt melts<sup>[16]</sup> as a reaction media.

In the course of the temperature-dependant condensation of C/N/H precursors, several intermediates are formed with compounds like melem  $C_6N_{10}H_6 \equiv C_6N_7(NH_2)_3$  or melam  $C_6N_{11}H_9 \equiv (NH_2)_2C_3N_3(NH)C_3N_3(NH_2)_2$  are prominent examples (see Scheme 1). The melam molecule consists of two  $NH_2$ -substituted triazine nuclei bridged by an NH group. Historically, melam was one of the first C/N/H compounds to be mentioned in the literature. It was actually is the first compound reported in *Liebig's* initial publication dealing with carbon nitride-type molecules.<sup>[17]</sup> However, this compound has repeatedly puzzled researchers for a century and a half.<sup>[18, 19]</sup> Questions concerning the actual existence and structure of melam were not adequately resolved until recently.<sup>[20]</sup> Single-crystal XRD investigations on melam have established the conformation depicted in Scheme 1.

Melam was observed during condensation of pure melamine but remains an intermediary product.<sup>[20]</sup> As we have recently shown, the formation of melem or adduct phases of melamine and melem<sup>[21]</sup> usually preferential under equilibrium conditions. A general trend that pyrolysis of C/N/H precursors in the presence of acids favors the generation of melam(ium) containing species has been claimed in the literature.<sup>[22]</sup>

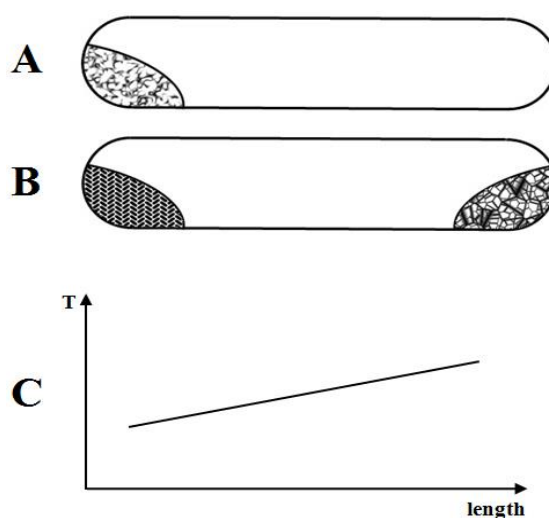


**Figure 1.** Reaction ampoule before (A) and after reaction (B), sketch of temperature gradient (C).

Melamium adducts with the formula  $C_6N_{11}H_{10}Cl \cdot 0.5 NH_4X$  ( $X = Cl, Br$ ) have been reported by *Jürgens*<sup>[23]</sup> as products formed by reaction of ammonium halides and various basic C/N/H molecules or ions (e.g. melamine, tricyanomelaminates, dicyandiamide). Such melamium compounds have also received attention in the literature.<sup>[24]</sup> However, the structures of these compounds could not be elucidated and their chemical nature was not unequivocally established. Preparative amounts of melam were liberated from such compounds<sup>[20]</sup> adding to their synthetic importance since no direct synthesis of pure and adduct-free melam has hitherto been reported. Herein, we present a comprehensive study of precursor systems yielding melamium adduct phases. We were able to identify several key pyrolysis intermediates thus furthering our understanding of the formation of melam, as well as melamine, melem and their adducts.

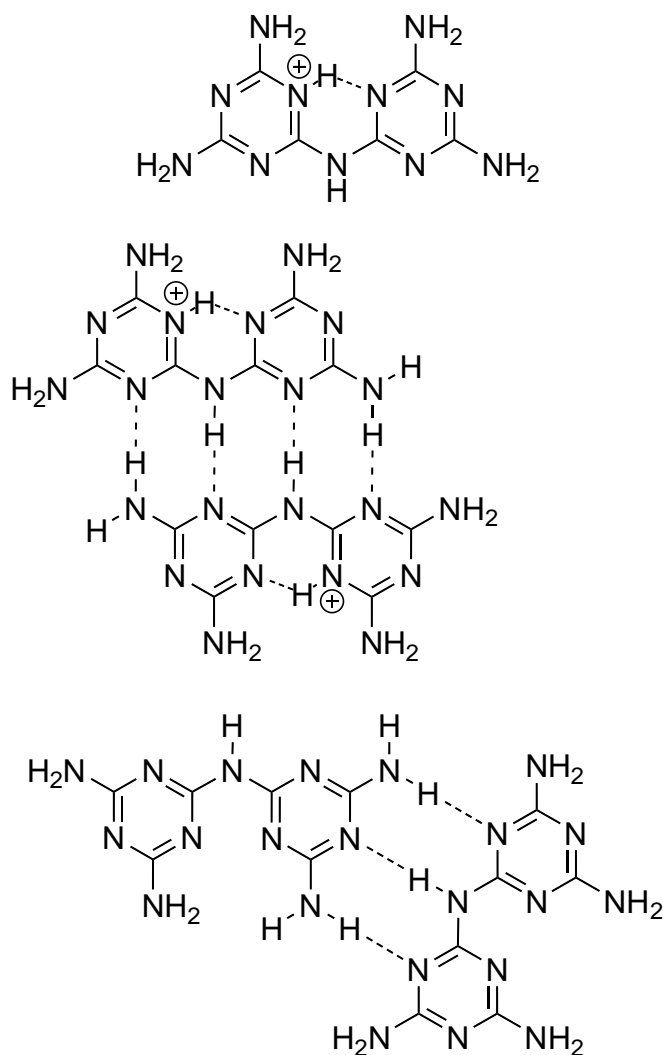
### 3.1.2. Results and Discussion

#### Melamium adducts by pyrolysis of melamine/ $NH_4Cl$ mixtures

To provide reliable information concerning the nature of the melamium adduct phases, the reported literature procedures<sup>[23]</sup> for synthesis of the claimed melamium ammonium chloride adduct were optimized for better crystal growth. In particular, reaction times were greatly extended (see Experimental Section for details). For pyrolysis, ampoules were loaded with melamine and  $NH_4Cl$  at one end and subsequently placed horizontally in a tube furnace. Due to the thermal gradient and the initial pressure within the ampoule several products were deposited at both ends of the ampoule (Figure 1). At the cooler part  $C_6N_{11}H_{10}Cl \cdot 0.5 NH_4Cl$  (**1**) was deposited. In the warmer zone, melem,  $NH_4Cl$  and  $C_6N_{11}H_{10}Cl \cdot 0.5 NH_4Cl$  (**1**) were deposited.  $NH_3$  was detected in the gas phase. Due to the deposition of large amounts of starting material at the hotter end and the loss in the gas phase only a marginal 5 % yield of pure crystalline  $C_6N_{11}H_{10}Cl \cdot 0.5 NH_4Cl$  (**1**) could be recovered from the lower part of the ampoule.

The highly crystalline melamium  $\text{NH}_4\text{Cl}$  adduct **1** thus obtained was studied by single-crystal XRD.  $\text{C}_6\text{N}_{11}\text{H}_{10}\text{Cl} \cdot 0.5 \text{NH}_4\text{Cl}$  (**1**) crystallizes in the triclinic space group  $P\bar{1}$ . The unit cell was found to be identical to that reported by *Jürgens* (obtained by indexing the PXRD diagram).<sup>[23]</sup> The asymmetric unit contains one single-protonated melamium ion with the formula  $\text{C}_6\text{N}_{11}\text{H}_{10}^+$ , one respective chloride counter ion and half equivalent of ammonium chloride. The  $\text{NH}_4^+$  ion exhibits disordered proton positions since the central atom (N12) of the tetrahedral (and thus non-centrosymmetric) cation is located on an inversion center. Such dynamical disordered positions have already been discussed in the literature.<sup>[25]</sup> The ammonium ion can best be viewed as two interfering tetrahedra and was refined as such. This resulted in a cube-like arrangement of 8 hydrogen atoms of occupancy 0.5 around the central nitrogen atom. Restraints were applied to limit the geometry of the disordered ion to reasonable parameters. All possible proton positions are part of hydrogen bonds supporting the structural description.

The melamium ion is built up of two amino-substituted triazine rings connected by an NH. The protonation site is located between the two rings allowing the formation of the intra-molecular and inter-annular hydrogen bridge  $\text{N4-H10}\cdots\text{N3}$  (see Figure 2). Thus the planes defined by the two triazine rings are no longer mutually tilted against each other, as is the case in pure melam,<sup>[20]</sup> but are found to be coplanar in the  $\text{C}_6\text{N}_{11}\text{H}_{10}^+$  ion. Two melamium ions are connected to each other by a total of four hydrogen bonds resulting in a dimer.



**Scheme 2.** Molecular structure of the  $C_6N_{11}H_{10}^+$  ion. H-bonding motifs observed in melamium adduct phases (top) and in pure melam (bottom).<sup>[20]</sup>

As this hydrogen-bonding motif incorporates a total of four hydrogen bonds it can be expected to possess a high degree of stability.<sup>[26]</sup> In melam, however, another hydrogen bonding motif is observed (see Scheme 2).<sup>[20]</sup> It seems plausible, that the tilting of the NH group found in this case, renders the four hydrogen-bond-motif less favorable.

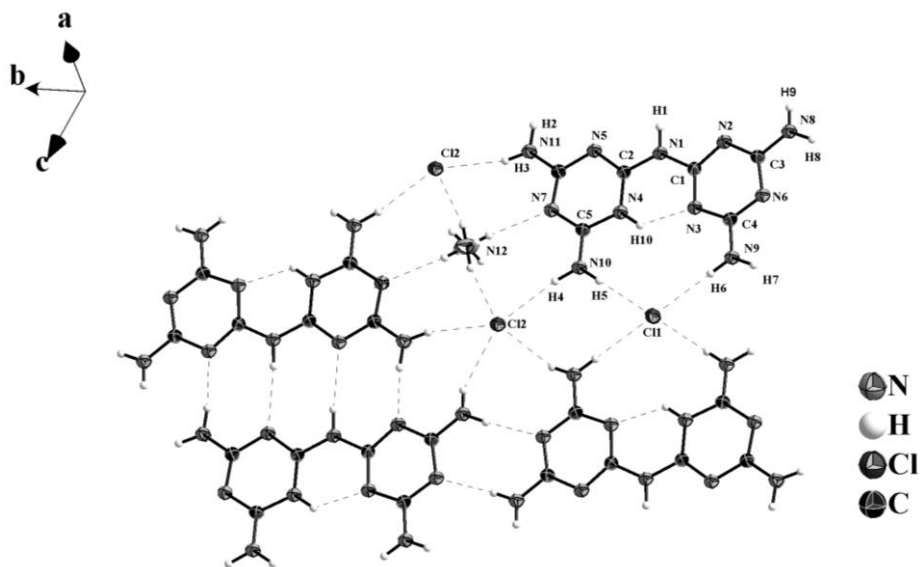


**Figure 2.** H-bonding interactions observed for  $C_6N_{11}H_{10}Cl \cdot 0.5NH_4Cl$  (1). Ellipsoids for non-hydrogen atoms are drawn at the 50 % probability level.

Bond lengths and angles within the melamium ion  $C_6N_{11}H_{10}^+$  are within the expected range for melam<sup>[20]</sup> and other triazine-based molecules such as melamine<sup>[27]</sup> and tricyanomelaminates.<sup>[28]</sup> Bonds lengths within both  $C_3N_3$  rings are indicative of intermediate states between double (C=N) and single bonds (C-N), reflecting delocalization due to the aromatic character. The triazine rings are slightly distorted and thus deviate from their idealized symmetry.

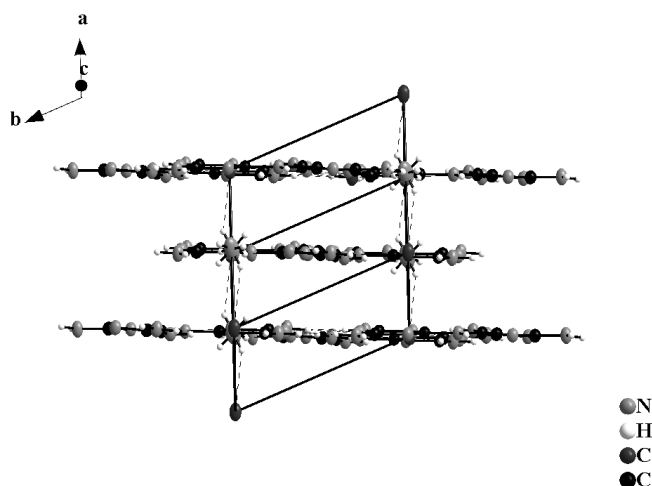


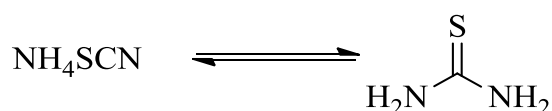
**Figure 3.** Layer-like structure of  $C_6N_{11}H_{10}Cl \cdot 0.5 NH_4Cl$  (1).

This is in accordance with observations made for a number of triazine-based compounds.<sup>[27]</sup> The protonation at N4 causes a slight elongation of adjacent bonds.

The melamium, the chloride and the ammonium ions are found to be almost coplanar resulting in a layer-like arrangement (see Figure 3). Whereas a dense hydrogen-bonding network is found within such layers, inter-layer interactions apparently are rather weak. The inter-layer stacking distance is about 3.4 Å which is rather large in comparison to the corresponding distance in the majority of heptazine or triazine compounds, that adopt layer-like structures (e.g. melon 3.19 Å<sup>[11]</sup> and melem 3.27 Å).<sup>[29]</sup>

### Melamium adducts by pyrolysis of thiourea

Sulfur-containing C/N precursors are reactive and thus promising intermediates for synthesis of carbon nitride-type materials, although they have not yet been systematically considered for this purpose. However, the use of ammonium thiocyanate as a precursor for preparation of several C/N/H compounds has to be mentioned in this context. Liebig described formation of C/N/H compounds such as melamine and melem as reaction products starting from ammonium thiocyanate.<sup>[17]</sup>



**Scheme 3.** Equilibrium reaction between thiourea and ammonium thiocyanate.

In the melt, ammonium thiocyanate transforms into thiourea (Scheme 3). This conversion is analogous to *Wöhler's* synthesis of urea from ammonium cyanate, but represents a true equilibrium reaction. The molar ratio of thiourea to ammonium thiocyanate in a fully equilibrated melt has been reported as 1 : 3.<sup>[30]</sup> The fraction of thiourea present in the melt is dependent on temperature and pressure, with high pressures and low temperatures shifting the equilibrium towards thiourea. Several investigations have been concerned with detailed analyses of these dependences.<sup>[31]</sup> Because of their mutual interconversion, it is not possible to clearly distinguish the thermal reactivity of both compounds.

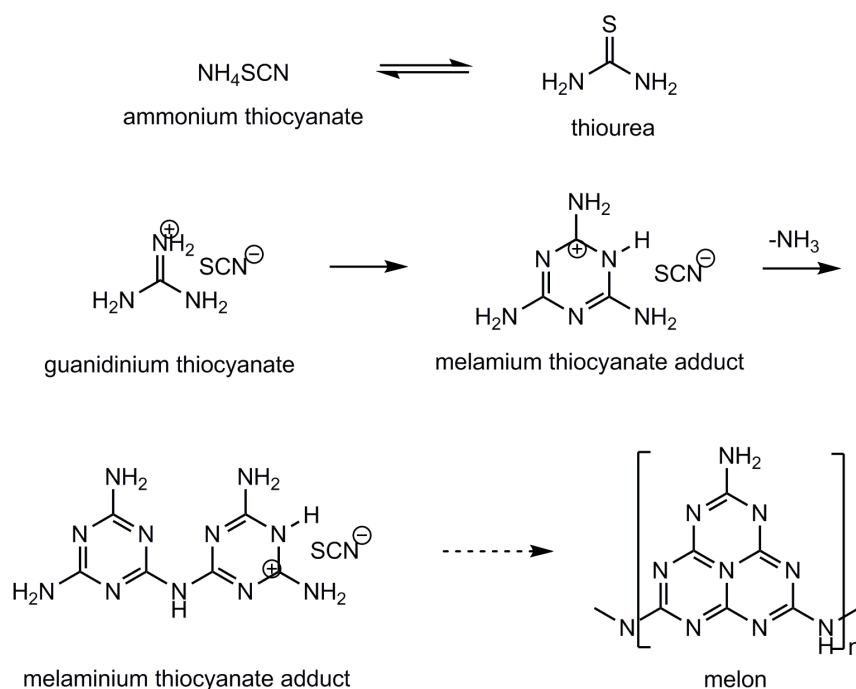
Apart from its partial conversion into thiourea in the melt, additional thermal reactivity of ammonium thiocyanate at higher temperatures has been reported. The formation of guanidinium thiocyanate takes place at temperatures around

180 °C.<sup>[32]</sup> The evolution of CS<sub>2</sub> from ammonium thiocyanate melts or mixtures of ammonium chloride and potassium thiocyanate upon further heating has been described by Liebig.<sup>[17]</sup> The formation of melam and ultimately melon upon heating with a burner has been described long ago but was queried by later studies.<sup>[33]</sup> Reports on the pyrolysis of thiourea mention the evolution of CS<sub>2</sub> and NH<sub>3</sub> as main gaseous products between 182 and 240 °C, but intermediates have not been isolated.<sup>[34]</sup> Recently, decomposition of thiosemicarbazide SC(NH)(NH)<sub>2</sub> leading to formation of graphitic carbon nitride-type materials has been reported. This suggests that sulfur-containing compounds might be prospective precursors for several polymeric C/N/H materials.<sup>[35]</sup>

In this present study we have used thiourea SC(NH<sub>2</sub>)<sub>2</sub> as a precursor for synthesis of carbon nitride-type materials. The employment of thiourea instead of ammonium thiocyanate was considered for several practical reasons: Ammonium thiocyanate undergoes typical dissociation of ammonium salts and thus generates a significant amount of gases (HSCN and NH<sub>3</sub>) when heated. As a consequence, the initial pressure during pyrolysis of NH<sub>4</sub>SCN is often significantly higher than that at the actual pyrolysis temperature after a large part of the NH<sub>4</sub>SCN has been consumed by the reaction. Thus, in comparison to thiourea, the use of ammonium thiocyanate can cause uncontrolled pressure development when using closed reaction vessels. Furthermore, product loss by sublimation may occur in open systems, leading to lower yields. Last but not least, in contrast to thiourea, ammonium thiocyanate is rather hygroscopic thus making storage, purification and reactions technically more demanding.

Analogously to the previous experiment ampoules were loaded with thiourea and placed horizontally in a tube furnace (see Experimental Section for further details). Due to the thermal gradient and the initial pressure (Figure 1) several products were generated (see Scheme 4). An overview of investigated reaction conditions is given in Table 1, with the indicated products being recovered from the hot zone of the ampoule. At the cooler end mostly guanidinium thiocyanate was formed. NH<sub>3</sub>

and CS<sub>2</sub> were detected in the gas phase. Further heating up to 500 °C leads to an amorphous melon-type polymeric material.



**Scheme 3.** Pyrolysis products of thiourea.

The two new phases were obtained at higher reaction temperatures as described in the following.

Pyrolysis at 300 °C in sealed glass ampoules yielded a new adduct phase with the formula C<sub>6</sub>N<sub>11</sub>H<sub>10</sub>SCN · 2 C<sub>3</sub>N<sub>3</sub>(NH<sub>2</sub>)<sub>3</sub> (**2**) comprising melamium thiocyanate and melamine. The compound was obtained in crystalline form allowing structural investigations. C<sub>6</sub>N<sub>11</sub>H<sub>10</sub>SCN · 2 C<sub>3</sub>N<sub>3</sub>(NH<sub>2</sub>)<sub>3</sub> (**2**) crystallizes in the triclinic space group *P*  $\bar{1}$ . Its structure could be solved by single-crystal XRD. The asymmetric unit contains the melamium ion C<sub>6</sub>N<sub>11</sub>H<sub>10</sub><sup>+</sup>, a thiocyanate ion and two neutral melamine molecules. The molecular structure of the melamium ion resembles that observed for the adduct C<sub>6</sub>N<sub>11</sub>H<sub>10</sub>Cl · 0.5 NH<sub>4</sub>Cl (**1**).

The two triazine rings are coplanar and connected by an intra-molecular hydrogen bridge. The melamine molecules show only minor deviations from their idealized structure (mainly torsions of the NH<sub>2</sub> groups with respect to the cyanuric nucleus), which may be due to packing effects in the crystal. The thiocyanate ion adopts the

expected linear form. The bond length and angles are in good agreement with those in other melam compounds.<sup>[20]</sup>

Rosette-like motifs, built up of melamine ions and melamine molecules, are present (Figure 5). Two different types of these rosettes can be identified. One type of rosettes is almost circular, whereas the other type is elongated due to the incorporation of larger melamium ions. Both motifs display a central void which is occupied by thiocyanate ions.

**Table 1.** Pyrolysis products of thiourea at different reaction conditions.

Temperature / °C	Initial atmosphere	Products <sup>[a]</sup>
150	Ar	$C(NH_2)_3SCN$
200	Ar	$C(NH_2)_3SCN + C_6N_{11}H_{10}SCN \cdot 2C_3N_3(NH_2)_3$
250	Ar	$C(NH_2)_3SCN + C_6N_{11}H_{10}SCN \cdot 2C_3N_3(NH_2)_3$
300	Ar	$C_6N_{11}H_{10}SCN \cdot 2C_3N_3(NH_2)_3$
400	Ar	$C_6N_{11}H_{10}SCN \cdot 2C_3N_3(NH_2)_3$
500	Ar	$C_6N_{11}H_{10}SCN \cdot 2C_3N_3(NH_2)_3$
200	vacuum	$HC_3N_3(NH_2)_3SCN \cdot 2C_3N_3(NH_2)_3 + \text{side phases}$
250	vacuum	$HC_3N_3(NH_2)_3SCN \cdot 2C_3N_3(NH_2)_3 + \text{side phases}$
300	vacuum	$HC_3N_3(NH_2)_3SCN \cdot 2C_3N_3(NH_2)_3 + \text{side phases}$
350	vacuum	$HC_3N_3(NH_2)_3SCN \cdot 2C_3N_3(NH_2)_3 + \text{side phases}$

- [a] identified by PXRD.

These  $\text{SCN}^-$  ions are connected to the amino groups of melamine or melam, respectively, by hydrogen bonds. They point towards the central voids, acting as hydrogen-bond acceptors. The nitrogen atoms of the thiocyanate ions all point towards the smaller circular voids, whereas the sulfur atoms point towards the elongated voids.

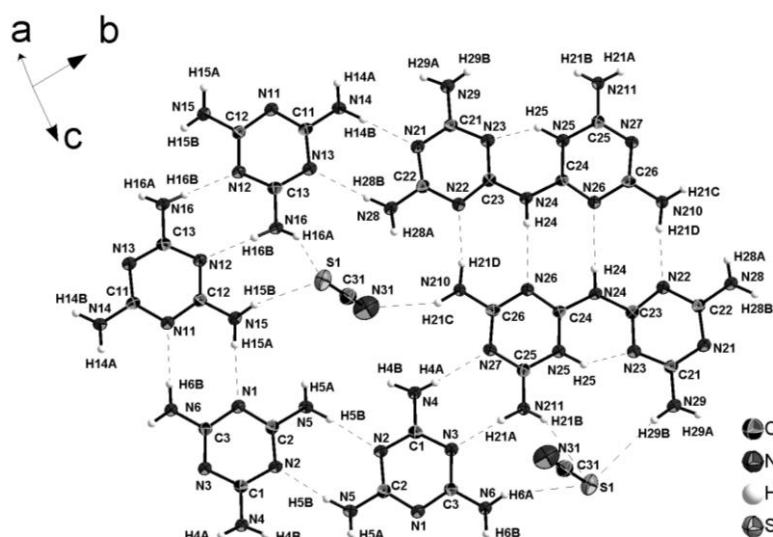


**Figure 4.** Structural motifs observed for the melamium adduct  $\text{C}_6\text{N}_{11}\text{H}_{10}\text{SCN} \cdot 2 \text{C}_3\text{N}_3(\text{NH}_2)_3 (2)$ .  
H-bonding interactions for  $\text{C}_6\text{N}_{11}\text{H}_{10}\text{SCN} \cdot 2 \text{C}_3\text{N}_3(\text{NH}_2)_3 (2)$ .  
Ellipsoids for non-hydrogen atoms are drawn at the 50 % probability level.

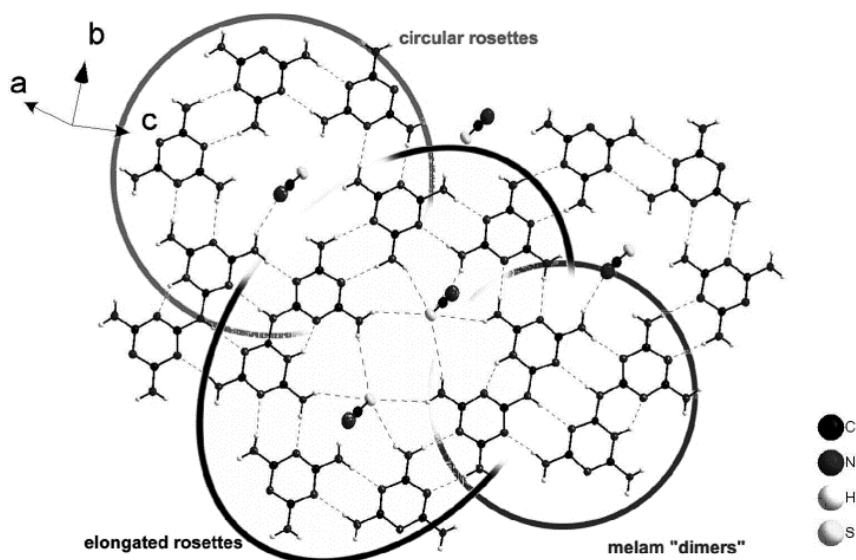


**Figure 5.** Structural motifs observed for the melamium adduct  $\text{C}_6\text{N}_{11}\text{H}_{10}\text{SCN} \cdot 2 \text{C}_3\text{N}_3(\text{NH}_2)_3 (2)$ .

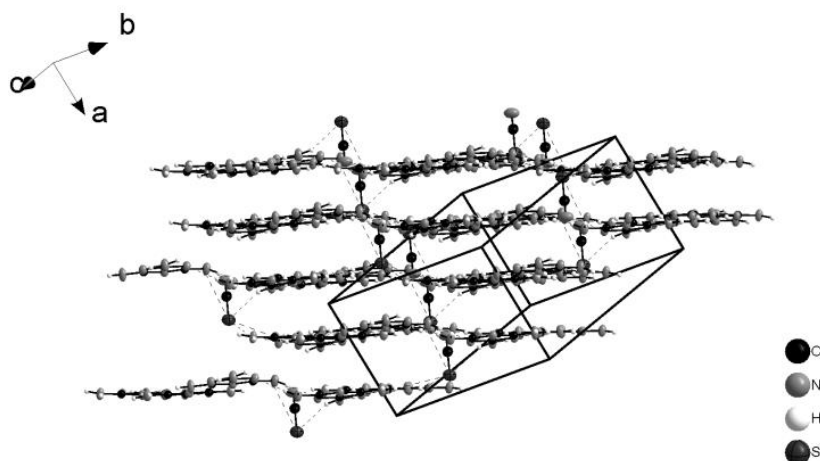


**Figure 6.** Layer-like arrangement of  $C_6N_{11}H_{10}SCN \cdot 2 C_3N_3(NH_2)_3$  (2).

The different layers are only inter-connected by  $SCN^-$  ions since no hydrogen bonding occurs between melamine or melam molecules of different layers (Figure 6). This layer-like assembly is slightly corrugated with  $SCN^-$  ions acting like pillars. The inter-layer distance is around 3.0 to 3.2 Å and thus rather small in comparison to most other C/N/H compounds. Melon has an interlayer spacing of 3.19 Å,<sup>[11]</sup> the interlayer spacing of melem is about 3.27 Å.<sup>[29]</sup> This may possibly be explained in terms of the thiocyanate ion (length = 2.79 Å) acting as fixed length connectors, dragging the layers into close proximity.

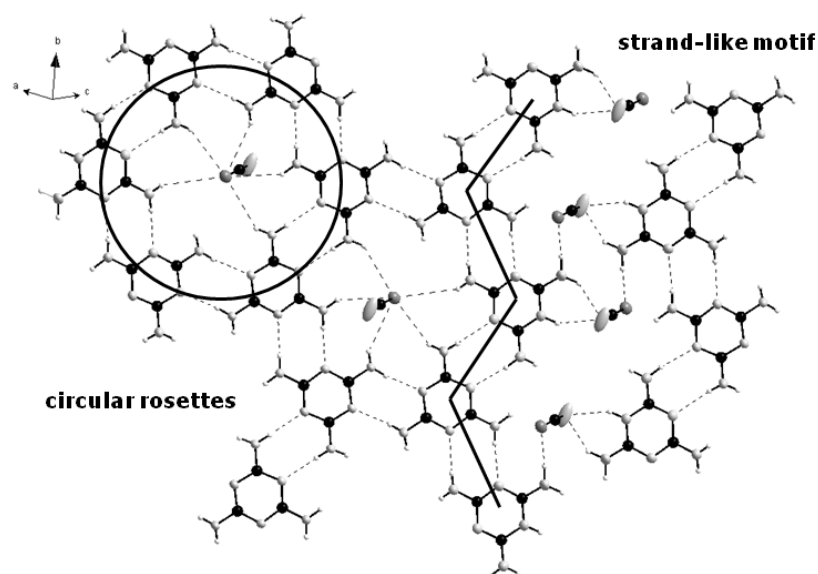


**Figure 7.** Structural motifs observed for the melaminium adduct  $HC_3N_3(NH_2)_3SCN \cdot 2 C_3N_3(NH_2)_3$  (3).

Guanidinium thiocyanate is not directly transformed into the above-mentioned melamium thiocyanate melamine adduct  $C_6N_{11}H_{10}SCN \cdot 2 C_3N_3(NH_2)_3$  (**2**) (Scheme 4). A melaminium thiocyanate melamine adduct with the formula  $HC_3N_3(NH_2)_3SCN \cdot 2 C_3N_3(NH_2)_3$  (**3**) was also found as an intermediate. Though this adduct remains but an intermediary product and ultimately transforms into  $C_6N_{11}H_{10}SCN \cdot 2 C_3N_3(NH_2)_3$  (**2**) at the temperature of its formation, its structure could be elucidated by single-crystal XRD.  $HC_3N_3(NH_2)_3SCN \cdot 2 C_3N_3(NH_2)_3$  (**3**) crystallizes in the triclinic space group  $P \bar{1}$  with two formula units per unit cell. Single protonated melaminium ions are found among neutral melamine molecules and the respective amount of thiocyanate anions. Bond lengths and angles of these molecules and ions are in line with general expectations thus found in  $C_6N_{11}H_{10}SCN \cdot 2 C_3N_3(NH_2)_3$  (**2**). Indeed, several structural features of this compound resemble the findings for the melamium thiocyanate adduct (**2**). The structure is dominated by a layer like arrangement linked by a dense H-bonding network. A rosette-like motif consisting of six melamine molecules is found here as well (Figure 7). The other predominant motif is formed by zigzag strands running along *b*. The thiocyanate ions form hydrogen bridges involving the centers of the rosettes and the middle of the strand-like motif thus serving as both inter- and intra-layer connectors. The resulting stacking pattern of the layers in  $HC_3N_3(NH_2)_3SCN \cdot 2 C_3N_3(NH_2)_3$  (**3**) is reminiscent of  $C_6N_{11}H_{10}SCN \cdot 2 C_3N_3(NH_2)_3$  (**2**). The inter-layer distance is 3.2 Å.

### NMR – investigations

We have conducted a multi-nuclear solid-state NMR investigation of both the melamium adducts  $C_6N_{11}H_{10}Cl \cdot 0.5 NH_4Cl$  (**1**) and  $C_6N_{11}H_{10}SCN \cdot 2 C_3N_3(NH_2)_3$  (**2**). Taking the reported literature data for melam<sup>[20]</sup> and its  $NH_4Cl$  adduct<sup>[23]</sup> as a reference, the melamium ions could readily be identified in both compounds.

The  $^1H$  NMR spectra of both compounds show rather broad signals. Thus individual proton positions could not be resolved. The peaks are found at  $\delta = 6.2$  and 7.2 ppm (shoulder) for  $C_6N_{11}H_{10}Cl \cdot 0.5 NH_4Cl$  (**1**) and at  $\delta = 5.9$  and 7.2 ppm for  $C_6N_{11}H_{10}SCN \cdot 2 C_3N_3(NH_2)_3$  (**2**). For many other protonated C/N compounds, such as

melemium salts, signals at notably higher chemical shifts are usually observed.<sup>[36]</sup> The  $^1\text{H}$  spectra thus suggest a relatively low acidity of the melamium ion  $\text{C}_6\text{N}_{11}\text{H}_{10}^+$  and therefore a correspondingly high basicity of the unprotonated melam. This supports the conclusions drawn from the thermal reactivity of the precursor compounds.

The  $^{13}\text{C}$  NMR spectrum (Figure 8) of  $\text{C}_6\text{N}_{11}\text{H}_{10}\text{Cl} \cdot 0.5 \text{NH}_4\text{Cl}$  (**1**) shows two signals at  $\delta = 162.2$  and  $156.2$  ppm (see Table 2) which is well in line with expectations for triazine based compounds. For the thiocyanate adduct (Figure 9)  $\text{C}_6\text{N}_{11}\text{H}_{10}\text{SCN} \cdot 2 \text{C}_3\text{N}_3(\text{NH}_2)_3$  (**2**) the signals of the carbon atoms within the triazine rings are found between  $\delta = 170$  and  $155$  ppm. Since, according to the structure elucidation, there are a total of 12 respective sites within the asymmetric unit individual atoms could not be resolved and the peaks are rather broad.

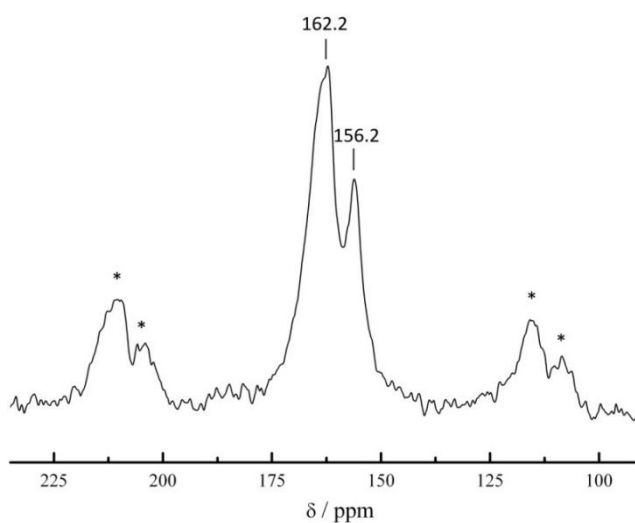


**Figure 8.**  $^{13}\text{C}$  MAS solid-state NMR spectrum for  $\text{C}_6\text{N}_{11}\text{H}_{10}\text{Cl} \cdot 0.5 \text{NH}_4\text{Cl}$  (**1**). Rotational sidebands labeled with \*.

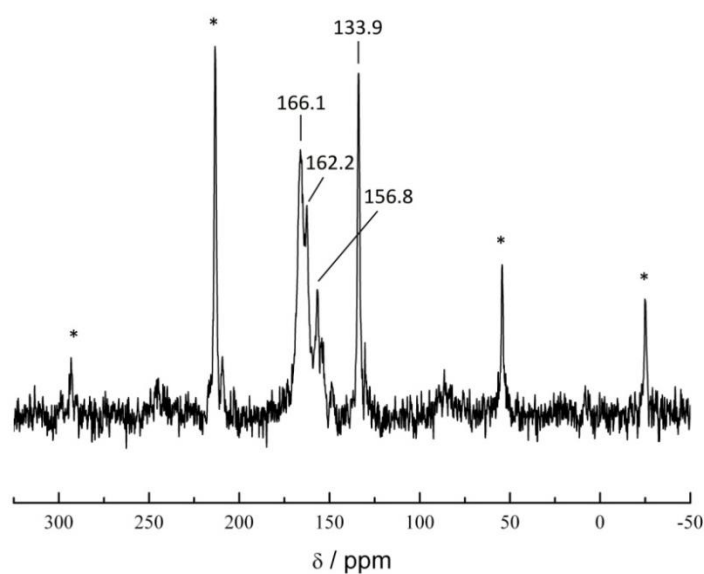
Three peaks are seen at  $\delta = 166.1$ ,  $162.2$  and  $156.8$  ppm. The  $^{13}\text{C}$  NMR signal of the thiocyanate anion is found at  $\delta = 133.9$  ppm (Table 2) which is considered with literature values for thiocyanates.<sup>[37]</sup>

**Table 2.**  $^{13}\text{C}$  NMR: chemical shifts of  $\text{C}_6\text{N}_{11}\text{H}_{10}\text{Cl} \cdot 0.5 \text{NH}_4\text{Cl}$  (1) and  $\text{C}_6\text{N}_{11}\text{H}_{10}\text{SCN} \cdot 2 \text{C}_3\text{N}_3(\text{NH}_2)_3$  (2).

C (located to $-\text{NH}_2$ )	C (located to $-\text{NH}$ )	$\text{SCN}^-$
$\delta = 162.2 \text{ ppm}$ (1)	$\delta = 156.2 \text{ ppm}$ (1)	$\delta = 133.9 \text{ ppm}$ (2)
$\delta = 166.1 \text{ ppm}$ (2)	$\delta = 156.8 \text{ ppm}$ (2)	
$\delta = 162.2 \text{ ppm}$ (2)		

In the  $^{15}\text{N}$  NMR spectrum of  $\text{C}_6\text{N}_{11}\text{H}_{10}\text{Cl} \cdot 0.5 \text{NH}_4\text{Cl}$  (**1**) (Figure 10) seven signals are observed (see Table 3).

The peak at  $\delta = -205.7 \text{ ppm}$  corresponds to the protonated nitrogen of the triazine ring. Those at  $\delta = -252.1$  and  $-261.3 \text{ ppm}$  correspond to  $\text{NH}$  groups. The single signals  $\text{NH}_2$  groups are observed at  $\delta = -285.1$ ,  $-282.8$  and  $-273.6 \text{ ppm}$ . The signal at  $\delta = -341.3 \text{ ppm}$  can be attributed to  $\text{NH}_4^+$ , in line with reported literature values.<sup>[28]</sup>

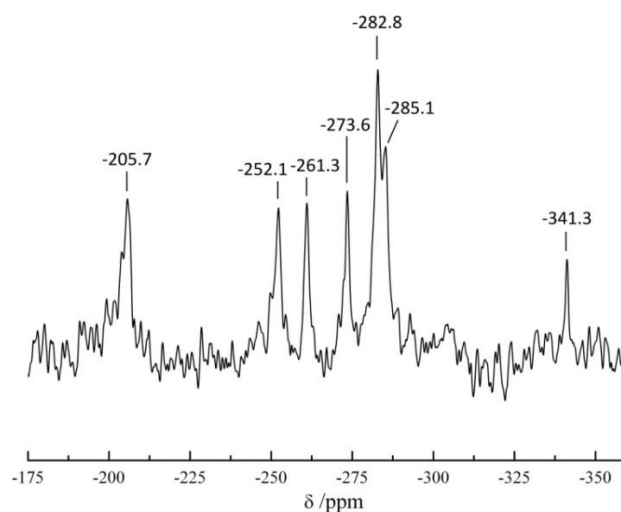


**Figure 9.**  $^{13}\text{C}$  MAS solid state NMR spectrum for  $\text{C}_6\text{N}_{11}\text{H}_{10}\text{SCN} \cdot 2 \text{C}_3\text{N}_3(\text{NH}_2)_3$  (2). Rotational sidebands labeled with \*.

**Table 3.**  $^{15}\text{N}$  NMR: chemical shifts of  $\text{C}_6\text{N}_{11}\text{H}_{10}\text{Cl} \cdot 0.5 \text{NH}_4\text{Cl}$  (**1**).

N (ring, protonated)	-NH	-NH <sub>2</sub>	NH <sub>4</sub> <sup>+</sup>
$\delta = -205.7$ ppm	$\delta = -252.1$ ppm	$\delta = -285.1$ ppm	$\delta = -341.3$ ppm
	$\delta = -261.3$ ppm	$\delta = -282.8$ ppm	
		$\delta = -273.6$ ppm	

Though it was impossible to record a well resolved  $^{15}\text{N}$  NMR spectrum of  $\text{C}_6\text{N}_{11}\text{H}_{10}\text{SCN} \cdot 2 \text{C}_3\text{N}_3(\text{NH}_2)_3$  (**2**) in this study, key spectral features of the adduct could nevertheless be identified. The resonance of the  $\text{SCN}^-$  ion<sup>[37]</sup> was found at  $\delta = -346$  ppm and the peaks of the  $\text{NH}_2$  groups of the melamium ion were observed at  $\delta = -206.8$  ppm and  $171.4$  ppm. Although the other atoms could not be resolved the reported finding confirmed the nature of this compound as a  $\text{SCN}^-$  salt.

**Figure 10.**  $^{15}\text{N}$  MAS solid state NMR spectrum for  $\text{C}_6\text{N}_{11}\text{H}_{10}\text{Cl} \cdot 0.5 \text{NH}_4\text{Cl}$  (**1**). Rotational sidebands labeled with \*.

### 3.1.3. Conclusion

Adjusting structures and properties of carbon nitride-type materials is becoming increasingly important and precursor pyrolysis is the only established route for the synthesis of this class of materials. Hence, controlling the condensation process from the precursor side is an especially important issue. By studying novel precursor compounds leading to new products the understanding of the thermal condensation of carbon nitride-type materials could be advanced.

When  $\text{NH}_4\text{Cl}$  is added to melamine the usual thermal reactivity of the latter is drastically altered. The melamium adduct  $\text{C}_6\text{N}_{11}\text{H}_{10}\text{Cl} \cdot 0.5 \text{NH}_4\text{Cl}$  (**1**) is formed instead of melam in this case.

Based on our experimental observations, thiourea can be considered a very interesting precursor for carbon nitride type materials. Substitution of ammonium thiocyanate with thiourea can be widely recommended. Two new thiocyanate containing adduct phases could thereby be prepared. The initial condensation step of thiourea leads to the formation of guanidinium thiocyanate. The next condensation step affords melamine which is found as an intermediate adduct with the formula  $\text{HC}_3\text{N}_3(\text{NH}_2)_3\text{SCN} \cdot 2 \text{C}_3\text{N}_3(\text{NH}_2)_3$  (**3**). The stable reaction product is  $\text{C}_6\text{N}_{11}\text{H}_{10}\text{SCN} \cdot 2 \text{C}_3\text{N}_3(\text{NH}_2)_3$  (**2**), the first example of a melamium melamine adduct to be structurally investigated. This shows that there is a vast potential for additional adduct phases involving various C/N/H molecules.

Single-crystal structural investigations of melamium salts grown from solution have already been described in the literature.<sup>[23]</sup> Whereas disorder involving the proton positions was observed in those studies, the melamium ions found in  $\text{C}_6\text{N}_{11}\text{H}_{10}\text{Cl} \cdot 0.5 \text{NH}_4\text{Cl}$  (**1**) and  $\text{C}_6\text{N}_{11}\text{H}_{10}\text{SCN} \cdot 2 \text{C}_3\text{N}_3(\text{NH}_2)_3$  (**2**) allow unambiguous proton localization. Only melam and not melamine is protonated in the two compounds  $\text{C}_6\text{N}_{11}\text{H}_{10}\text{Cl} \cdot 0.5 \text{NH}_4\text{Cl}$  (**1**) and  $\text{C}_6\text{N}_{11}\text{H}_{10}\text{SCN} \cdot 2 \text{C}_3\text{N}_3(\text{NH}_2)_3$  (**2**). This illustrates that melam is more basic than melamine (melamine being more basic than melam). This effect can be explained in terms of the formation of a favorable intramolecular hydrogen bridge as observed in the  $\text{C}_6\text{N}_{11}\text{H}_{10}^+$  ion.

The formation of melam can thus be promoted by Brønsted acids. This acid is  $\text{NH}_4\text{Cl}$  for  $\text{C}_6\text{N}_{11}\text{H}_{10}\text{Cl} \cdot 0.5 \text{NH}_4\text{Cl}$  (**1**). In the case of  $\text{C}_6\text{N}_{11}\text{H}_{10}\text{SCN} \cdot 2 \text{C}_3\text{N}_3(\text{NH}_2)_3$  (**2**) the respective acid is HSCN. HSCN which is formed by the degradation of thiourea used as starting material.

**Table 4.** Crystallographic data for the reported compounds.

Formula	$\text{C}_6\text{N}_{11}\text{H}_{10}\text{Cl} \cdot 0.5 \text{NH}_4\text{Cl}$ (1)	$\text{C}_6\text{N}_{11}\text{H}_{10}\text{SCN} \cdot 2 \text{C}_3\text{N}_3(\text{NH}_2)_3$ (2)	$\text{HC}_3\text{N}_3(\text{NH}_2)_3\text{SCN} \cdot 2 \text{C}_3\text{N}_3(\text{NH}_2)_3$ (3)
Formula weight / g mol <sup>-1</sup>	298.45	546.61	437.51
Crystal system	triclinic	triclinic	triclinic
Space group	$P \bar{1}$ (no. 2)	$P \bar{1}$ (no. 2)	$P \bar{1}$ (no. 2)
Lattice parameters / Å, °	$a = 6.7785(14)$	$a = 7.8625(16)$	$a = 7.9766(16)$
	$b = 7.7528(16)$	$b = 10.237(2)$	$b = 10.551(2)$
	$c = 12.182(2)$	$c = 14.519(3)$	$c = 11.353(2)$
	$\alpha = 98.94(3)$	$\alpha = 91.92(3)$	$\alpha = 86.67(3)$
	$\beta = 103.23(3)$	$\beta = 91.61(3)$	$\beta = 74.86(3)$
Volume / Å <sup>3</sup>	$\gamma = 93.33(3)$	$\gamma = 112.26(3)$	$\gamma = 86.04(3)$
	591.6(2)	1118.4(4)	919.3(3)
Z	2	2	2
Diffractometer	IPDS	Kappa-CCD	Kappa-CCD
Temperature / K	140	200	193(2)
Data / restraints / parameters	3144 / 19 / 228	4134 / 0 / 411	4011 / 0 / 347
R-indices	$R_1 = 0.0587$ all data	$R_1 = 0.0840$ all data	$R_1 = 0.0812$ all data
	$R_1 = 0.0516 F_0^2 > 2\sigma(F_0^2)$ (2539 reflections)	$R_1 = 0.0528 F_0^2 > 2\sigma(F_0^2)$ (2843 reflections)	$R_1 = 0.0660 F_0^2 > 2\sigma(F_0^2)$ (3178 reflections)
	$wR_2 = 0.1436$ all data	$wR_2 = 0.1356$ all data	$wR_2 = 0.2026$ all data
GooF	$wR_2 = 0.1398 F_0^2 > 2\sigma(F_0^2)$	$wR_2 = 0.1227 F_0^2 > 2\sigma(F_0^2)$	$wR_2 = 0.1945 F_0^2 > 2\sigma(F_0^2)$
	1.000 (0.997 for 19 restraints)	0.995	1.075
Weighting scheme [a]	$w^{-1} = \sigma^2(F_0^2) + (0.1153P)^2$	$w^{-1} = \sigma^2(F_0^2) + (0.0707P)^2$	$w^{-1} = \sigma^2(F_0^2) + (0.1065P)^2 + 0.8359P$
Largest peak deepest hole / e Å <sup>-3</sup>	0.355 / -0.497	0.349 / -0.326	0.832 / -0.368

[a]  $P = (F_0^2 + 2F_c^2)/3$ .

### 3.1.4. Experimental Section

**Synthesis: Preparation of  $[\text{C}_6\text{N}_{11}\text{H}_{10}]\text{Cl} \cdot 0.5 \text{NH}_4\text{Cl}$  (1):** A dried glass ampoule (outer diameter: 16 mm, inner diameter: 12 mm) was charged with melamine (99%, Fluka,) (390 mg, 3.1 mmol) and ammonium chloride ( $\geq 99\%$ , Fluka) (110 mg, 2.1 mmol). The ampoule was sealed under argon at a length of about 120 mm and heated to 450 °C at a rate of 2 °C  $\text{m}^{-1}$ . After 24 h the ampoule was slowly cooled (1 °C  $\text{min}^{-1}$ ) to room temperature. After the ampoule was opened, a smell of ammonia was detected. The product (150 mg, 0.25 mmol, 5 %) was recovered as a colorless solid from both the cooler and warmer parts of the ampoule, and was identified by X-ray powder diffractometry. Elemental analysis (wt.-%): N 52.48 (calcd. 53.98), C 24.16 (calcd. 24.15), H 4.0 (calcd. 4.05), Cl 20.60 (calcd. 17.82), deviation of composition from theory may be due to presence of amorphous side phases. IR:  $\tilde{\nu} = 791$  (m), 1270 (vs), 1419 (m), 1634 (m), 3116 (w), 3314  $\text{cm}^{-1}$  (w).

**Preparation of  $[\text{C}_6\text{N}_{11}\text{H}_{10}]\text{SCN} \cdot 2 \text{C}_3\text{N}_3(\text{NH}_2)_3$  (2):** A dried glass ampoule (outer diameter: 10 mm, inner diameter: 7 mm) was charged with thiourea (99%, Grüssing) (150 mg, 2.0 mmol). The ampoule was sealed under argon at a length of about 120 mm and heated to 400 °C at a rate of 2 °C  $\text{m}^{-1}$ . After 24 h the ampoule was slowly cooled (1 °C  $\text{min}^{-1}$ ) to room temperature. After opening the ampoule the product was dried under vacuum for 5 h. The product (60 mg, 0.11 mmol, 5.5 %) was recovered as a light green powder in the warmer part of the ampoule, and was identified by X-ray powder diffractometry. Elemental analysis (wt.-%): N 56.47 (calcd. 61.51), C 25.86 (calcd. 28.57), H 3.91 (calcd. 4.06), S 10.51 (calcd. 5.87), deviation of composition from theory may be due to presence of amorphous side phases. IR:  $\tilde{\nu} = 797$  (m), 1415 (m), 1641 (m), 2059 (v), 3147 (w), 3331  $\text{cm}^{-1}$  (w).

**Preparation of  $[\text{C}_3\text{N}_6\text{H}_7]\text{SCN} \cdot 2 \text{C}_3\text{N}_3(\text{NH}_2)_3$  (3):** A dried glass ampoule (outer diameter: 16 mm, inner diameter: 12 mm) was charged with thiourea (99%, Grüssing) (200 mg, 2.6 mmol).

The ampoule was sealed under vacuum at a length of about 120 mm and heated to 300 °C at a rate of 2 °C  $\text{min}^{-1}$ . After 24 h the ampoule was slowly cooled (1 °C  $\text{min}^{-1}$ )

to room temperature. A single crystal of  $[\text{C}_3\text{N}_6\text{H}_7]\text{SCN} \cdot 2 \text{C}_3\text{N}_3(\text{NH}_2)_3$  (**3**) was isolated from the product which was recovered in a total yield of 56 mg as a colorless inhomogeneous solid in the warmer part of the ampoule.

**Structure determination:** Single crystal XRD data were measured on a STOE IPDS and a Kappa CCD diffractometer using Mo- $K_\alpha$  radiation ( $\lambda = 71.073$  pm) in all cases. The crystal structures were solved by direct methods (SHELXS-97) and refined against  $F^2$  on all data by full-matrix least-squares (SHELXL-97).<sup>[38]</sup> Lorentz and polarization corrections were applied for all structures. SCALEPACK correction was applied to the Kappa CCD data.

Crystallographic data are summarized in Table 4. CCDC-821352, CCDC-821353 and CCDC-821354 contain the supplementary crystallographic data for this paper. These data can be obtained free of charge from The Cambridge Crystallographic Data Centre via [www.ccdc.cam.ac.uk/data\\_request/cif](http://www.ccdc.cam.ac.uk/data_request/cif). The crystals of  $\text{C}_6\text{N}_{11}\text{H}_{10}\text{Cl} \cdot 0.5 \text{NH}_4\text{Cl}$  (**1**) show an inherent tendency for twinning. Although the twinning is non-merohedral, it was not possible to select a single individual. The crystal examined in the present structural investigation consisted of a total of three individuals. With the largest of them accounting for almost 90 % of the diffraction intensity, the sizes of these individuals were very different. Only non-overlapping reflections of the largest individual were used during the structure elucidation, all other data were discarded. However, this method resulted in a rather low overall completeness of the dataset. The incompleteness of the data is mainly due to the fact that the software allowing data separation was only available on the IPDS diffractometer. Thus the triclinic crystal had to be measured using  $\phi$ -scans only. The actual data separation only caused a minor loss of data, as the other individuals were rather weak

**X-ray powder diffraction** patterns (PXRD) were recorded on a Huber G670 Guinier Imaging Plate. Measurements were conducted using monochromatic Cu- $K_\alpha$  radiation at room temperature. Theoretical powder diffraction patterns were simulated from single-crystal data using the Win XPOW software package.<sup>[39]</sup>

**Solid-state NMR** spectra were recorded at room temperature on a DSX 500 Avance (Bruker) FT-NMR spectrometer with an external magnetic field of 11.4 T. Magic angle spinning (MAS) spectra were recorded using double resonance probes (Bruker) operated with 2.5 mm ( $^1\text{H}$ ) and 4.0 mm ( $^{13}\text{C}$ ,  $^{15}\text{N}$ )  $\text{ZrO}_2$  rotors.

The rotation frequencies were 6-10 kHz ( $^{15}\text{N}$ ,  $^{13}\text{C}$ ) or 10 kHz ( $^1\text{H}$ ). Cross-polarization (CP) experiments were used for  $^{15}\text{N}$  and  $^{13}\text{C}$  measurements. Chemical shifts are referenced with respect to TMS ( $^1\text{H}$ ,  $^{13}\text{C}$ ) and nitromethane ( $^{15}\text{N}$ ) as external standards. Additional data for the individual experiments is given in the captions of the respective figures.

**Elemental analysis:** The elements **H, C, N and S** were determined by combustion analysis at the micro-analytical laboratory of the Department of Chemistry, LMU Munich, using a ele vario EL (Elementar) elemental analyzer. Analyses of sulfur-containing samples were conducted using vario micro cubes.

**Fourier-transformed infra-red (FTIR) spectra** were recorded in reflection geometry on a Spektrum BX II FTIR spectrometer (Perkin Elmer) equipped with a DuraSampler diamond ATR (attenuated total reflectance) unit. All spectra were corrected of baseline and ATR specific effects. All measurements involving IR spectroscopy were conducted at room temperature. Signal shapes and intensities of the signals are addressed using the following abbreviations: s = strong, m = medium, w = weak, vw = very weak, br = broad, vbr = very broad, sh = shoulder.

### **Acknowledgements**

The authors would like to thank Thomas Miller and Peter Mayer (both Department Chemie, LMU München) for collecting the X-ray diffraction data. Financial support by the Deutsche Forschungsgemeinschaft DFG (project SCHN 377/12) as well as the Fonds der Chemischen Industrie (FCI) is gratefully acknowledged.

### 3.1.5. Bibliography

- [1] R. P. Subrayan, P. G. Rasmussen, *Trends Polym. Sci.* **1995**, *3*, 165.
- [2] Z. B. Zhou, R. Q. Cui, Q. J. Pang, G. M. Hadi, Z. M. Ding, W. Y. Li, *Solar Energy Mater. Solar Cells* **2002**, *70*, 487.
- [3] a) F. Goettmann, A. Fischer, M. Antonietti, A. Thomas, *Angew. Chem.* **2006**, *118*, 4579; *Angew. Chem. Int. Ed.* **2006**, *45*, 4467; b) F. Goettmann, A. Thomas, M. Antonietti, *Angew. Chem.* **2007**, *119*, 2773; *Angew. Chem. Int. Ed.* **2007**, *46*, 2717.
- [4] D. M. Teter, R. J. Hemley, *Science* **1996**, *271*, 53.
- [5] a) A. Y. Liu, M. L. Cohen, *Science* **1989**, *245*, 841; b) A. Y. Liu, M. L. Cohen, *Phys. Rev. B* **1990**, *41*, 10727; c) A. Y. Liu, R. M. Wentzcovitch, *Phys. Rev. B* **1994**, *50*, 10362.
- [6] A. Thomas, A. Fischer, F. Goettmann, M. Antonietti, J.-O. Müller, R. Schlögl, J. M. Carlsson, *J. Mater. Chem.* **2008**, *18*, 4893.
- [7] a) F. Goettmann, A. Fischer, M. Antonietti, A. Thomas, *Chem. Commun.* **2006**, 450; b) F. Goettmann, A. Fischer, M. Antonietti, A. Thomas, *New. J. Chem.* **2007**, *31*, 1455.
- [8] X. Wang, K. Maeda, A. Thomas, K. Takanabe, G. Xin, J.M Carlsson, K. Domen, M. Antonietti, *Nat. Mater.* **2009**, *8*, 76.
- [9] P. Kuhn, A. Thomas, M. Antonietti, *Macromolecules* **2009**, *42*, 319.
- [10] P. Kuhn, A. Forget, D. Su, A. Thomas, M. Antonietti, *J. Am. Chem. Soc.* **2008**, *130*, 13333.
- [11] B. V. Lotsch, M. Döblinger, J. Sehnert, L. Seyfarth, J. Senker, O. Oeckler, W. Schnick, *Chem. Eur. J.* **2007**, *13*, 4969.
- [12] M. Döblinger, B. V. Lotsch, J. Wack, J. Thun, J. Senker, W. Schnick, *Chem. Commun.* **2009**, 1541.

- [13] a) C. L. Schmidt, M. Jansen, *J. Mater. Chem.* **2010**, *20*, 4183; b) C. L. Schmidt, M. Jansen, *J. Mater. Chem.* **2010**, *20*, 110.
- [14] a) D. R. Miller, D. C. Swenson, E. G. Gillan, *J. Am. Chem. Soc.* **2004**, *126*, 5372; b) D. R. Miller, J. R. Holst, E. G. Gillan, *Inorg. Chem.* **2007**, *46*, 2767.
- [15] a) S. Tragl, K. Gibson, H.-J. Meyer, *Z. Anorg. Allg. Chem.* **2004**, *630*, 2373; b) S. Tragl, K. Gibson, J. Glaser, G. Heydenrych, G. Frenking, V. Duppel, A. Simon, H.-J. Meyer, *Z. Anorg. Allg. Chem.* **2008**, *634*, 2754; c) S. Tragl; K. Gibson, J. Glaser, V. Duppel, A. Simon, H.-J. Meyer, *Solid State Commun.* **2007**, *141*, 529.
- [16] J. Stenzel, W. Sundermeyer, *Chem. Ber.* **1967**, *100*, 3368; b) W. Sundermeyer, *Z. Anorg. Allg. Chem.* **1962**, *313*, 290; c) W. Sundermeyer, *Angew. Chem.* **1965**, *77*, 241; *Angew. Chem. Int. Ed.* **1965**, *4*, 222.
- [17] J. Liebig, *Ann. Chem. Pharm.* **1834**, *10*, 1.
- [18] J. Klason, *J. Prakt. Chem.* **1886**, *33*, 285.
- [19] A. I. Finkel'shtein, N. V. Spiridoova, *Russ. Chem. Rev.* **1964**, *33*, 400.
- [20] B. V. Lotsch, W. Schnick, *Chem. Eur. J.* **2007**, *13*, 4956.
- [21] A. Sattler, S. Pagano, M. Zeuner, A. Zurawski, D. Gunzelmann, J. Senker, K. Müller-Buschbaum, W. Schnick, *Chem. Eur. J.* **2009**, *15*, 13161.
- [22] N. K. Garvrilva, V. A. Gal'perin, A. I. Finkel'shtein, A. G. Koryakin, *Russ. J. Org. Chem.* **1977**, *13*, 616.
- [23] B. Jürgens, *Molekulare Vorstufen zur Synthese grafitischen Kohlenstoff(IV) - nitrids: Von Dicyanamiden über Tricyanomelamine zu Melem*, PhD Thesis, Universität München, Shaker Verlag, Aachen, **2004**.
- [24] L. Costa, G. Camino, G. Martinasso, *Polym. Prepr. Am. Chem. Soc. Div. Polym. Chem.* **1989**, *30*, 531.
- [25] B.V. Lotsch, J. Senker, W. Kockelmann, W. Schnick, *J. Solid State Chem.* **2003**, *176*, 180.

- [26] T. Steiner, *Angew. Chem.* **2002**, *114*, 50; *Angew. Chem. Int. Ed.* **2002**, *41*, 48.
- [27] J. N. Varghese, A. O'Connor, E.N. Malsen, *Acta Crystallogr.* **1977**, *B33*, 2102.
- [28] A. Nag, B. V. Lotsch, J. Schmedt auf der Günne, O. Oeckler, P.J. Schmidt, W. Schnick, *Chem. Eur. J.* **2007**, *13*, 3512.
- [29] B. Jürgens, E. Irran, J. Senker, P. Kroll, H. Müller, W. Schnick, *J. Am. Chem. Soc.* **2003**, *125*, 10288.
- [30] *Gmelins Handbuch der Anorganischen Chemie*, Vol. D6, 8.Aufl., Berlin, Heidelberg, New York, **1978**, 91.
- [31] a) W. Klemt, *Chem. Tech.* **1942**, *15*, 1; b) S. Kodama, S. Kukushima, S. Nose, J. Nakajima, *J. Chem. Soc. Japan Ind. Chem Sect.* **1953**, *56*, 1; c) T. Yanagimoto, *Rev. Phys. Chem. Japan* **1954**, *24*, 1.
- [32] H. Krall, *J. Chem. Soc., Trans.* **1913**, *103*, 1378.
- [33] B. A. Tadatomo, S.Choichiro, H. Shuhei, *J. Chem. Soc. Japan* **1970**, *73*, 2619.
- [34] J. Madarász, G. Pokol, *J. Therm. Anal. Calorim.* **2007**, *88*, 329.
- [35] A. Sattler, L. Seyfarth, J. Senker, W. Schnick, *Z. Anorg. Allg. Chem.* **2005**, *631*, 2545.
- [36] R. M. Dickson, M. S. McKinnon, J. F. Britten, R. E. Wasylshen, *Can. J. Chem.* **1987**, *65*, 941.
- [37] a) G. M. Sheldrick, *Acta Crystallogr., Sect. A*, **2008**, *64*, 112; b) G. M. Sheldrick, *SHELX-97, Program package for the solution and refinement of crystal structures*, Release 97-2, Universität Göttingen, **1997**.
- [38] *Win XPOW*, v2.12, STOE & Cie GmbH, Darmstadt, **2005**.

### 3.2. New Heptazine Based Materials with a Divalent Cation – $\text{Sr}[\text{H}_2\text{C}_6\text{N}_7\text{O}_3]_2 \cdot 4 \text{H}_2\text{O}$ and $\text{Sr}[\text{HC}_6\text{N}_7(\text{NCN})_3] \cdot 7 \text{H}_2\text{O}$

Nicole E. Braml and Wolfgang Schnick

published in: *Z. Anorg. Allg. Chem.* **2013**, 639, 275

DOI: 10.1002/zaac.201200345

Copyright © 2014 WILEY-VCH

<http://onlinelibrary.wiley.com/doi/10.1002/zaac.201200345/abstract>

**Keywords:** heptazine · cyamelurate · crystal structure · strontium

**Abstract.** The new heptazine based compounds  $\text{Sr}[\text{H}_2\text{C}_6\text{N}_7\text{O}_3]_2 \cdot 4 \text{H}_2\text{O}$  and  $\text{Sr}[\text{HC}_6\text{N}_7(\text{NCN})_3] \cdot 7 \text{H}_2\text{O}$  have been synthesized by metathesis reaction in aqueous solution. Crystal structures were studied by single-crystal X-ray diffraction and Rietveld refinement. Strontium cyamelurate tetrahydrate exhibits distorted zigzag strands embedding  $\text{Sr}^{2+}$  ions surrounded by crystal water molecules (*Fdd2*,  $a = 1194.0(17)$ ,  $b = 6358.14(97)$ ,  $c = 602.73(89)$  pm,  $Z = 8$ ,  $\text{GOF} = 1.034$ ,  $R_p = 0.033$ ,  $wR_p = 0.043$ ,  $R_B = 0.84$ ). Strontium melonate heptahydrate crystallizes in a layer-like structure characteristic for heptazine based compounds (*P1*,  $a = 660.76(13)$ ,  $b = 1080.7(2)$ ,  $c = 1353.8(3)$  pm,  $\alpha = 101.67(3)$ ,  $\beta = 101.40(3)$ ,  $\gamma = 94.60(3)^\circ$ ,  $Z = 2$ ,  $R_1 = 0.032$ ,  $wR_2 = 0.072$ ). Additionally, the thermal behavior has been studied by DTA/TG measurements and FTIR spectroscopy data are presented.

### 3.2.1. Introduction

The first carbon nitride type materials have been studied in the middle of the 18<sup>th</sup> century by Liebig.<sup>[1]</sup> Since that time C/N/(H) compounds have gained increasing relevance in the literature and in modern materials chemistry.<sup>[2,3]</sup>

One of the most intriguing aspects was the quest for  $sp^3$ -hybridized  $C_3N_4$  as ultrahard material which initiated the revival for the interest in carbon nitride type materials in the 1980s.<sup>[3-6]</sup> The existence and nature of ultrahard  $C_3N_4$  still remains elusive, however synthesis and materials properties of graphitic carbon nitride type materials have gained increasing importance instead. Recent work is dealing with applications of compounds like melon  $[C_6N_7(NH_2)(NH)]_n$  as semiconductor<sup>[7]</sup> or with related compounds as suitable metal free catalysts for  $CO_2$  fixation or hydrogen production from water.<sup>[8,9]</sup>

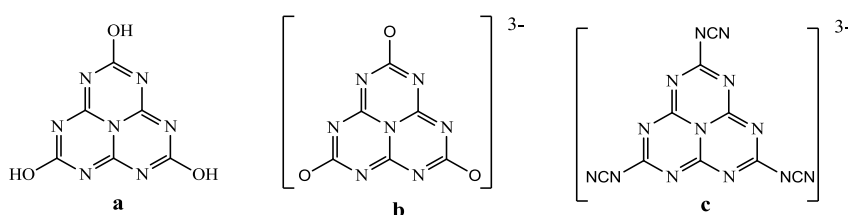


**Figure 1.** a cyameluric acid, b cyamelurate, c melonate.

Molecular, oligomeric and polymeric C/N/(H) materials exhibit a large structural variety. During the last decades a number of precursors have been described which, upon thermal treatment, are supposed to form polymeric carbon nitride type materials.

The first heptazine based C/N/(O)/(H) compound which has been structurally elucidated was cyameluric acid  $H_3C_6N_7O_3$  (see Figure 1), first mentioned by *Henneberg* in 1850.<sup>[10]</sup> Its structure has been investigated in the literature for several times.<sup>[11,12]</sup> Subsequently, a number of deriving alkali salts have been reported.<sup>[13]</sup> Quite recently, the first metal(II) cyamelurates have been characterized. Due to their preparation in aqueous ammonia these Cu, Zn and Ca salts include additional  $NH_3$  or  $NH_4^+$  groups.<sup>[14]</sup>

Another important heptazine based molecular ion is melonate comprising the anion  $[\text{C}_6\text{N}_7(\text{NCN})_3]^{3-}$  (see Figure 1), which was already mentioned by *Gmelin*,<sup>[15]</sup> *Pauling* and *Sturdivant*.<sup>[16]</sup> The first structural elucidation of potassium melonate pentahydrate has been published by *Kroke et al.*,<sup>[17]</sup> subsequently, anhydrous potassium melonate was characterized by *Sattler et al.*<sup>[18]</sup> Since then, various alkali melonate salts,<sup>[19]</sup> including monoprotonated bivalent melonate salts have been studied as well.<sup>[20]</sup>

In this contribution we describe both a new Sr-containing cyamelurate, namely  $\text{Sr}[\text{H}_2\text{C}_6\text{N}_7\text{O}_3]_2 \cdot 4 \text{H}_2\text{O}$ , and a melonate,  $\text{Sr}[\text{HC}_6\text{N}_7(\text{NCN})_3] \cdot 7 \text{H}_2\text{O}$ . Their structural properties and thermal behavior is discussed.

### 3.2.2. Results and Discussion

Our aim was the preparation of new cyamelurate salts with divalent cations (preferentially  $\text{Sr}^{2+}$ ) avoiding incorporation of  $\text{NH}_3$  or  $\text{NH}_4^+$  ligands. To this end recrystallization from acidified water has been chosen. This approach has already been used for synthesis of monoprotonated alkaline earth melonates,<sup>[20]</sup> and has now led to a new diprotonated Sr salt.

Strontium cyamelurate tetrahydrate,  $\text{Sr}[\text{H}_2\text{C}_6\text{N}_7\text{O}_3]_2 \cdot 4 \text{H}_2\text{O}$ , was synthesized by metathesis reaction of potassium cyamelurate with strontium chloride. After filtration, strontium cyamelurate was recrystallized from aqueous solution acidified by HCl.

#### Crystal structure of $\text{Sr}[\text{H}_2\text{C}_6\text{N}_7\text{O}_3]_2 \cdot 4 \text{H}_2\text{O}$

Strontium cyamelurate tetrahydrate crystallizes in the orthorhombic space group *Fdd2*. The product was obtained as thin microcrystalline platelets whose crystal quality was sufficient for single-crystal X-ray diffraction solution but not for refinement. However, the high microcrystallinity of the product allowed for Rietveld refinement by using the starting parameters obtained from single-crystal data. Experimental and calculated powder patterns agree well in position and intensity (see Figure 2).

Details regarding the data collection and refinement are summarized in Table 1.

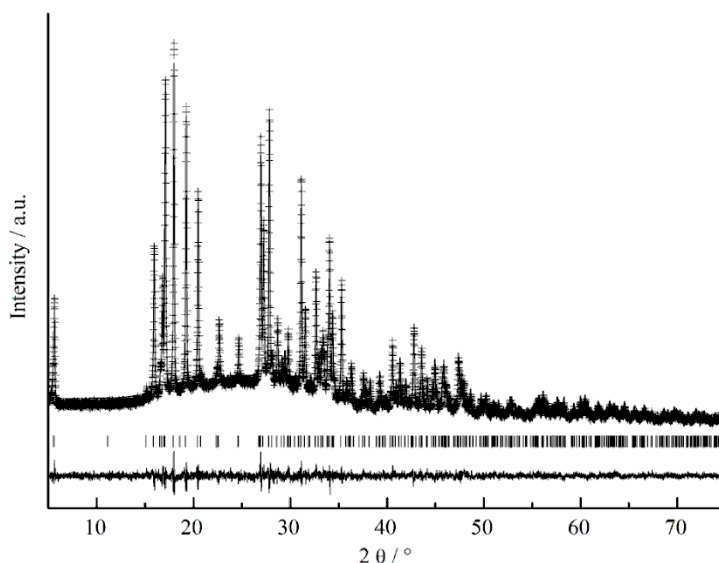


**Figure 2.** Rietveld refinement of X-ray diffraction data for  $\text{Sr}[\text{H}_2\text{C}_6\text{N}_7\text{O}_3]_2 \cdot 4 \text{H}_2\text{O}$ . Measured data are indicated by crosses, refined data and reference profile are given by solid lines. Bragg peaks are indicated as vertical bars.

The asymmetric unit comprises one diprotonated cyamelurate ion, one  $\text{Sr}^{2+}$  and four crystal water molecules.

The geometry of the planar hydrogencyamelurate ion found in strontium cyamelurate tetrahydrate is very similar with the respective anion found in the Zn compound  $(\text{NH}_4)_2[\text{Zn}(\text{H}_2\text{O})_6](\text{HC}_6\text{N}_7\text{O}_3)_2 \cdot \text{H}_2\text{O}$ .<sup>[14]</sup> Its bond lengths and angles agree well with other heptazine based compounds.<sup>[14,20]</sup>

In contrast to known cyamelurates<sup>[14]</sup> or melonates<sup>[20]</sup> with divalent cations, whose anions are typically arranged in parallel strands connected by hydrogen bonds, parallel distorted zigzag strands running along *b* are found in  $\text{Sr}[\text{H}_2\text{C}_6\text{N}_7\text{O}_3]_2 \cdot 4 \text{H}_2\text{O}$  (see Figure 3). The interlayer distance is 296 pm. This value is rather small in comparison to most other C/N/H compounds, like melon which has an interlayer spacing of 319 pm<sup>[21]</sup> or melem which interlayer distance is about 327 pm.<sup>[22]</sup>

**Table 1.** Crystallographic data of the Rietfeld refinement of  $\text{Sr}[\text{H}_2\text{C}_6\text{N}_7\text{O}_3]_2 \cdot 4 \text{H}_2\text{O}$ .

<b><math>\text{Sr}[\text{H}_2\text{C}_6\text{N}_7\text{O}_3]_2 \cdot 4 \text{H}_2\text{O}</math></b>	
Formula mass /g mol <sup>-1</sup>	651.88
space group	<i>Fdd2</i> (no. 43)
T [K]	293
diffractometer	Stoe STADI P
Radiation, $\lambda$ / pm	Cu-K $\alpha_1$ , 154.06
<i>a</i> / pm	1194.000(17)
<i>b</i> / pm	6358.140(97)
<i>c</i> / pm	602.7278(89)
<i>V</i> / 10 <sup>6</sup> pm <sup>3</sup>	4575.68(12)
<i>Z</i>	8
Calculated density / g·cm <sup>-1</sup>	1.893
Diffraction range [°]	5 ≤ 2 $\theta$ ≤ 75
No. data points	7000
Observed reflections	349
Independent parameters	111
GOF	1.034
R-indices (all data) [%]	$R_p = 0.033$ , $wR_p = 0.042$ , $R_B = 0.8396$

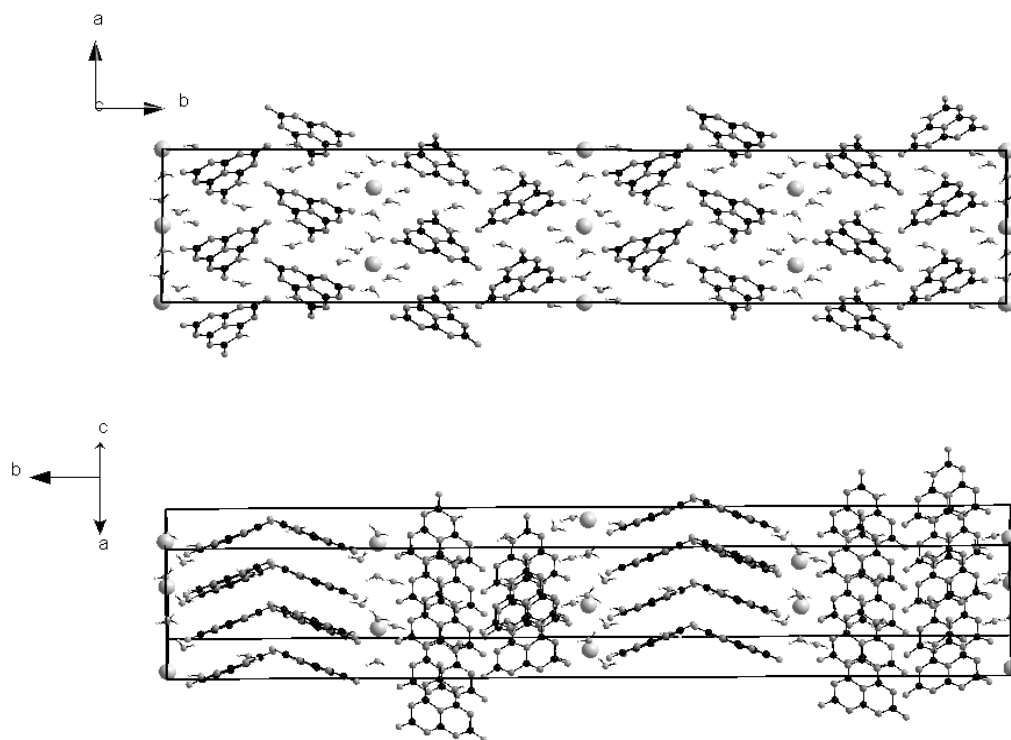


**Figure 3.** Layer arrangement of  $\text{Sr}[\text{H}_2\text{C}_6\text{N}_7\text{O}_3]_2 \cdot 4 \text{H}_2\text{O}$  (top), layer rotated about  $90^\circ$  (bottom).

Within the strands  $\text{Sr}^{2+}$  is located between the anions (see Figure 3). Six crystal water molecules and two O atoms of the dihydrogencyamelurate ion coordinate the metal ions (see Figure 4). The distances Sr-O are in the range of the sum of the respective ionic radii.<sup>[23]</sup>

Additionally, one crystal water molecule without any coordinative function is arranged between the layers.

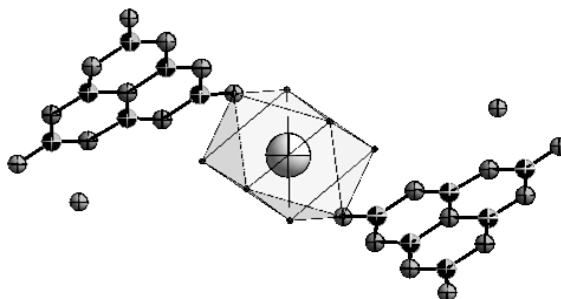


**Figure 4.** Representation of one formula unit and coordination of  $\text{Sr}^{2+}$  by oxygen in  $\text{Sr}[\text{H}_2\text{C}_6\text{N}_7\text{O}_3]_2 \cdot 4 \text{H}_2\text{O}$ .

### Thermal Behavior

DTA and TG curves of  $\text{Sr}[\text{H}_2\text{C}_6\text{N}_7\text{O}_3]_2 \cdot 4 \text{H}_2\text{O}$  are represented in Figure 5. The broad endothermic signal between 90 and 210 °C can be attributed to dehydration. The continuous mass loss starting at 400 °C indicates thermal decomposition of the sample.

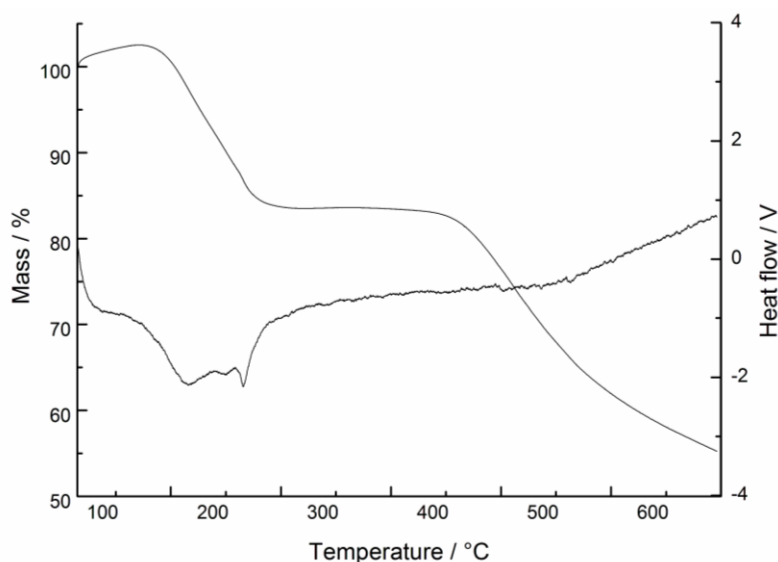


**Figure 5.** TG and DTA curves of  $\text{Sr}[\text{H}_2\text{C}_6\text{N}_7\text{O}_3]_2 \cdot 4 \text{H}_2\text{O}$  (16.2 mg), recording with a heating rate of  $5 \text{ °C} \cdot \text{min}^{-1}$ .

A relatively low thermal stability and a constant mass loss during heating have been observed for other protonated *s*-heptazine based compounds. Compared to melonates,<sup>[20]</sup> whose decomposition starts already at 250 °C, cyamelurates seem to be slightly more stable.

However, the comparable non-protonated compound cyameluric acid is thermally stable up to 500 °C. Protonation of the heptazine ring leads possibly to a different decomposition pathway and consequently to a lower thermal stability.

### FTIR Spectroscopy

Strontium cyamelurate tetrahydrate was analyzed by a BX II FTIR spectrometer (Perkin Elmer) equipped with a DuraSampler diamond ATR. The spectrum displayed in Figure 6 agrees well with the data reported in the literature for cyamelurates.<sup>[15]</sup>

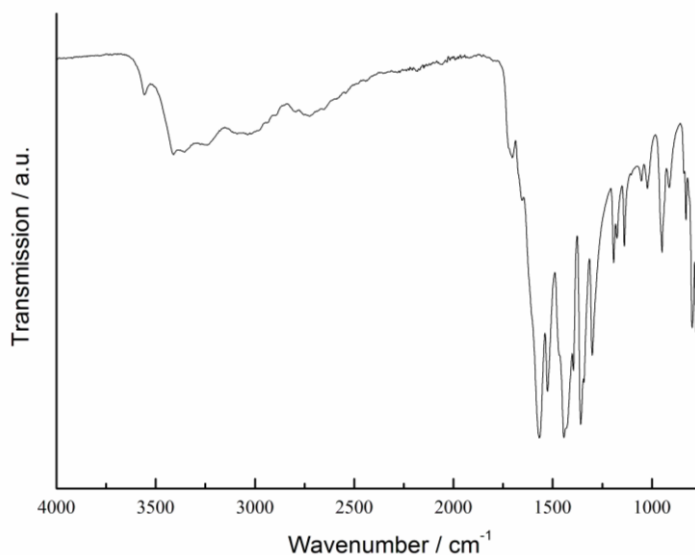


**Figure 6.** FTIR spectrum of  $\text{Sr}[\text{H}_2\text{C}_6\text{N}_7\text{O}_3]_2 \cdot 4 \text{H}_2\text{O}$  (ATR).

Very strong and sharp bands occur between  $790$  and  $1200 \text{ cm}^{-1}$  characterizing bending and stretching vibrations of the *s*-heptazine ring. The weak signals between  $3300 - 3000 \text{ cm}^{-1}$  correspond to N-H stretching vibrations of the imino group. Stretching vibration of the water molecules can be observed at  $3500 - 3740 \text{ cm}^{-1}$ .

### Crystal structure of $\text{Sr}[\text{HC}_6\text{N}_7(\text{NCN})_3] \cdot 7 \text{H}_2\text{O}$

Strontium hydrogenmelonate was obtained by metathesis reaction of potassium melonate and strontium chloride. The structure is isotypic to that of calcium melonate heptahydrate.<sup>[20]</sup> It crystallizes in the triclinic spacegroup *P1* comprising one monoprotonated melonate, one  $\text{Sr}^{2+}$  and seven crystal water molecules in the asymmetric unit (see Figure 7).

Crystallographic data are summarized in Table 2.

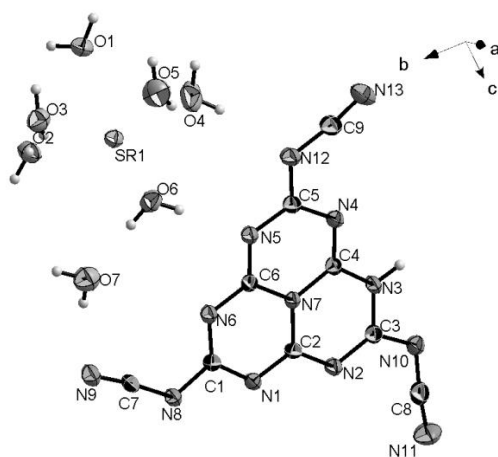


**Figure 7.** Representation of one formula unit of  $\text{Sr}[\text{HC}_6\text{N}_7(\text{NCN})_3] \cdot 7 \text{H}_2\text{O}$ . Ellipsoids are drawn at 50 % probability value.

In analogy with the respective calcium salt a layered structure was found (Figure 8).  $\text{Sr}^{2+}$  is arranged within the layers surrounded by six crystal water molecules. Hydrogen bonds are very similar to those which were found in calcium melonate heptahydrate.<sup>[20]</sup> Due to the isotype structure thermal behavior as well as FTIR spectroscopy are similar to monoprotonated calcium melonate.<sup>[20]</sup>

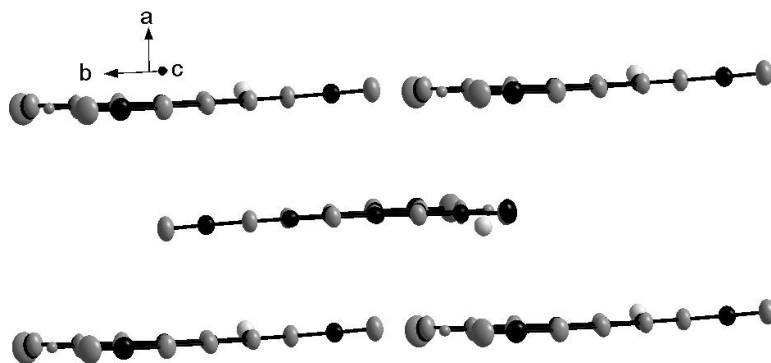


**Figure 8.** Layer-like structure for  $\text{Sr}[\text{HC}_6\text{N}_7(\text{NCN})_3] \cdot 7 \text{H}_2\text{O}$ .

**Table 2.** Crystallographic data and details of the structure refinement for Sr[HC<sub>6</sub>N<sub>7</sub>(NCN)<sub>3</sub>] · 7 H<sub>2</sub>O.

<b>Sr[HC<sub>6</sub>N<sub>7</sub>(NCN)<sub>3</sub>] · 7 H<sub>2</sub>O</b>	
Formula mass / g mol <sup>-1</sup>	504.96
Crystal system	triclinic
Space group	<i>P</i> 1
T / K	293(2)
Diffractometer	Nonius Kappa-CCD
Radiation, λ / pm	Mo-Kα, 71.073
<i>a</i> / pm	660.76(13)
<i>b</i> / pm	1080.7(2)
<i>c</i> / pm	1353.8(3)
α / °	101.67(3)
β / °	101.40(3)
γ / °	94.60(3)
<i>V</i> / 10 <sup>6</sup> pm <sup>3</sup>	920.80(3)
<i>Z</i>	2
Calculated density / g·cm <sup>-3</sup>	1.821
Crystal size / mm <sup>3</sup>	0.12 x 0.12 x 0.9
Absorption coefficient / mm <sup>-1</sup>	2.996
Diffraction range	3.15° ≤ θ ≤ 27.57°
	-8 ≤ <i>h</i> ≤ 8
Index range	-14 ≤ <i>k</i> ≤ 14
	-17 ≤ <i>l</i> ≤ 17
Parameters / restraints	316 / 15
Total no. of reflections	8046
No. of independent reflections	4344
No. of observed reflections	3697
Min. / max. residual electron density / e 10 <sup>-6</sup> pm <sup>-3</sup>	-0.363 / 0.388
GoF	1.047
Final R indices [ <i>I</i> > 2σ( <i>I</i> )]	<i>R</i> <sub>1</sub> = 0.0319
	<i>wR</i> <sub>2</sub> = 0.0727 <sup>a)</sup>
Final R indices (all data)	<i>R</i> <sub>1</sub> = 0.0404
	<i>wR</i> <sub>2</sub> = 0.0759 <sup>a)</sup>

$$a) \quad w = [\sigma^2(F_o^2) + (0.0300P)^2 + 0.6121P]^{-1}, \quad P = (F_o^2 + 2F_c^2)/3.$$

### 3.2.3. Conclusions

In this contribution, we have reported on the new strontium cyamelurate tetrahydrate,  $\text{Sr}[\text{H}_2\text{C}_6\text{N}_7\text{O}_3]_2 \cdot 4 \text{H}_2\text{O}$ , solved by single-crystal structure analysis and refined by the Rietveld method based on single-crystal data. The results expand the diversity of *s*-heptazine derivates. Comparing the newly described structure with other *s*-heptazine derivates a new stacking order arranged in zigzag strands could be found. Due to protonation thermal stability seems to be lowered. This observation is in accordance with several analogous compounds containing protonated melonate or cyamelurate ions. A second compound, namely  $\text{Sr}[\text{HC}_6\text{N}_7(\text{NCN})_3] \cdot 7 \text{H}_2\text{O}$ , which is isotypic to calcium melonate heptahydrate could be synthesized either.

Future work will focus on heptazine based compounds of divalent cations to establish new applications of C/N/(O)/(H) materials.

### 3.2.4. Experimental Section

#### *Syntheses*

#### **$\text{Sr}[\text{H}_2\text{C}_6\text{N}_7\text{O}_3]_2 \cdot 4 \text{H}_2\text{O}$**

Melon was prepared according to the literature<sup>[12]</sup> by heating melamine (Fluka, purum) in an open porcelain crucible at 490 °C for 4 days.

Potassium cyamelurate was obtained by refluxing 25 g melon powder in 250 ml of a 2.5 molar aqueous KOH solution for 45 minutes.<sup>[13]</sup> The hot reaction mixture was filtered. After cooling to room temperature needles precipitated from the filtrate. The product was washed with EtOH and dried in air over night.

Strontium cyamelurate tetrahydrate was synthesized by metathesis of 0.736 g (2 mmol) potassium cyamelurate and 1.6 g (6 mmol)  $\text{SrCl}_2 \cdot 6\text{H}_2\text{O}$  in aqueous solution.  $\text{SrCl}_2 \cdot 6\text{H}_2\text{O}$  and potassium cyamelurate were dissolved separately in 100 ml deionized water under heating up to 60 °C. Subsequently, potassium cyamelurate was added dropwise to the potassium cyamelurate solution. The eluate was collected by filtration and dried under air for 24 h. For recrystallization strontium

cyamelurate was dissolved in deionized water by heating up to 80 °C. Subsequently, few drops of concentrated HCl were added. The product was yielded as colorless thin platelets. Elemental analysis(wt.-%): N 29.47 (calcd. 31.3), C 21.65 (calcd. 22.0), H 2.89 (calcd. 2.2).

#### **Sr[HC<sub>6</sub>N<sub>7</sub>(NCN)<sub>3</sub>] · 7 H<sub>2</sub>O**

Potassium melonate was synthesized according to the literature,<sup>[13]</sup> KSCN (20.0 g, 206 mmol, Acros, ≥ 99 %) was melted and small amounts of melon were added step by step. After heating for 1 hour the yellow product was cooled, filtered and dissolved in boiling water. While cooling down to room temperature the product precipitated. It was recrystallized in water for 3 times and dried at 75 °C over night.

Strontium melonate heptahydrate was obtained by metathesis of strontium chloride and potassium melonate. To a solution of potassium melonate pentahydrate (1 g, 2.01 mmol) in 100 ml deionized water, SrCl<sub>2</sub> · 6H<sub>2</sub>O (1.6 g, 6 mmol) equally dissolved in 100 ml water was added dropwise. The eluate was collected by filtration and dried in air for 24 h. For recrystallization strontium melonate was dissolved in deionized water by heating up to 80 °C, subsequently few drops of concentrated hydrochloric acid were added. The product was yielded as colorless crystals. Elemental analysis (wt.-%): N 36.37 (calcd. 36.06), C 21.88 (calcd. 21.41), H 2.95 (calcd. 2.99).

#### **X-ray Structure Determination**

Single-crystal X-ray diffraction data of Sr[H<sub>2</sub>C<sub>6</sub>N<sub>7</sub>O<sub>3</sub>]<sub>2</sub> · 4 H<sub>2</sub>O and Sr[HC<sub>6</sub>N<sub>7</sub>(NCN)<sub>3</sub>] · 7 H<sub>2</sub>O were measured on a Kappa CCD diffractometer using Mo-K<sub>α</sub> radiation (λ = 71.073 pm). The diffraction intensities were scaled using the SCALEPACK software package. The crystal structure was solved by direct methods (SHELXS-97) and refined against F<sup>2</sup> by full-matrix least-squares (SHELXL-97).<sup>[24,25]</sup> Hydrogen positions could be determined from difference Fourier syntheses and were refined isotropically. All non hydrogen atoms were refined anisotropically. Final atomic positions of Sr[H<sub>2</sub>C<sub>6</sub>N<sub>7</sub>O<sub>3</sub>]<sub>2</sub> · 4H<sub>2</sub>O could be obtained by Rietveld refinement. It was performed with the TOPAS<sup>[26]</sup> package using the fundamental

parameters approach as reflection profiles. Preferred orientation of the crystallites was described with a spherical harmonics function of 4th order. Hydrogen atoms of crystal water or protonation could not be located due to low scattering power and were restrained in the Rietveld refinement. Further details of the crystal structure investigations can be obtained from the Fachinformationszentrum Karlsruhe, 76344 Eggenstein-Leopoldshafen, Germany (fax: (+49) 7247-808-666; e-mail: [crysdata@fiz-karlsruhe.de](mailto:crysdata@fiz-karlsruhe.de), [http://www.fiz-karlsruhe.de/request\\_for\\_deposited\\_data.html](http://www.fiz-karlsruhe.de/request_for_deposited_data.html)) on quoting the depository number CSD-424625 for  $\text{Sr}[\text{H}_2\text{C}_6\text{N}_7\text{O}_3]_2 \cdot 4 \text{H}_2\text{O}$  and CSD- 424622 for  $\text{Sr}[\text{HC}_6\text{N}_7(\text{NCN})_3] \cdot 7 \text{H}_2\text{O}$ .

### General Techniques

X-ray powder diffraction patterns (PXRD) were recorded on a Stoe STADI P diffractometer. The measurement was conducted using monochromatic Cu-K $\alpha$  ( $\lambda = 154.06 \text{ pm}$ ) radiation at room temperature.

Thermoanalytical measurements were performed under inert atmosphere (He) with a Thermoanalyzer TG-DTA92 (Setaram). The sample was heated in an alumina crucible from room temperature to 700 °C with a heating rate of 5 °C min $^{-1}$ .

Fourier-transformed infra-red (FTIR) spectra were recorded in reflection geometry on a Spektrum BX II FTIR spectrometer (Perkin Elmer) equipped with a DuraSampler diamond ATR (attenuated total reflectance) unit. All spectra were corrected with regard to baseline and ATR specific effects. IR spectroscopy was measured at room temperature.

Elemental analyses for C, H and N were performed with the elemental analyzer systems Vario EL and Vario Micro (Elementar Analysensysteme GmbH).

### Acknowledgement

The authors acknowledge financial support by the Fonds der Chemischen Industrie (FCI) and the Deutsche Forschungsgemeinschaft (DFG) (project SCHN377/15-1) and thank Dr. P. Mayer (Department Chemie, LMU München) for single-crystal data collection.

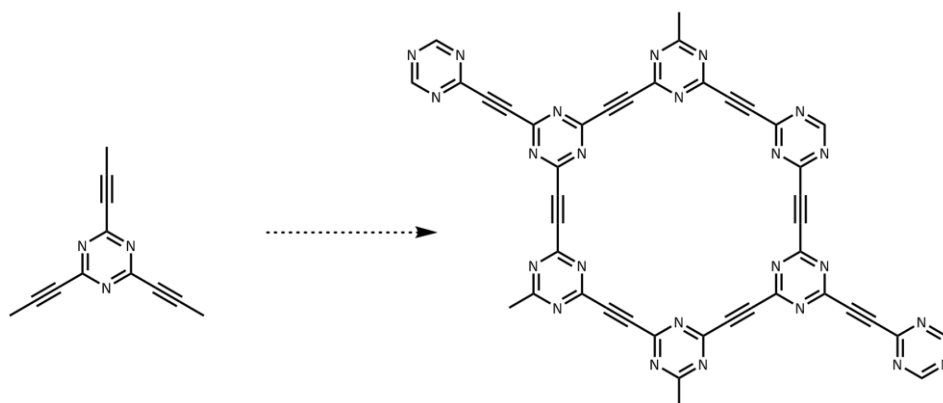
### 3.2.5. Bibliography

- [1] J. Liebig, *Ann. Pharm.* **1834**, *10*, 1.
- [2] E. Kroke, M. Schwarz, *Coord. Chem. Rev.* **2004**, *248*, 493.
- [3] G. Goglio, D. Foy, G. Demazeau, *Mater. Sci. Eng. R* **2008**, *58*, 195.
- [4] A. Y. Liu, M. L. Cohen, *Phys. Rev. B* **1990**, *41*, 10727.
- [5] A. Y. Liu, M. L. Cohen, *Science* **1989**, *245*, 841.
- [6] M. L. Cohen, *Phys. Rev. B* **1985**, *32*, 7988.
- [7] X. Wang, K. Maeda, A. Thomas, K. Takanahe, G. Xin, J. M. Carlsson, K. Domen, M. Antonietti, *Nat. Mater.* **2009**, *8*, 76.
- [8] A. Thomas, A. Fischer, F. Goettmann, M. Antonietti, J.-O. Müller, R. Schlögl, J. M. Carlsson, *J. Mater. Chem.* **2008**, *18*, 4893.
- [9] F. Goettmann, A. Thomas, M. Antonietti, *Angew. Chem.* **2007**, *119*, 2773; *Angew. Chem. Int. Ed.* **2007**; *Angew. Chem. Int. Ed.* **2007**, *46*, 2717.
- [10] W. Henneberg, *Ann. Chem. Pharm.* **1850**, *73*, 228.
- [11] J. Wagler, N. E. A. El-Gamel, E. Kroke, *Z. Naturforsch.* **2006**, *61b*, 975.
- [12] A. Sattler, W. Schnick, *Z. Anorg. Allg. Chem.* **2006**, *632*, 1518.
- [13] E. Horvath-Bordon, E. Kroke, I. Svoboda, H. Fueß, R. Riedel, S. Neeraj, A. K. Cheetham, *Dalton Trans.* **2004**, 3900.
- [14] A. Sattler, M. R. Budde, W. Schnick, *Z. Anorg. Allg. Chem.* **2009**, *635*, 1933.
- [15] L. Gmelin, *Ann. Pharm.* **1835**, *15*, 252.
- [16] L. Pauling, J. H. Sturdivant, *Proc. Natl. Acad. Sci USA* **1937**, *23*, 615.
- [17] E. Horvath-Bordon, E. Kroke, I. Svoboda, H. Fuess, R. Riedel, *New J. Chem.* **2005**, *29*, 693.
- [18] A. Sattler, W. Schnick, *Eur. J. Inorg. Chem.* **2009**, 4972.
- [19] S. J. Makowski, W. Schnick, *Z. Anorg. Allg. Chem.* **2009**, *635*, 2197.

- [20] S. J. Makowski, D. Gunzelmann, J. Senker, W. Schnick, *Z. Anorg. Allg. Chem.* **2009**, 635, 2434.
- [21] B. V. Lotsch, M. Döblinger, J. Sehnert, L. Seyfarth, J. Senker, O. Oeckler, W. Schnick, *Chem. Eur. J.* **2007**, 13, 4969.
- [22] B. Jürgens, E. Irran, J. Senker, P. Kroll, H. Müller, W. Schnick, *J. Am. Chem. Soc.* **2003**, 125, 10288.
- [23] R. D. Shannon, C. T. Prewitt, *Acta Crystallogr. Sect. B* **1969**, 25, 925.
- [24] G. M. Sheldrick, SHELXS-97 **1997**.
- [25] G. M. Sheldrick, SHELXL-97, Program for the Refinement of Crystal Structures, Universität Göttingen **1997**.
- [26] A. Coelho, TOPAS Academic, v.4.1, Coelho Software, Brisbane, **2007**.

## 4. From Alkyne-triazines to New Triazine-based Networks

Precursors for polymeric carbon nitrides were described only in regard of condensation reactions thus far. In this chapter new types of precursors were characterized and have successfully been applied for polymerization and metathesis reactions to obtain new networked compounds.



**Scheme 1.** Polymerisation of alkyne-triazine.

As a first step the functionalization of *s*-triazine units with alkynes by organic cross coupling reactions were investigated. Especially the structure and the thermal behavior of tris(1-propynyl)-1,3,5-triazine  $C_3N_3(C_3H_3)_3$  (TPT) and tris(1-butynyl)-1,3,5-triazine  $C_3N_3(C_4H_5)_3$  have been investigated.

Such alkyne-triazines are capable of forming new polymeric carbon nitrides. Through thermal treatment alkyne fragments forming a ring closing mechanism to mesitylene units which are linkers between the triazine cores. Subsequently a first disordered polymer, poly-TPT, with high surface area could be investigated by pyrolysis of  $C_3N_3(C_3H_3)_3$ .

Due to the expected pore size distribution of triazine-based polymers connected by acetylene units, alkyne-metathesis reactions of alkyne-triazines were conducted in order to obtain polymeric compounds as demonstrated in Scheme 1.

The occasional release of gaseous but-1-yne and hex-1-yne is a promoting factor for metathesis reactions. An overview of various catalysts as well as different reaction conditions is represented in this study. The successful synthesis and characterization of first oligomers are described as well.

## 4.1. Synthesis of Novel Triazine-based Materials by Functionalization with Alkynes

Nicole E. Braml, Linus Stegbauer, Bettina V. Lotsch and Wolfgang Schnick

Published in: *Chem. Eur. J.* **2015**, *21*, 7866.

DOI: 10.1002/chem.201405023

Copyright © 2015 WILEY-VCH

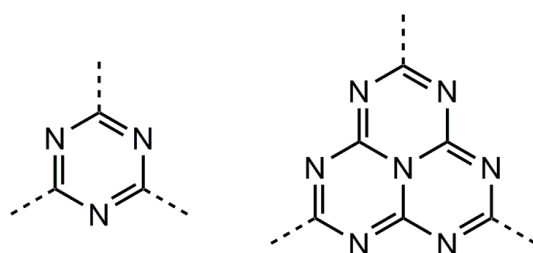
<http://onlinelibrary.wiley.com/doi/10.1002/chem.201405023/abstract>

**Keywords:** carbon nitrides · triazine · alkyne · crystal structure · hydrogen bonding

**Abstract.** In this contribution, we report on novel functionalized triazines, which represent new precursors for C/N/(H) compounds or suitable building blocks for carbon-based functional networks. Our results furnish new insights into the structural properties of molecular carbon nitride materials and their design principles. Tris(1-propynyl)-1,3,5-triazine  $C_3N_3(C_3H_3)_3$  and tris(1-butynyl)-1,3,5-triazine  $C_3N_3(C_4H_5)_3$  were prepared by substitution reactions of cyanuric chloride  $C_3N_3Cl_3$  with prop-1-yne and but-1-yne. The crystal structure of tris(1-propynyl)-1,3,5-triazine was solved in the orthorhombic space group *Pbcn* ( $Z = 4$ ,  $a = 1500.06$  (14),  $b = 991.48(10)$ ,  $c = 754.42(6)$  pm,  $V = 1122.03(18) \cdot 10^6$  pm<sup>3</sup>), whereas tris(1-butynyl)-1,3,5-triazine crystallized in the triclinic space group *P-1* ( $Z = 6$ ,  $a = 1068.36(12)$ ,  $b = 1208.68(12)$ ,  $c = 1599.38(16)$  pm,  $\alpha = 86.67(3)$ ,  $\beta = 86.890(4)$ ,  $\gamma = 86.890(4)^\circ$ ,  $V = 1997.7(4) \cdot 10^6$  pm<sup>3</sup>). For both structures planar triazine units and layer-like packing of the molecules were observed. Tris(1-propynyl)-1,3,5-triazine is built up from hydrogen-bonded zig-zag strands while tris(1-butynyl)-1,3,5-triazine shows parallel layered arrangements. Both compounds were investigated by NMR, IR spectroscopy and DTA/TG, providing insights into their structural, chemical and thermal properties. In addition,  $C_3N_3(C_3H_3)_3$  was pyrolyzed and a new polymeric triazine based compound containing mesitylene units was obtained. Its structural features and properties are discussed in detail.

### 4.1.1. Introduction

Triazine- as well as heptazine-based materials, although known for decades, have surfaced recently as functional materials with a broad set of interesting properties ranging from abrasion resistance to photoactivity.<sup>[1,2]</sup> Substantial research efforts are currently being devoted to the synthesis of precursors and intermediate compounds for the design of novel C/N/(H) networks.<sup>[3,4]</sup> In addition, the utilization of triazine- and heptazine-based precursors as suitable building blocks for covalent organic frameworks (COFs) has been gaining interest in recent years.<sup>[5-8]</sup> COFs have been developed into a versatile class of ordered polymeric materials with high porosities, which bodes well for numerous applications in gas storage, energy conversion, and catalysis. Lately, the prospective use of polymeric carbon nitride-type materials as “organic semiconductors”<sup>[9]</sup> or metal free catalysts<sup>[10]</sup> for hydrogen production from water or CO<sub>2</sub> fixation has been discussed in the literature as well.<sup>[11]</sup> Furthermore, triazine- or heptazine-based compounds (see Scheme 1) are potential precursors for the design of new molecular solid-state materials with complex supramolecular topologies.<sup>[12-14]</sup> As a result of the large structural variety and chemical robustness of the precursors, the synthesis of new functional materials with interesting structural properties, for example hydrogen-bonded architectures and low-dimensional solids, is within reach.



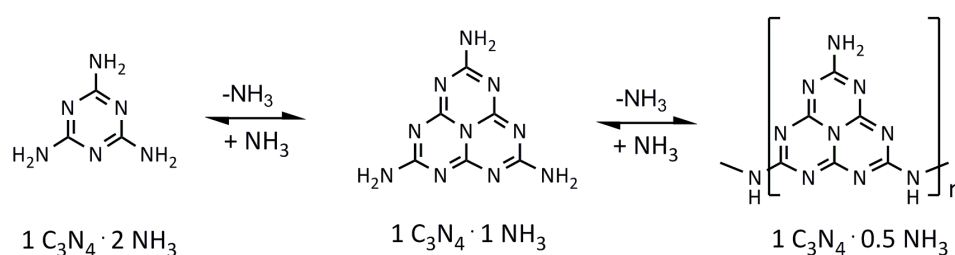
**Scheme 1.** Triazine C<sub>3</sub>N<sub>3</sub> and heptazine C<sub>6</sub>N<sub>7</sub> cores.

First pioneering work on carbon nitride chemistry was performed by Liebig<sup>[15]</sup> and other well-known<sup>[16-20]</sup> scientists such as Gmelin<sup>[19]</sup> or Henneberg.<sup>[20]</sup> Their achievements include the first description of the polymer melon and further “ammonocarbon acids” such as dicyandiamide, melamine or melem (Scheme 2). During the last few decades a great diversity of heptazine- and triazine-based

materials has been structurally elucidated. In addition, significant research efforts have been devoted to their thermal condensation reactions of these materials and the syntheses of highly condensed phases.

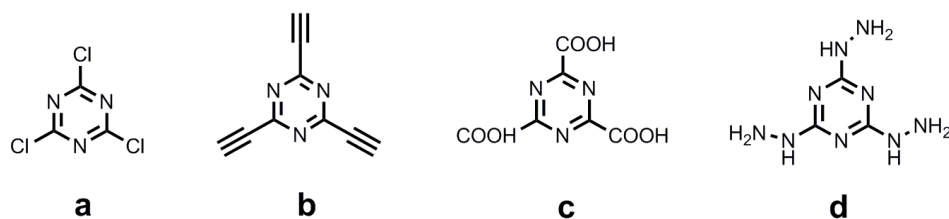
The structural characterization of melon was achieved by electron diffraction combined with solid-state NMR spectroscopy.<sup>[21]</sup> The first 3D carbon nitride network carbon nitride imide with a defective wurtzite-type structure was synthesized under high-pressure conditions.<sup>[22]</sup> In addition, the two-dimensional carbon nitride networks of poly(heptazine imide) (PHI)<sup>[23]</sup> and poly(triazine imide) (PTI)<sup>[24]</sup> built up from *s*-triazine and *s*-heptazine building units were prepared by using ionothermal reactions in salt melts or ampoule techniques. Just recently new investigations aiming at graphitic C<sub>3</sub>N<sub>4</sub> have been discussed in the literature.<sup>[25]</sup>

Less condensed C/N/H materials play a significant role as precursors but can also be used for further applications as described in the following section. Substitution of the above mentioned melamine (2,4,6-triamino-1,3,5-triazine) leads to ubiquitous reagents such as cyanuric chloride, C<sub>3</sub>N<sub>3</sub>Cl<sub>3</sub> and a number of derivatives<sup>[26]</sup> such as hydrazino-*s*-triazine which has been investigated as *s*-triazine herbicide (see Scheme 3a, d).<sup>[27]</sup>



**Scheme 2.** Condensation scheme of C/N/H materials, starting from melamine. Heptazine-based materials are obtained by thermal elimination of NH<sub>3</sub>.

Functionalized triazines are versatile and frequently used precursors because of their high reactivities. In addition, the supramolecular arrangement of 1,3,5-triazine-2,4,6-carboxylate,<sup>[28]</sup> C<sub>3</sub>N<sub>3</sub>(COOH)<sub>3</sub>, (Scheme 3c) with different types of heterocyclic aromatic systems by hydrogen-bonding was recently discussed in the literature.<sup>[12-14]</sup>



**Scheme 3.** **a** cyanuric chloride, **b** ethynyl-triazine, **c** triazine-carboxylate, **d** hydrazine-*s*-triazine.

Another structurally interesting triazine derivative is ethynyl-triazine (Scheme 3b).<sup>[29]</sup> Due to the layer-like structure and intermolecular interactions this compound has been discussed in the literature in quite some detail because it is built up from a two-dimensional network (Figure 1) similar to hypothetical graphyne<sup>[30]</sup> which can be derived from graphite interconnected with acetylene units. In addition, ethynyl-triazine is a suitable building-block for COFs.

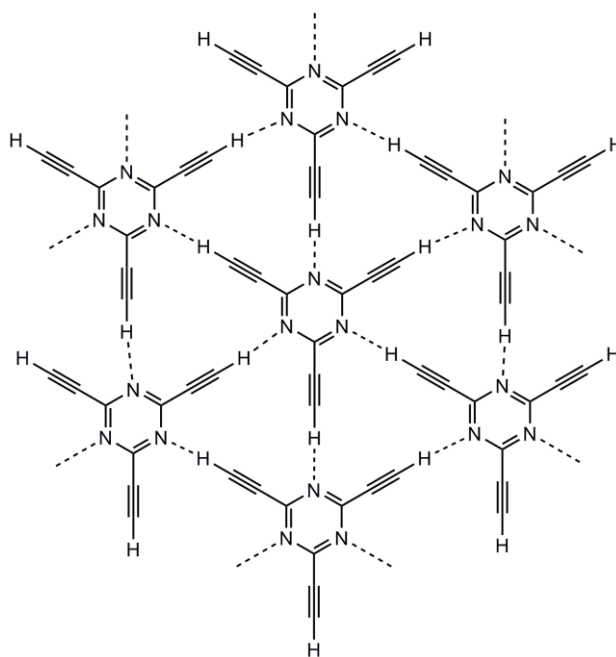


**Figure 1.** Two-dimensional H-bonding network of ethynyl-triazine.

In this contribution we report a generic strategy for the functionalization of the triazine core with alkynes by reaction of cyanuric chloride with prop-1-yne or but-1-yne in a Negishi-like coupling. This approach targets the formation of molecular carbon nitride precursors for the synthesis of mixed aryl-triazine networks through atom efficient trimerization reactions.

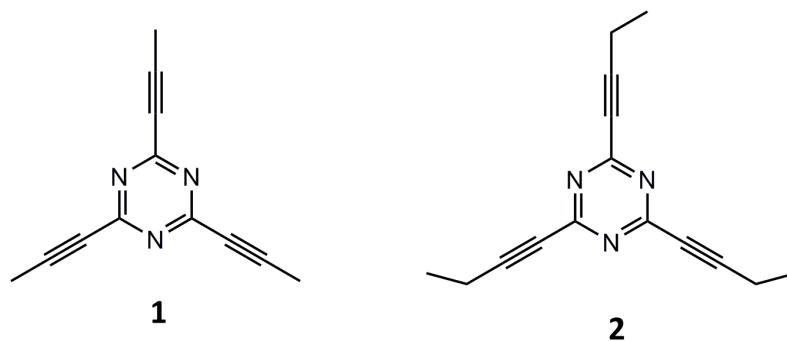
We describe the structural characterization of the corresponding tris(1-propynyl)-1,3,5-triazine  $C_3N_3(C_3H_3)_3$  and tris(1-butynyl)-1,3,5-triazine  $C_3N_3(C_4H_5)_3$ . With these compounds a novel approach to form new polymeric compounds could be established. The thermal behavior indicates that tris(1-propynyl)-1,3,5-triazine is especially capable to form new polymeric compounds.

#### 4.1.2. Results and Discussion

As mentioned above, functionalized triazine-based materials are of interest as potential intermediates for polymeric carbon nitride-type materials or as building blocks for supramolecular architectures. Along these lines, our contribution aims at the synthesis and structural characterization of new alkyne-substituted triazines as potential precursors for carbon nitride networks. The crystal structure of ethynyl-triazine,<sup>[29]</sup> a  $\pi$ -stacked hexagonal layered structure (Figure 1), has already been discussed in the literature.

Related alkyne-triazines may form similar structures or may be suitable precursors for new carbon nitride networks (Scheme 4) with interesting properties. The formation of polymeric compounds with high porosity and surface areas and their use of such compounds as tailor-made catalysts are possible scenarios.

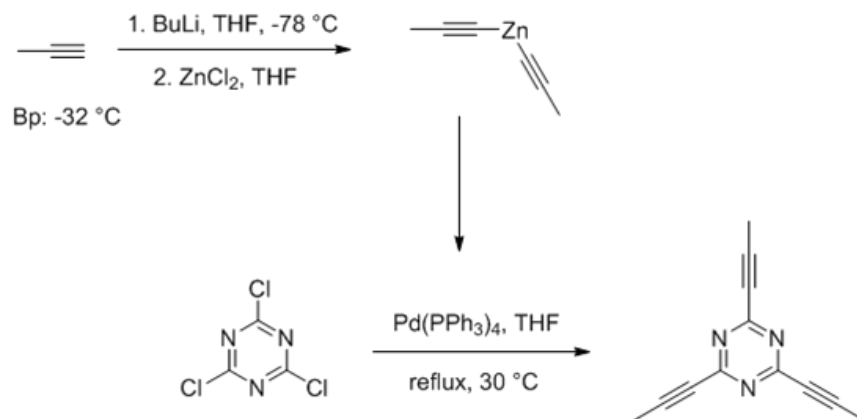
The first step in our investigation is the synthesis of two new monomeric alkyne compounds, namely tris(1-propynyl)-1,3,5-triazine  $C_3N_3(C_3H_3)_3$  (1) and tris(1-butynyl)-1,3,5-triazine  $C_3N_3(C_4H_5)_3$  (2) (Scheme 4).



**Scheme 4.** Tris(1-propynyl)-1,3,5-triazine (1) and tris(1-butynyl)-1,3,5-triazine (2).

The individual reaction steps in the synthesis of tris(1-propynyl)-1,3,5-triazine  $C_3N_3(C_3H_3)_3$  (1) are outlined in Scheme 5. Prop-1-yne was deprotonated with butyllithium and treated with  $ZnCl_2$  in THF. The resulting product was allowed to react in a Negishi-like coupling<sup>[31]</sup> with cyanuric chloride,  $C_3N_3Cl_3$ , to form  $C_3N_3(C_3H_3)_3$  (1) with a yield of about 30 % which can be traced back to the presence of partially substituted side products. By using the Grignard reagent propyne-1-yle magnesium chloride, the yield could be increased. Tris(1-butynyl)-1,3,5-triazine  $C_3N_3(C_4H_5)_3$  (2) was prepared under analogous reaction conditions using but-1-yne as the starting reagent. Both products are stable in air, however slightly volatile. Additional data are provided in the Experimental Section.

Both compounds were characterized by solution NMR spectroscopy, which confirms the expected molecular structure for both compounds. Detailed NMR data are summarized in the supporting information. IR spectroscopy and mass spectrometry were also carried out and further confirm the successful synthesis of both compounds.



**Scheme 5.** Synthetic procedure for  $C_3N_3(C_3H_3)_3$  (1).

Besides the spectroscopic analysis, we determined the crystal structures of (1) and (2). Despite severe disorder effects in conjunction with the organic moieties in the structures, we were able to solve and refine the structure of tris(1-propynyl)-1,3,5-triazine (1) based on single-crystal X-ray diffraction. Despite the low data quality for single crystals of tris(1-butynyl)-1,3,5-triazine (2), a structural model could be derived, which is presented below.

**Structural investigation of tris(1-propynyl)-1,3,5-triazine (TPT) (1):**  $C_3N_3(C_3H_3)_3$  (1) was obtained as thin colorless platelets. It crystallizes in the orthorhombic space group  $Pbcn$ . The asymmetric unit comprises four planar tris(1-propynyl)-1,3,5-triazine  $C_3N_3(C_3H_3)_3$  fragments (Figure 2 and Table 1). All corresponding H-atoms could be localized, while methyl groups are disordered. Special regard has to be paid to the terminal C-atom C8 which has a specific location and therefore exhibits six disordered proton positions. C-N bond lengths of the planar triazine ring are intermediate between single and double bonds in agreement with the aromatic character of the triazine unit.<sup>[32]</sup> Angles within the triazine ring are quite similar to those of comparably functionalized triazines.

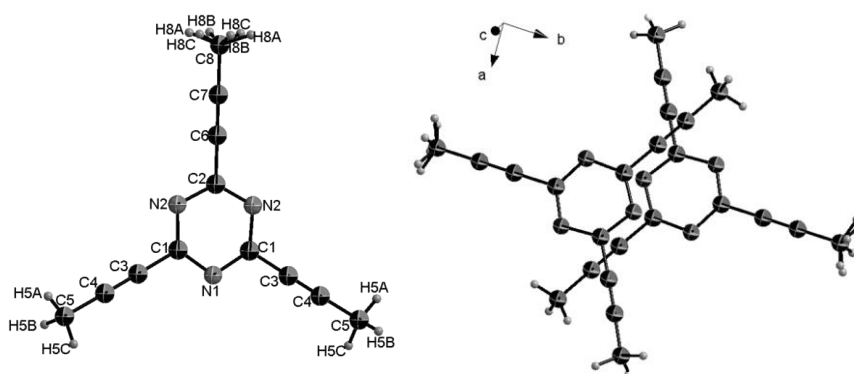


**Figure 2.** Representation of one formula unit of  $C_3N_3(C_3H_3)_3$  (1). Ellipsoids are drawn at the 50 % probability level. Shifted fragments of  $C_3N_3(C_3H_3)_3$  (1), viewed along  $c$ .

The majority of triazine-based compounds are made up of parallel layer-like arrangements in the crystal (see Figure S 3 in the Supporting Information).<sup>[32,33]</sup> By the contrast,  $C_3N_3(C_3H_3)_3$  (1) forms zig-zag strands running along  $a$  axis with an interlayer spacing of 320 pm which is well in line with values known from the literature for triazine- and heptazine-based materials.<sup>[32,33]</sup> Between the layers, stacked  $C_3N_3(C_3H_3)_3$  (1) fragments are displaced so that negatively polarized N-atoms and negatively polarized C-atoms of the alkyne groups are located above positively polarized C-atoms of the triazine core (Figure 2).

The layers are connected and stabilized by hydrogen-bonding motifs. We observe inter- as well as intralayer donor–acceptor distances with moderate values that range from 254 to 296 pm (see Figure S 4 in the Supporting Information).<sup>[34]</sup> The corresponding interlayer distance of N2 and protons attached to the terminal C8 is 279 pm. Within the layer, protons of C8 are engaged in hydrogen-bonding to N1 with a distance of 296 pm. Further intralayer connections of N2 and protons of the terminal methyl group C5 are observed with a distance of 254 pm.  $C_3N_3(C_3H_3)_3$  was additionally characterized by NMR spectroscopy. Further information can be found in the Supporting Information.

**Table 1.** Crystallographic data for  $C_3N_3(C_3H_3)_3$ .

$C_3N_3(C_3H_3)_3$	
Formula mass /g mol <sup>-1</sup>	195.22
Crystal system/space group	orthorhombic / <i>Pbcn</i> (no. 60)
T [K]	100(2)
Diffractometer	Bruker Venture D8
Radiation, $\lambda$ / pm	Mo-K $\alpha$ , 71.073
<i>a</i> / pm	1500.06(14)
<i>b</i> / pm	991.48(10)
<i>c</i> / pm	754.42(6)
<i>V</i> / 10 <sup>6</sup> pm <sup>3</sup>	1122.03(18)
<i>Z</i>	4
Diffraction range [°]	5 ≤ 2 $\theta$ ≤ 52
Data / parameters / restraints	1166 / 73 / 0
GOF	1.056
R-indices (all data) [%]	$R_1 = 0.0498$ $wR_2 = 0.1251$

**Structural investigation of tris(1-butynyl)-1,3,5-triazine (2):**  $C_3N_3(C_4H_5)_3$  (2) crystallizes in the triclinic space group *P*-1 with six formula units in the unit cell (see Figure 3 and Table 1). Similar to (1) it was obtained as colorless thin crystal blocks. Due to disordered terminal CH<sub>3</sub>-groups and possible variances of these fragments, the solution of the crystal structure was challenging. In particular, mechanical distortion and shifting of the layered structure is probably responsible for the bad data quality. Nevertheless, the structure solution and refinement lead to a plausible structural model.

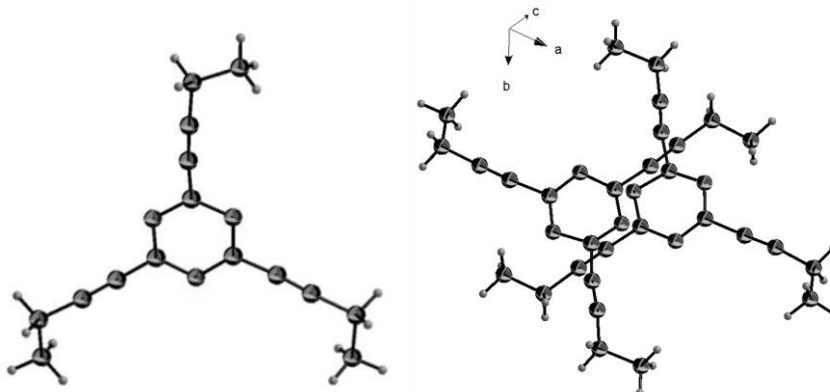


**Figure 3.** Representation of one formula unit of  $C_3N_3(C_4H_5)_3$  (2).  
Shifted molecules due to interaction of negatively and positively polarized atoms of (2).

One formula unit comprises a triazine ring with three substituted butin-1-yle groups (Figure 3). The triazine ring and the triply bonded C-atoms of the butyn-1-yle fragments are planar, except for the terminal  $CH_3$ -group which is tilted with an angle of  $113.5^\circ$ . Angles and bond lengths are quite similar to those in (1). By comparison with structural data for triazines reported in the literature,<sup>[32]</sup> the observed angles and bond lengths can be confirmed. Bond lengths of the triazine core are intermediate between double and single bonds due to the aromatic character of the triazine ring. Bond lengths of the C-C bonds are in the expected ranges. C-C single bonds between the triazine ring and the triple bonds and between the triple bonds and the terminal single bonds are around 145 pm, the triple bonds ( $\approx 120$  pm) are significantly shorter. The bond lengths between the  $CH_2$ - and the  $CH_3$  groups are around 155 pm which is well in line with  $sp^3$ - $sp^3$  single bonds.

As with the zig-zag strands of (1), fragments of (2) are stacked along  $a$  (see Figure S 3 in the Supporting Information) to form linear planes with an interplanar distance of about 300 pm. The distance between the parallel layers is accordingly smaller than the distance of zig-zag strands of  $C_3N_3(C_3H_3)_3$  (1). However, it is well in line with values known from the literature for layered carbon nitride-type materials.<sup>[32,33]</sup> Similar to (1), the molecules are shifted such that negatively polarized and positively polarized atoms are located on top of each other (see Figure 3).

**Table 2.** Crystallographic data for  $C_3N_3(C_4H_5)_3$  (2).

$C_3N_3(C_4H_5)_3$ (2)	
Formula mass /g mol <sup>-1</sup>	222.18
Crystal system/space group	Triclinic / <i>P</i> -1
T [K]	100(2)
diffractometer	Bruker Venture D8
Radiation, $\lambda$ / pm	Mo-K $\alpha$ , 71.073
<i>a</i> / pm	1068.36(12)
<i>b</i> / pm	1208.68(12)
<i>c</i> / pm	1599.38(16)
$\alpha$ / °	81.33(3)
$\beta$ / °	86.890(4)
$\gamma$ / °	78.162(4)°
<i>V</i> / 10 <sup>6</sup> pm <sup>3</sup>	1997.7
<i>Z</i>	6
Diffraction range [°]	4 ≤ 2 $\theta$ ≤ 52
Data / parameters / restraints	5732 / 229 / 0
GOF	1.06
R-indices (all data) [%]	$R_1 = 0.1341$ $wR_2 = 0.2694$

All protons have been added by using constraints and are involved in various hydrogen-bonding motifs (see Figure S 4 in the Supporting Information). The layers are stabilized by interaction of CH<sub>2</sub>- as well as CH<sub>3</sub>-protons with N atoms of the triazine unit with a donor–acceptor distance of 291 pm. Equal connections could be found within the layer. The carbon atoms of CH<sub>2</sub>- as well as CH<sub>3</sub>-groups build up a H-bonding network with slightly stronger hydrogen bonding than that in (1). The bond lengths are between 253 pm and 284 pm. Stronger H-bonds can be explained by tilted CH<sub>3</sub>-groups, which reduce the distance to adjacent triazine units.

Additional NMR data can be found in the Supporting Information.

**FTIR Spectroscopy:** Compounds 1 and 2 were analyzed by attenuated total reflectance (ATR) IR spectroscopy. The corresponding spectra are depicted in Figure 4. The signals are well in line with data reported in the literature for triazine-based

compounds.<sup>[32]</sup> The signals are between  $\lambda = 790$  and  $1200\text{ cm}^{-1}$  represent bending and stretching vibrations of the triazine ring. Strong signals occur at  $\lambda = 2200 - 2300\text{ cm}^{-1}$ , which are characteristic stretching vibrations of the alkyne groups. At  $\lambda = 2800 - 3000\text{ cm}^{-1}$  weak signals indicate the presence of  $\text{CH}_3$ - and  $\text{CH}_2$ -groups.

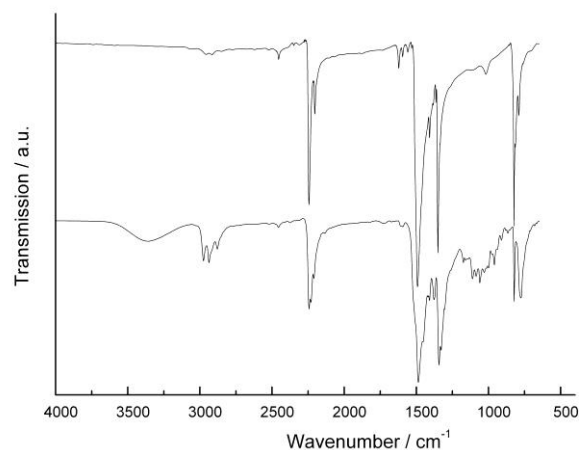


**Figure 4.** FTIR spectrum of  $\text{C}_3\text{N}_3(\text{C}_3\text{H}_3)_3$  (1) (above) and  $\text{C}_3\text{N}_3(\text{C}_4\text{H}_5)_3$  (2) (below) (ATR).

As expected,  $\text{C}_3\text{N}_3(\text{C}_4\text{H}_5)_3$  (2) shows stronger signals between  $\lambda = 2800 - 3000\text{ cm}^{-1}$  than  $\text{C}_3\text{N}_3(\text{C}_3\text{H}_3)_3$  (1) due to the presence of additional  $\text{CH}_2$ -groups.

**Thermal Behavior:** The thermal stability of the alkynyl-triazines was investigated by determination of the melting point and differential thermal analysis/thermogravimetric (DTA/TG) analyses. Accordingly,  $\text{C}_3\text{N}_3(\text{C}_3\text{H}_3)_3$  (1) decomposes at  $200\text{ }^\circ\text{C}$ , while  $\text{C}_3\text{N}_3(\text{C}_4\text{H}_5)_3$  (2) melts at  $200\text{ }^\circ\text{C}$  and decomposes subsequently at  $350\text{ }^\circ\text{C}$ . The decomposition process for 1 was observable by a color change at  $200\text{ }^\circ\text{C}$  of the initial white powder to a black powdery substance. These findings were verified by DTA and TG measurements in He inert atmosphere. For  $\text{C}_3\text{N}_3(\text{C}_3\text{H}_3)_3$  (1; Figure 5) the plots show a mass loss beginning at  $200\text{ }^\circ\text{C}$  with a sharp exothermic signal at  $250\text{ }^\circ\text{C}$ . An amount of (1) was transformed into gaseous C/N/H products under heating. This indicates thermal stability up to  $200\text{ }^\circ\text{C}$  and a rapid, complete decomposition at higher temperatures.

The signals for  $C_3N_3(C_4H_5)_3$  (2) (see Figure S 5 in the Supporting Information) are less well-defined. The compound melts at about 200 °C with no significant mass loss, while at 350 °C a gradual mass loss during heating occurs. Compared to  $C_3N_3(C_3H_3)_3$  (1), the thermal behavior of (2) is slightly different, implying a slightly higher thermal stability. This difference may result from the additional  $CH_2$ -group, which is responsible for stronger dispersive interactions. There is no plateau at low mass loss for (2) as observed for compound 1. As a consequence, we have pyrolyzed  $C_3N_3(C_3H_3)_3$  (1) on a preparative scale to obtain further insights into the decomposition process.

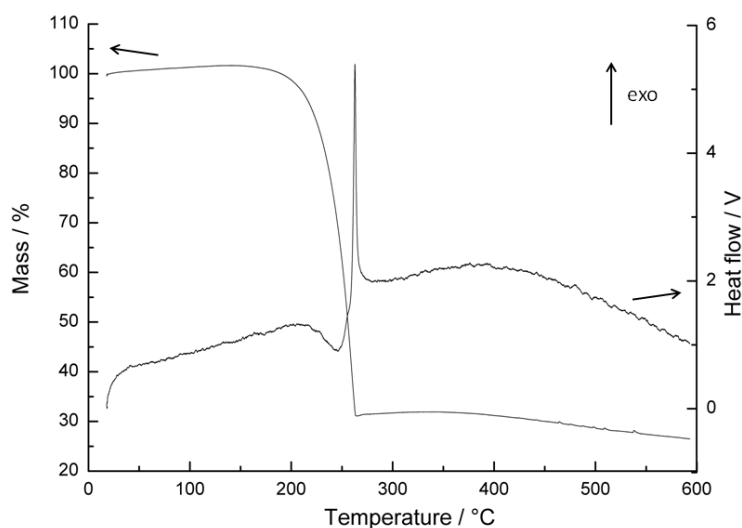


**Figure 5.** DTA and TG curves of  $C_3N_3(C_3H_3)_3$  (1), measured in He inert atmosphere.

**Polymerization:** Corresponding with the DTA/TG measurements  $C_3N_3(C_3H_3)_3$  (1) was heated at 250 °C for one hour in inert atmosphere. During heating gaseous side products evaporate as indicated by the overpressure built up in the schlenk tube and a pungent smell of volatiles. A glossy black powder, poly-TPT, could be isolated and was analyzed with respect to its composition and molecular connectivity.

Powder X-ray diffraction of the polymerization product of (1) (see Figure S 6 in the Supporting Information) indicates that an amorphous polymeric product was obtained. A broad shoulder at about  $25 \ 2\theta / ^\circ$  suggests a layered material with a stacking distance of roughly 3.5 Å. To identify the building units and their assembly,

FTIR and NMR spectroscopy studies were conducted. The corresponding FTIR spectra (Figure 6) show signals at  $\lambda = 1000 - 1600 \text{ cm}^{-1}$  which correspond to aromatic C=C and C=N vibrations, while the broad bands indicate a disordered structure. Additionally, between  $\lambda = 3000 - 3500 \text{ cm}^{-1}$  very weak  $\text{C}_{\text{sp}^3}\text{-H}$  vibrations could be observed.

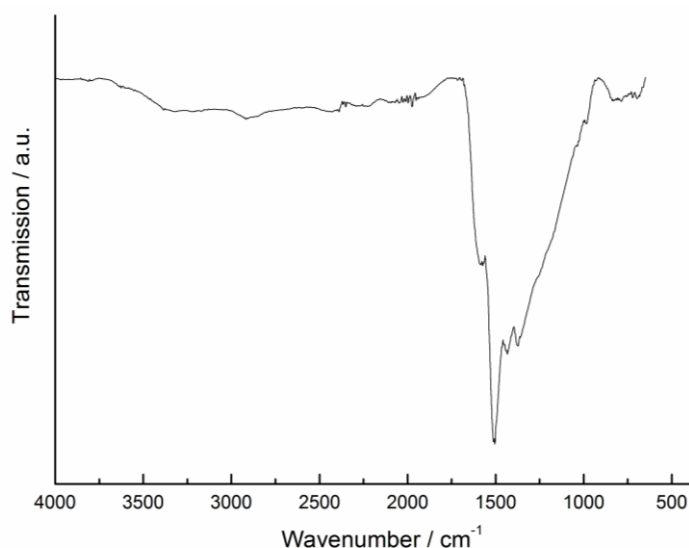


**Figure 6.** FTIR-spectrum of poly-TPT (ATR).

Additionally, multinuclear solid-state NMR measurements show the presence of alkyl groups, triazine- and further aromatic fragments as well. In the  $^1\text{H}$  spectrum (see Figure S 7 in the Supporting Information) the signal at 2.2 ppm was assigned to a methyl group, showing an only slight downfield shift compared to the corresponding monomeric  $\text{C}_3\text{N}_3(\text{C}_3\text{H}_3)_3$  (1) (2.1 ppm). The  $^{13}\text{C}$  NMR spectrum exhibits three signals (Figure 7). The signal located at 171 ppm corresponds to the C atoms in the triazine unit. The broad signal at 134 ppm can be assigned to aromatic C atoms that are absent in the starting material (see Figure S 1 in the Supporting Information) and, hence, suggest the formation of a benzene ring through trimerization of the alkynyl moieties. The third signal at 20 ppm is assigned to C atoms of the methyl groups which exhibit a rather significant upfield shift compared with those in monomeric  $\text{C}_3\text{N}_3(\text{C}_3\text{H}_3)_3$  (1) (5 ppm). The total absence of any  $^{13}\text{C}$  signal between 20 and 100 ppm in the solid-state NMR clearly shows a total loss of all alkyne groups.

The above findings suggest that a disordered network based on known structural motifs mesitylene and triazine units has been synthesized. The initial alkynes apparently undergo a thermally induced Reppe-like [2+2+2] cyclotrimerization, which may be assisted by traces of leached<sup>[35]</sup> palladium<sup>[36]</sup> from the earlier Pd catalyzed Negishi-like coupling, leading to aromatic mesitylene units in poly-TPT (Figure 8 for a tentative structure). The idealized structure highlights the expected transformation product which is likely formed alongside structurally related polymers and a large amount of gaseous decomposition products. Nevertheless, solid-state NMR indicates structural motifs which are in line with the proposed model presented in Figure 8.

The material properties of such networked compounds, especially regarding their porosity and surface area, are of substantial interest for applications in gas storage and catalysis. Therefore, scanning electron microscopy/energy dispersive X-ray spectroscopy (SEM-EDX) and sorption measurements of poly-TPT were conducted to investigate its properties.

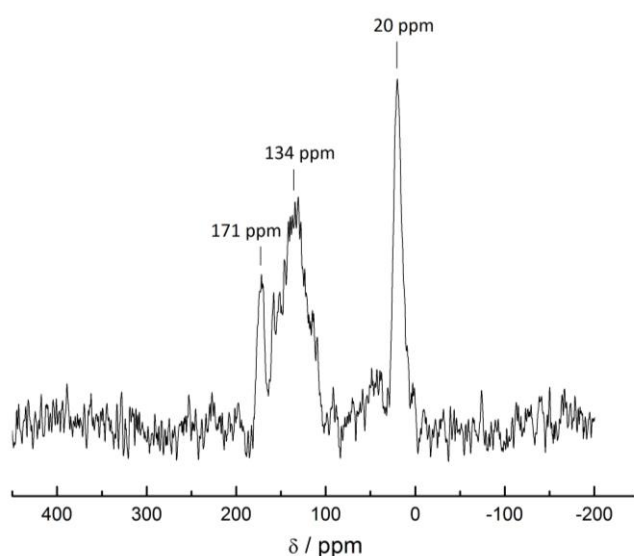


**Figure 7.** <sup>13</sup>C CP-MAS solid-state NMR spectrum (4 mm rotor, 10 kHz spinning speed at room temperature).

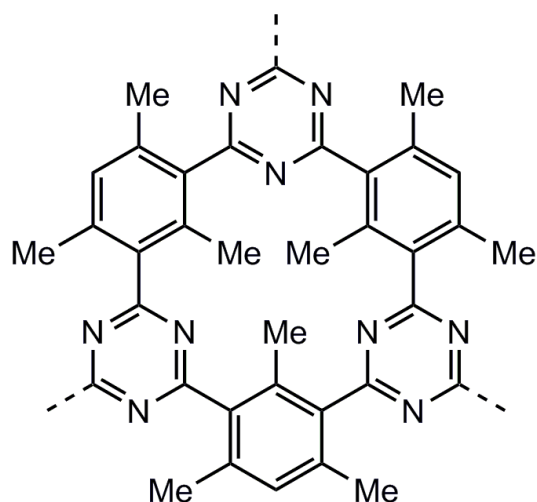


**Figure 8.** Tentative local structure of Poly-TPT.

SEM analysis of poly-TPT (see Figure S 8 in the Supporting Information), shows large amorphous flakes. EDX measurements show evidence of the presence of a high amount of nitrogen, whereas the carbon content cannot be quantified due to the carbon coating. Therefore, the amount of carbon, nitrogen and hydrogen was determined by elemental analyses, which show 68.6 % carbon, 19.0 % nitrogen and 4.5 % hydrogen. This composition is similar to that found in the starting materials (73 % carbon, 21 % nitrogen and 5 % hydrogen) and hence supports the formation of a mesitylene-triazine-based structure, along with a large amount of gaseous decomposition products.

Although Ar physisorption was hampered by extraordinary long equilibrium times, CO<sub>2</sub> sorption at 273 K shows a fully reversible isotherm (Figure 9) with an uptake of 1.59 mmol/g at 1 bar. The surface area was determined as 360 m<sup>2</sup>/g with a pore volume of 0.12 ml/g and predominantly ultramicropores with diameters between 0.4 and 0.8 nm (see supporting information for more details).

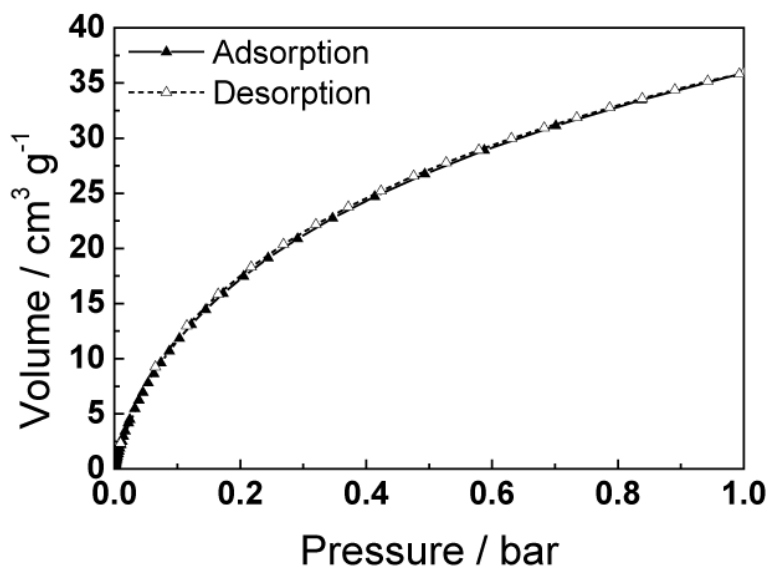


Figure 9. CO<sub>2</sub> sorption of poly-TPT at 273 K.

#### 4.1.3. Conclusion

Two new triazine derivatives were prepared by nucleophilic substitution reactions of cyanuric chloride with prop-1-yne and but-1-yne. Tris(1-propynyl)-1,3,5-triazine C<sub>3</sub>N<sub>3</sub>(C<sub>3</sub>H<sub>3</sub>)<sub>3</sub> (1) and tris(1-butynyl)-1,3,5-triazine C<sub>3</sub>N<sub>3</sub>(C<sub>4</sub>H<sub>5</sub>)<sub>3</sub> (2) are composed of planar molecular units arranged into supramolecular structures by hydrogen bonding.

C<sub>3</sub>N<sub>3</sub>(C<sub>3</sub>H<sub>3</sub>)<sub>3</sub> (1) involves planar fragments with disordered H positions at the CH<sub>3</sub>-groups. C<sub>3</sub>N<sub>3</sub>(C<sub>4</sub>H<sub>5</sub>)<sub>3</sub> (2) is also planar with tilted terminal and rather disordered CH<sub>2</sub>- and CH<sub>3</sub>-groups. The structures are characterized by a dense network of moderately strong hydrogen bonds which stabilize a layer like arrangement in both compounds. While (1) forms a layered zig-zag strand arrangement, (2) is built up from co-planar, parallel strands. The single crystal investigations are consistent with the molecular structures based on NMR and IR spectroscopy data. DTA and TG measurements suggest that tris(1-butynyl)-1,3,5-triazine is slightly more stable than tris(1-propynyl)-1,3,5-triazine.

C<sub>3</sub>N<sub>3</sub>(C<sub>3</sub>H<sub>3</sub>)<sub>3</sub> (1) was pyrolyzed in an inert atmosphere and a new triazine based polymer was isolated. NMR spectroscopy data suggest that a ring closing mechanism of the alkyne groups lead to 1,3,5-trimethylbenzene units as linkers. The

presence of ultramicropores in the as-obtained material merit future investigations into applications of poly-TPT-type materials as catalyst supports or CO<sub>2</sub> storage materials.

As a result of the above investigations, we have added another set of potential precursors and a polymerization route for the synthesis of new carbon nitride-type materials or carbon-based solids. Functionalization of triazines with alkynes establishes a new approach in carbon nitride chemistry, which previously has been focused on condensation reactions. Future research will be directed towards the use of alkyne-triazines as precursors for further polymeric carbon nitrides or building blocks for covalent organic networks. In addition, the formation of supramolecular architectures based on alkyne-triazines and other heterocyclic building blocks will be studied.

#### **4.1.4. Experimental Part**

##### **Preparation of tris(1-propynyl)-1,3,5-triazine (1):**

n-Butyllithium (33.9 mL, 84.7 mmol; 2.5M in hexane; Sigma–Aldrich) was added dropwise to a solution of prop-1-yne (4.74 mL, 77 mmol; ≥99%; Sigma–Aldrich) in THF (10 mL; ≥99%; Sigma–Aldrich) at -78 °C. The solution was stirred for 5 min. With the temperature maintained at -78 °C, a solution of anhydrous zinc chloride (10.50 g, 77 mmol; ≥ 99%; Sigma–Aldrich) dissolved in THF (20 mL) was added dropwise. The mixture was stirred for 15 min and then slowly warmed up to room temperature. [Pd(PPh<sub>3</sub>)<sub>4</sub>] (58 mg, 0.050 mmol; 99%; Sigma–Aldrich) and 2-propynyl zinc (10 mL, 5.00 mmol) were added to trichlorotriazine (184.41 mg, 1.00 mmol; 99%; Sigma–Aldrich) in THF (2 mL). The mixture was heated to reflux under a nitrogen atmosphere for 30 min. Subsequently, 0.1 M HCl (10 mL) was added and the reaction mixture was extracted with diethyl ether (3x20 mL). The combined organic layers were washed with brine (20 mL) and dried over MgSO<sub>4</sub>. The solvent was evaporated and the residue was purified by chromatography on silica gel (eluent: hexane/AcOEt, 8:2). The product was additionally purified by flash column chromatography.

HRMS (desorption electronimpact):  $m/z$  calcd: 195.22 ( $C_{12}H_9N_3$ ); found: 195.08.

#### **Preparation of tris(1-butynyl)-1,3,5-triazine (2):**

*n*-Butyllithium (8.8 mL, 22 mmol; 2.5M in hexane; Sigma–Aldrich) was added dropwise to a solution of but-1-yne (1.67 mL, 20 mmol; 98%; ABCR) in THF (10 mL;  $\geq 99\%$ ; Sigma–Aldrich) at  $-78\text{ }^\circ\text{C}$ . The solution was stirred for 5 min. With the temperature maintained at  $-78\text{ }^\circ\text{C}$ , a solution of anhydrous zinc chloride (2.72 g, 20 mmol;  $\geq 99\%$ ; Sigma–Aldrich) dissolved in 5 mL THF was added dropwise. The mixture was stirred for 15 min and then slowly warmed up to room temperature.  $[Pd(PPh_3)_4]$  (58 mg, 0.050 mmol; 99%; Sigma–Aldrich) and 2-butynyl zinc (10 mL, 5.00 mmol) were added to a three-necked flask containing trichlorotriazine (184.41 mg, 1.00 mmol; 99%; Sigma–Aldrich) in THF (2 mL). The mixture was heated to reflux under a nitrogen atmosphere for 30 min. Subsequently, 0.1M HCl (10 mL) was added and the reaction mixture was extracted with diethyl ether (3x20 mL). The combined organic layers were washed with brine (20 mL) and dried over  $MgSO_4$ . The solvent was evaporated and the residue was purified by chromatography on silica gel (eluent: hexane/AcOEt, 8:2). The product was additionally purified by flash column chromatography.

HRMS(ESI, positive):  $m/z$  calcd: 238.30 ( $C_{15}H_{15}N_3$ )  $[M+H]^+$ ; found: 238.13.

#### **Polymerization of TPT:**

Tris(1-propynyl)-1,3,5-triazine (1, 100 mg) was placed in a dried Schlenk flask and heated under argon atmosphere in a glass oven (Büchi) at  $250\text{ }^\circ\text{C}$  for one hour. The resulting black powder was suspended in DMF, filtered and successively washed with distilled water (3 x 30 mL), DMF (3 x 30 mL), THF (3 x 30 mL), DCM (3 x 30 mL) and dried in *vacuo*.

#### **Acknowledgements**

The authors would like to thank Dr. Peter Mayer (Department Chemie, LMU München) for collecting the X-ray diffraction and Christian Minke for NMR and SEM-

EDX measurements and the Deutsche Forschungsgemeinschaft (DFG) (project SCHN 377/12 and LO 1801/1) as well as the Fonds der Chemischen Industrie (FCI) for financial support.≥

**Supporting information**

Additional structural features and analytical data on (1), (2) and poly-TPT can be found in the supporting information.

#### 4.1.5. Bibliography

- [1] K. Schwinghammer, B. Tuffy, M.B. Mesch, E. Wirnhier, C. Martineau, F. Taulelle, W. Schnick, J. Senker, B.V. Lotsch, *Angew. Chem.* **2013**, 125, 2495; *Angew. Chem. Int. Ed.* **2013**, 52, 2435.
- [2] K. Schwinghammer, M. B. Mesch, V. Duppel, C. Ziegler, J. Senker, B. V. Lotsch, *J. Am. Chem. Soc.* **2014**, 136, 1730.
- [3] E. Kroke, M. Schwarz, *Coord. Chem. Rev.* **2004**, 248, 493.
- [4] G. Goglio, D. Foy, G. Demazeau, *Mater. Sci. Eng. R* **2008**, 58, 195.
- [5] S. Ren, M. J. Bojdys, R. Dawson, A. Laybourn, Y. Z. Khimyak, D. J. Adams, A. I. Cooper, *Adv. Mater.* **2012**, 1.
- [6] P. Kuhn, M. Antonietti, A. Thomas, *Angew. Chem.* **2008**, 120, 3499; *Angew. Chem. Int. Ed.* **2008**, 47, 3450.
- [7] P. Kuhn, A. Forget, D. Su, A. Thomas, M. Antonietti, *J. Am. Chem. Soc.* **2008**, 130, 3333.
- [8] P. Kuhn, A. Thomas, M. Antonietti, *Macromolecules* **2009**, 42, 319.
- [9] X. Wang, K. Maeda, A. Thomas, K. Takanabe, G. Xin, J. M. Carlsson, K. Domen, M. Antonietti, *Nat. Mater.* **2009**, 8, 76.
- [10] A. Thomas, A. Fischer, F. Goettmann, M. Antonietti, J.-O. Müller, R. Schlögl, J. M. Carlsson, *J. Mater. Chem.* **2008**, 18, 4893.
- [11] F. Goettmann, A. Thomas, M. Antonietti, *Angew. Chem.* **2007**, 119, 2773; *Angew. Chem. Int. Ed.* **2007**, 46, 2717.
- [12] S. J. Makowski, M. Lacher, C. Lermer, W. Schnick, *J. Mol. Struct.* **2012**, 1013, 19.
- [13] S. J. Makowski, P. Köstler, W. Schnick, *Chem. Eur. J.* **2012**, 18, 3248.
- [14] S. J. Makowski, E. Calta, M. Lacher, W. Schnick, *Z. Anorg. Allg. Chem.* **2011**, 638, 88.
- [15] J. Liebig, *Ann. Chem. Pharm.* **1834**, 10, 1.
- [16] J. Klason, *J. Prakt. Chem.* **1886**, 33, 285.

- [17] A. I. Finkel'shtein, N. V. Spiridoova, *Russ. Chem. Rev.* **1964**, *33*, 400.
- [18] L. Pauling, J. H. Sturdivant, *Proc. Natl. Acad. Sci USA* **1937**, *23*, 615.
- [19] L. Gmelin, *Ann. Pharm.* **1835**, *15*, 252.
- [20] W. Henneberg, *Ann. Chem. Pharm.* **1850**, *73*, 228.
- [21] B. V. Lotsch, M. Döblinger, J. Sehnert, L. Seyfarth, J. Senker, O. Oeckler, W. Schnick, *Chem. Eur. J.* **2007**, *13*, 4969.
- [22] E. Horvath-Bordon, E. Kroke, I. Svoboda, H. Fueß, R. Riedel, S. Neeraj, A. K. Cheetham, *Dalton Trans.* **2004**, 3900.
- [23] M. Döblinger, B. V. Lotsch, J. Wack, J. Thun, J. Senker, W. Schnick, *Chem. Commun.* **2009**, 1541.
- [24] E. Wirnhier, M. Döblinger, D. Gunzelmann, J. Senker, B. V. Lotsch, W. Schnick, *Chem. Eur. J.* **2011**, *17*, 3213; b) M. J. Bojdys, J.-O. Müller, M. Antonietti, A. Thomas, *Chem. Eur. J.* **2008**, *14*, 8177.
- [25] G. Algara-Siller, N. Severin, S. Y. Chong, T. Björkman, R. G. Palgrave, A. Laybourn, M. Antonietti, Y. Z. Khimiyak, A. V. Krasheninnikov, J. P. Rabe, U. Kaiser, A. I. Cooper, A. Thomas, M. J. Bojdys, *Angew. Chem.* **2014**, *126*, 7580; *Angew. Chem. Int. Ed.* **2014**, *53*, 7450.
- [26] S. Tragl, K. Gibson, H.-J. Meyer, *Z. Anorg. Allg. Chem.* **2004**, *630*, 2373; b) S. Tragl, K. Gibson, J. Glaser, G. Heydenrych, G. Frenking, V. Duppel, A. Simon, H.-J. Meyer, *Z. Anorg. Allg. Chem.* **2008**, *634*, 2754.
- [27] D. S. Brown, J. D. Lee, P. R. Russell, *Acta Cryst.* **1976**, *B32*, 2101.
- [28] C. Grundmann, E. Kober, *J. Org. Chem.* **1956**, *21*, 1392; b) J.-R. Galán-Mascarós, J.-M. Clemente-Juan, K. R. Dunbar, *J. Chem. Soc., Dalton Trans.* **2002**, *13*, 2710.
- [29] M. Ohkita, M. Kawano, T. Suzuki, T. Tsuji, *Chem. Commun.* **2002**, 3054.
- [30] A. T. Balaban, C. C. Rentia, E. Ciupitu, *Rev. Roum. Chim.* **1968**, *13*, 231.
- [31] M. Sonoda, A. Inabe, K. Itahashi, Y. Tobe, *Org. Lett.* **2001**, *3*, 2419.
- [32] B. V. Lotsch, W. Schnick, *Chem. Eur. J.* **2007**, *13*, 4956.

- [33] B. Jürgens, E. Irran, J. Senker, P. Kroll, H. Müller, W. Schnick, *J. Am. Chem. Soc.* **2003**, *125*, 10288.
- [34] T. Steiner, *Angew. Chem.* **2002**, *1*, 48; *Angew. Chem. Int. Ed.* **2002**, *42*, 58.
- [35] C. E. Garrett, K. Prasad, *Adv. Synth. Catal.* **2004**, *346*, 889.
- [36] C.-L. Lee , C. T. Hunt , A. L. Balch, *Inorg. Chem.* **1981**, *20*, 2498.

## 4.2. Polymerization of Tris(1-proynyl)-1,3,5-triazine by Alkyne-metathesis

### 4.2.1. Overview

Alkyne-substituted triazines of section 4.1. are potential precursors for hydrogen-free polymers with particular focus on triazine-based networks interconnected with acetylene units. The corresponding polymerization could be achieved by alkyne-metathesis, distinguishing it from thermal condensation reactions for networked carbon nitrides like melon<sup>[1]</sup> or PHI.<sup>[2]</sup>

Alkyne-metathesis, the exchange of terminal groups of two alkyne-containing compounds (see Figure 1), was first described by *Bayley* et al. in 1968.<sup>[3]</sup> Preliminary ideas included the use of tungsten oxide as catalyst. *Mortreux and Blanchard* have revised such metathesis reactions through utilisation of molybdenum hexacarbonyl as catalyst in 1974.<sup>[4]</sup> Further significant work by *Schrock* et al. marked the development of alkyne-metathesis by the use of tungsten catalysts such as tris(*tert*-butoxy)(neopentylidene)tungsten(VI) (see Figure 2a) which is up to now one of few commercially available catalysts.<sup>[5]</sup>

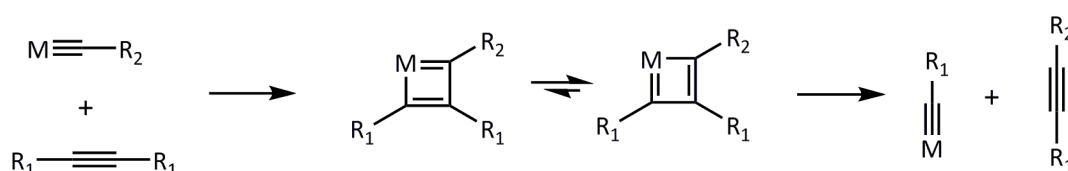


**Figure 1.** Reaction mechanism of alkyne-metathesis.

Subsequently, catalysts became more important and an increasing number of new effective catalysts, namely transition metal alkylidines, which enlarged the understanding of the reaction processes were characterized.<sup>[5,6]</sup> To avoid restraining interactions with polar side groups, catalysts with appropriate sterically hindering ligands like the molybdenum alkylidene complex pointed out in Figure 2b have been developed by *Fürstner* et al.<sup>[7,8]</sup>

Reactions by *Zhang* et al. that address porous organic polymers synthesized by molybdenum alkylidene catalyst (see Figure 2c) initiated the idea of the formation of porous polymeric compounds based on alkyne-triazines.<sup>[9]</sup>

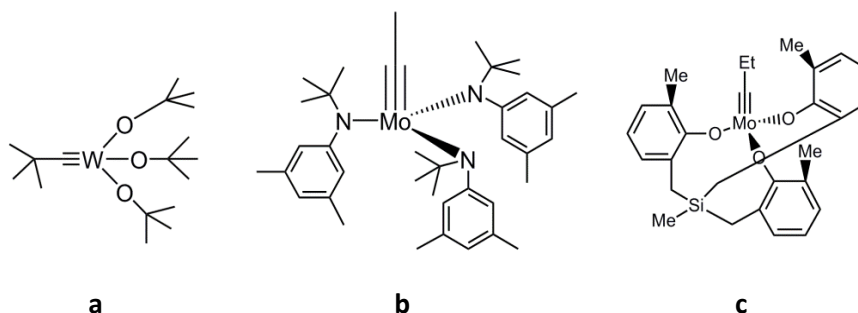


**Figure 2.** First catalysts for alkyne-metathesis.

Polymeric compounds which are derived from tris(1-propynyl)-1,3,5-triazine through alkyne-metathesis of residual propynyl-groups are rather likely. The formation of but-1-yne as side product shifts the equilibrium to the product side and therefore positively influences the polymerization process. The intended product is made up of  $C_3N_3$  units (see Figure 3), however intermediate compounds are no less interesting. The corresponding  $(C_6N_3)_n$  polymer is pretty similar to hypothetical graphyne<sup>[10]</sup> (see Figure 4) which is built up of graphite associated with acetylene units. Graphyne is predicted to be an interesting material for electronic applications such as conductivity elements or for nonlinear optics.

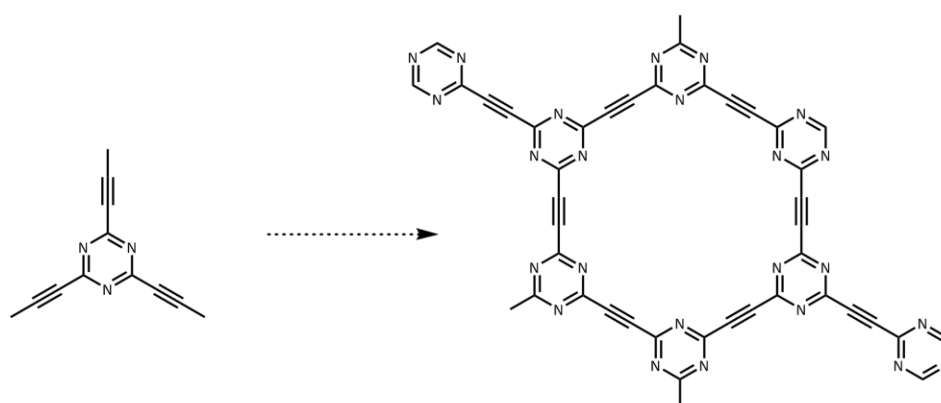


**Figure 3.** Reaction pathway and final polycondensation product.

Due to the postulated pore size of 1.2 nm and a layer like assembly the corresponding polymer is a potential catalyst for photocatalytic water splitting as well. Several polymeric carbon nitrides like PTI or melon used as metal-free catalysts are already known.<sup>[11-14]</sup> Networked materials with suitable bandgaps as well as porous materials which applies to hypothetical  $(C_6N_3)_n$  are very suitable for this purpose.

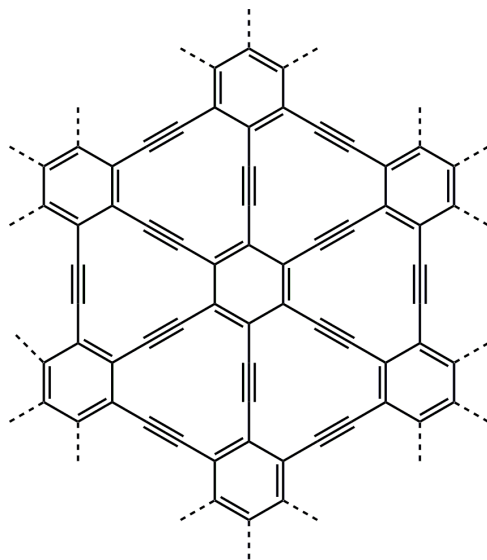


**Figure 4.** 2-dimensional structure of graphyne.

#### 4.2.2. Experimental section

In a dried schlenk flask 10 mg (1.92 mmol) of tris(1-propynyl)-1,3,5-triazine was suspended in 0.5 ml extra dry toluol or in mesitylene/dioxane 1:1 mixture in a second reaction series (see Table 1). In a second dried schlenk flask 10 mg of catalyst A, B, or C (catalyst A and B were prepared by the Fürstner group, MPI Mülheim; Catalyst C was synthesized according to Zhang<sup>[9]</sup>) (see Figure 5) were dissolved in 0.5 ml of toluol or accordingly in mesitylene/dioxane 1:1 mixture.

Previously, catalyst B and C were premixed with molybdenum alkylidene catalyst and corresponding silanole ligands (see Figure 5) and suspended in corresponding solvents. All reaction steps were conducted under argon atmosphere.

The catalysts were added to tris(1-propynyl)-1,3,5-triazine and the mixtures were heated in an oil bath. Corresponding reaction conditions are illustrated in Table 1. In all reactions gaseous side products could pass off over a pressure relief valve. Additionally, every 30 minutes resulting gases were removed with a vacuum pump.

**Table 1.** Reaction conditions for alkyne-metathesis of tris(1-propynyl)-1,3,5-triazine.

solvent	Temp.(°C)	time (h)	catalyst	progress (GC)
Tol	50	14	A	---
Tol	RT	14	B	94%
Mes/Diox 1:1	50	14	A	---
Mes/Diox 1:1	100	18	B	85%
Tol	110	18	C	100%
Tol	130	18	B	100%

Further reactions were conducted in special overpressure vials. The reaction progress was permanently observed by GC/MS. Finally the precipitants were filtrated and washed with THF and ether (2-Methoxy-2-methylpropane).

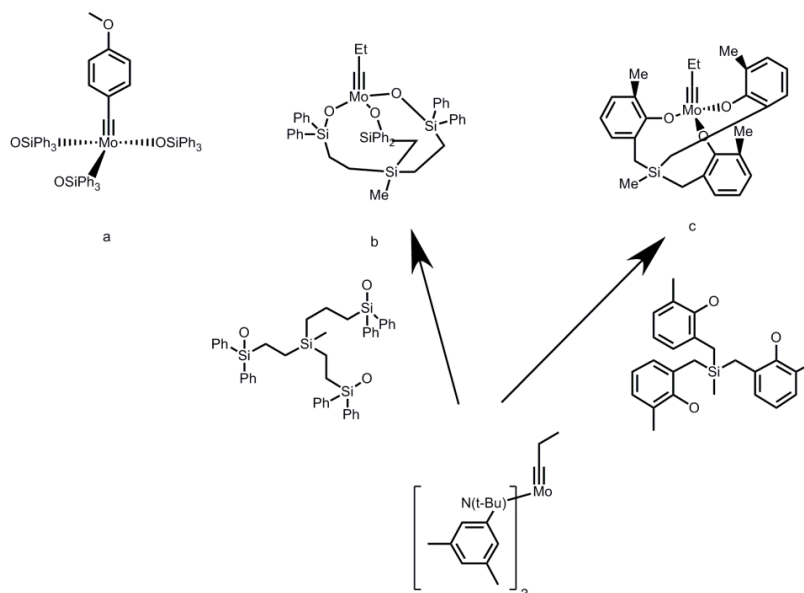


**Figure 5.** Used catalysts for alkyne-metathesis.

### 4.2.3. Results and Discussion

First reactions with tris(*tert*-butoxy)(neopentylidin)tungsten(VI) (Sigma-Alrich) have not been successful. The brownish colored solvated reactant tris(1-propynyl)-1,3,5-triazine immediately turned black after addition of the catalyst and no solvent or gaseous reaction which is essential for metathesis reactions could be observed. It can be assumed that the catalytic properties have been reduced due to air sensitivity. Several further experiments with catalyst A, B and C (see Figure 5 and experimental section) were conducted and interesting observations could be elaborated as follows.

In all reactions gas evolution and especially precipitation of a black solid could be observed which indicated a successful reaction progress. Especially, catalyst B and C could be regarded as suitable due to GC/MS monitoring which verifies the complete conversion of the reactant. 130 °C for 18 h could be figured out as the most effective reaction conditions. Gaseous side products have been removed using a pressure relief valve connected with a vacuum pump at first reaction series. To enhance the polymerization progress further reactions were conducted under closed system conditions in a special pressure vial. However, no significant enhancement of the reaction rate could be observed compared to an open system.

Nevertheless, mass-spectrometry as well as FTIR-spectroscopy of precipitated products confirm the successful process of alkyne-metathesis. A variety of mass spectrometry measurements (ESI, MALDI-TOF) present that catalyst A and B lead to a mixture of oligomeric compounds consisting of seven to 15 unit oligomers (see Figure 6). The corresponding mass values range between 600 and 2300 g/mol. Exact masses deviate from those of oligomers due to associated residual groups resulting from the endgroups of the catalysts (see Figure 6).

Sorption analysis shows no porosity properties therefore linear structures are more likely than 2 or 3-dimensional networks.

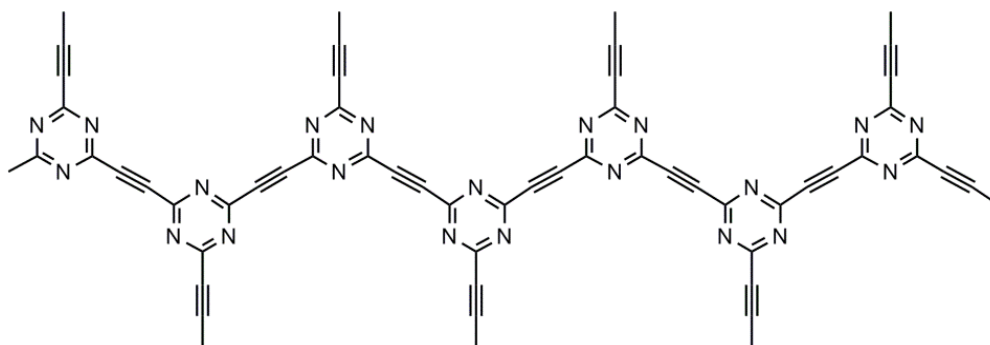


**Figure 6.** Seven unit oligomeric structure of catalyst B.

FTIR-data were recorded on a BX II FTIR spectrometer (Perkin Elmer) equipped with a DuraSampler diamond ATR. The spectrum illustrated in Figure 7 (recorded with product of catalyst B) agrees well with triazine-based materials.<sup>[15]</sup> Very strong and sharp bands occurring between 790 and 1700  $\text{cm}^{-1}$  are typical bending and stretching vibrations of *s*-triazine rings. Most interesting vibrational bands can be found at 2300  $\text{cm}^{-1}$  which corresponds to alkyne-groups.

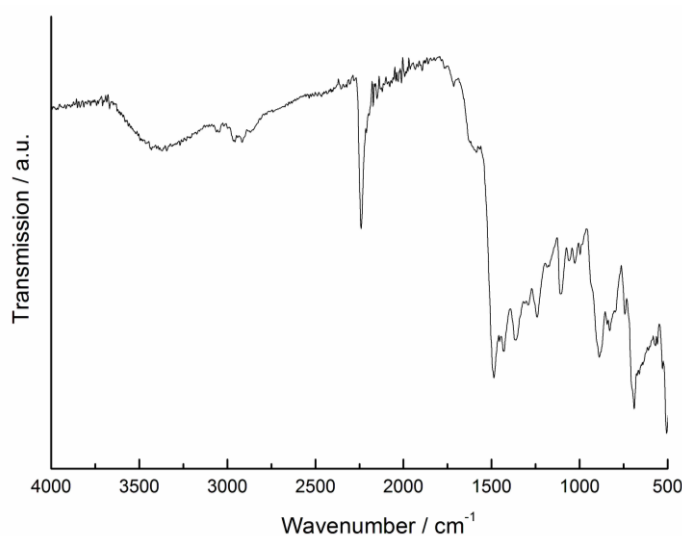


**Figure 7.** FTIR spectrum of oligomeric compound (catalyst B).

The FTIR spectrum of the product of catalyst A shows similar vibrations, only catalyst C results in no alkyne vibration and even no more triazine vibrations. Therefore catalyst A und B are best suited for extended metathesis reactions.

#### 4.2.4. Future plans

To summarize, catalyst B is the most suitable catalyst and first oligomeric compounds could be established. Nevertheless, the major aim is enlarging the polymerization from oligomeric to the polymeric compound  $(C_6N_3)_n$ . Reaction series with predominantly catalyst B, as well as catalyst A, have to be extended with different reaction conditions. More polar solvents which prevent precipitation of oligomeric compounds are possibly capable of promoting the polymerization process. It is also likely that pressure schlenk tubes are more suitable due to high sensitivity of the catalysts. Finally, further suitable catalysts, beside A and B, remain to be applied.

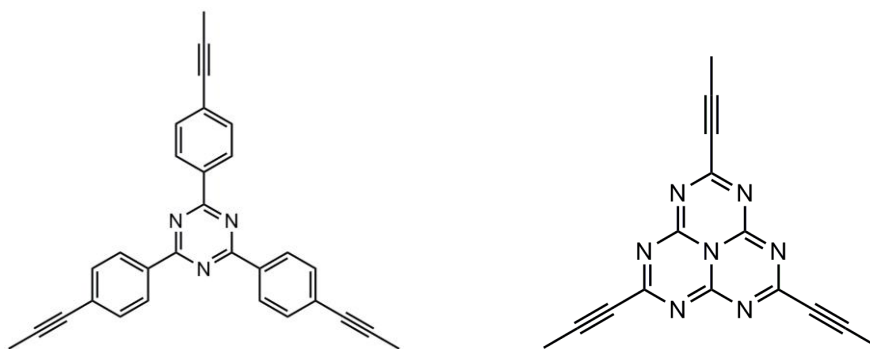


**Figure 6.** Propynyl-phenyl-triazine and propynyl-heptazine as potential precursors for alkyne-metathesis.

Further ideas are dealing with the use of other reactants. To avoid a possible coordination of metal ions of the catalysts by nitrogen atoms of the triazine-unit of tris(1-propynyl)-1,3,5-triazine, propynyl-phenyl-triazine (see Figure 6) could be a suitable alternative compound. Due to shielded nitrogen atoms catalysts are possibly more effective and propynyl-phenyl-triazine is also capable of forming porous polymeric compounds. However, propynyl-phenyl-triazine has not been successfully synthesized and work is still in progress. Additionally, heptazine-based alkynes rise particular attention due to interesting structural properties compared to corresponding triazine compounds and they are potential precursors for alkyne-metathesis as well.

#### 4.2.5. Bibliography

- [1] B. V. Lotsch, M. Döblinger, J. Sehnert, L. Seyfarth, J. Senker, O. Oeckler, W. Schnick, *Chem. Eur. J.* **2007**, *13*, 4969.
- [2] E. Wirnhier, M. Döblinger, D. Gunzelmann, J. Senker, B. V. Lotsch, W. Schnick, *Chem. Eur. J.* **2011**, *17*, 3213.
- [3] F. Penella, R.L. Banks, G.C. Bailey, *J. Chem. Soc., Chem. Commun.* **1968**, 1548.
- [4] A. Mortreux, M. Blanchard *J. Chem. Soc., Chem. Commun.* **1974**, 786.
- [5] J. H. Wengrovius, J. Sancho, R. R. Schrock, *J. Am. Chem. Soc.*, **1981**, *103*, 13, 3932; R. R. Schrock, D. N. Clark, J. Sancho, J. H. Wengrovius, S. M. Rocklage, S. F. Pedersen, *Organometallics*. **1982**, *1*, 1645.
- [6] McCullough, R. R. Schrock, *J. Am. Chem. Soc.* **1984**, *106*, 4067.
- [7] A. Fürstner, C. Mathes, C. W. Lehmann, *Chem. Eur. J.* **2001**, *7*, 5299.
- [8] A. Fürstner, C. Mathes, C. W. Lehmann, *J. Am. Chem. Soc.* **1999**, *121*, 9453.
- [9] Y. Zhu, H. Yang, Y. Jin, W. Zhang, *Chem. Mater.* **2013**, *25*, 3718.
- [10] M. Ohkita, M. Kawano, T. Suzuki, T. Tsuji, *Chem. Commun.* **2002**, 3054.
- [11] X. Wang, K. Maeda, A. Thomas, K. Takanabe, G. Xin, J. M. Carlsson, K. Domen, M. Antonietti, *Nat. Mater.* **2009**, *8*, 76.
- [12] A. Thomas, A. Fischer, F. Goettmann, M. Antonietti, J.-O. Müller, R. Schlögl, J. M. Carlsson, *J. Mater. Chem.* **2008**, *18*, 4893.
- [13] F. Goettmann, A. Thomas, M. Antonietti, *Angew. Chem.* **2007**, *119*, 2773; *Angew.Chem. Int. Ed.* **2007**, *46*, 2717.
- [14] K. Schwinghammer, B. Tuffy, M.B. Mesch, E. Wirnhier, C. Martineau, F. Taulelle, W.Schnick, J. Senker, B.V. Lotsch, *Angew. Chem.* **2013**, *125*, 2495; *Angew. Chem. Int.Ed.* **2013**, *52*, 2435.
- [15] B. V. Lotsch, W. Schnick, *Chem. Eur. J.* **2007**, *13*, 4956.

## **5. Investigations into the Polymerization Process of Carbon Nitrides**

Besides new precursor compounds for polymeric carbon nitrides, already elucidated polymerization processes play a significant role in carbon nitride chemistry and have to be investigated more precisely. This chapter deals with a novel approach which applies thermally induced decomposition reactions of melon. New intermediate phases as well as a deeper understanding regarding the synthesis of new highly condensed phases are of special interest.

Through reversibility reactions a better insight into condensation steps has been obtained. To initiate decomposition reactions bases like lithium nitride or lithium amide were used. Thermal treatment and further extreme parameters were elaborated to initiate a complete decomposition to cyanamides. Ammonothermal reactions prevent the complete decomposition to cyanamide and the triazine-core remains stable.

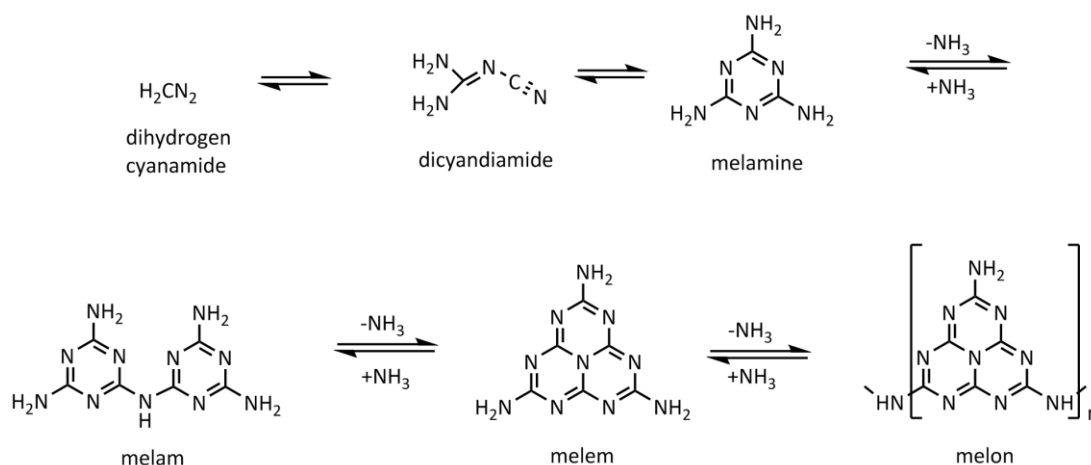
## 5.1. Decomposition of Melon

### 5.1.1. Introduction

#### Condensation mechanism

Thermal condensation reactions for the synthesis of novel polymeric C/N/H-materials have been extensively discussed in literature.<sup>[1,2]</sup> Several intermediate structures<sup>[3-9]</sup> as well as first polymers have been described in detail.<sup>[10-13]</sup>

The formation of melamine which could be generated by thermal treatment of dihydrogen cyanamide, dicyandiamide or pyrolysis of urea is the initial step for condensation. Continuing thermal treatment leads to melam, melem and the 1D polymer melon (see Scheme 1).



**Scheme 1.** Condensation scheme of C/N/H materials.

To achieve a better understanding of thermal reactions of carbon nitrides decomposition of melon was investigated. For this purpose a separation of the polymerization scheme is of major importance.

In particular dihydrogen cyanamide, dicyandiamide and melamine are in equilibrium and can be prepared by addition reactions. Dicyandiamide is built up of two parts of dihydrogen cyanamide, likewise C and N ratio of melamine and dicyandiamide are identical. Further reactions forming melam, melem and melon are induced by condensation with release of ammonia.

Decomposition of melon was initiated by deprotonation of the heptazine ring with bases like lithium amide or lithium nitride by variation of experimental parameters (pressure, temperature, ratio of educts). In respect of relevance of ammonia for condensation ammonothermal reactions are discussed in detail in the following section.

### 5.1.2. Results and Discussion

#### Thermal and high-pressure treatment of melon

Thermally induced decomposition reactions of melon with bases like lithium amide or lithium nitride were first realized in closed silica ampoules. All reactions indicate decomposition to lithium carbodiimide as could be shown by powder X-ray diffractometry. Most significant reaction conditions are summarized in Table 1. Different molecular ratios and temperatures between 400 and 700 °C were investigated. Decomposition of melon begins at 500 °C. The entire quantity was decomposed at 700 °C.

**Table 1.** Reaction conditions in closed ampoules.

<i>molar ratio melon:Li<sub>3</sub>N</i>	<i>temperature [°C]</i>	<i>time [h]</i>	<i>product</i>
1 : 6	500	24	Li <sub>3</sub> N/ melon/ Li <sub>2</sub> CN <sub>2</sub>
1 : 6	700	48	Li <sub>2</sub> CN <sub>2</sub>

By high-pressure and high-temperature reactions of melon with calcium nitride the formation of calcium carbodiimide was observed. We conducted the deprotonation step of melon under high pressure and temperature by employing the multianvil technique represented in the experimental section.<sup>[14]</sup>

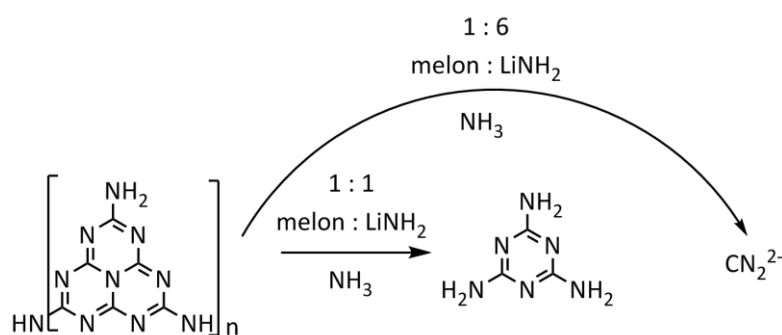
Consequently, high-pressure reactions extended the information on decomposition of melon. The small acyclic species carbodiimide initially forms with bases and further harsh conditions like high pressure or temperatures.

### Ammonothermal treatment of melon

Due to different synthesis steps for melon, first by forming melamine or dihydrogen cyanamide by addition reactions and secondary by further condensation reactions, the decomposition of melon to melamine has to be conducted in a new unusual approach.

The condensation of melamine is associated with release of ammonia, therefore ammonia pressure probably plays a significant role for decondensation reactions. Consequently, ammonothermal reactions of melon in a steel autoclave with a variation of lithium amide / melon ratio (see Table 2) were performed. Detailed experimental data are summarized in the experimental section.

Depending on the amount and molar ratio of bases or ammonia and melon, melon decomposes either partially to melamine or entirely to carbodiimide. An excess of lithium amide led to a complete decomposition of melon and the comprising heptazine ring to lithium carbodiimide (see Scheme 2). Up to three equivalents of lithium amide to one part melon the decomposition product melamine could be achieved. All products were identified by powder X-ray diffraction combined with FTIR- and solid-state NMR measurements.



**Scheme 2.** Decomposition of melon at autoclave reactions.

Reaction temperatures and reaction durations affect the decomposition process as well. Only at temperatures of above 500 °C and for reaction times of 48 h decomposition of melon was observed.

However, as expected, the most significant parameter for the reactions was the  $\text{NH}_3$  pressure which rises to 70 bar during the reactions. Ammonia pressure acts against

the complete decomposition of the heptazine ring (see Scheme 2) and the triazine-based intermediate product melamine was obtained instead of lithium carbodiimide.

**Table 2.** Reaction conditions for the decomposition of melon.

<i>Molar ratio [melon:LiNH<sub>2</sub>]</i>	<i>temperature [°C]</i>	<i>time [h]</i>	<i>product</i>
1 : 1	500	48	melamine
1 : 6	500	100	Li <sub>2</sub> CN

Thus, the reverse reaction of the condensation process starting from melon yielding melamine and carbodiimide could be demonstrated. Based on all presented experiments which could not lead to heptazine-based materials like melem or the dimeric compound melam it could be shown that carbodiimide and the triazine ring are most stable in this group of materials.

### 5.1.3. Experimental Part

#### Ammonothermal reactions

Melon [C<sub>6</sub>N<sub>7</sub>(NH<sub>2</sub>)(NH)]<sub>n</sub> synthesized starting from melamine (Fluka, 98 %) according to literature,<sup>[25]</sup> and LiNH<sub>2</sub> (Sigma-Aldrich, 95 %) were ground together in a glove box with dry argon atmosphere and filled in a 75 ml steel autoclave (Parr instrument co., 0.075 l, 586 bar) (see Table 3).

The autoclave was evacuated and NH<sub>3</sub> (air liquide, 99.98 %, micro torr gas purifier) (2 bar) was filled in for 20 min at -78 °C using an acetone/dry ice bath. After warming up to room temperature the reaction vessel was heated to 500 °C with a rate of 1 °C/min (see table 1). After 6 – 100 h (see Table 3) the reaction was cooled down to room temperature with 1 °C · min<sup>-1</sup>.

**Table 3.** Reaction conditions.

<i>melon</i> [mg]/[mmol]	<i>LiNH<sub>2</sub></i> [mg]/[mmol]	<i>Temperature</i> [°C]	<i>time</i> [h]
150/0.75	17/0.75	500	48
120/0.60	83/3.60	500	100
120/0.60	14/0.60	500	6
120/0.60	14/0.60	400	48

### Ampoule preparation

Melon  $[C_6N_7(NH_2)(NH)]_n$  and  $LiN_3$  (most significant experiments see Table 4) were ground together in a glove box with dry argon atmosphere and filled into dried, graphitized silica ampoules (outer diameter: 16 mm, inner diameter: 12 mm). The ampoules were sealed under vacuum at a length of 120 mm and heated to 400 - 700 °C at a rate of 2 °C min<sup>-1</sup>. After 24 - 48 h the ampoules were slowly cooled (1 °C · min<sup>-1</sup>) to room temperature.

**Table 4.** Reaction conditions.

<i>melon</i> [mg]/[mmol]	<i>Li<sub>3</sub>N</i> [mg]/[mmol]	<i>temperature</i> [°C]	<i>time</i> [h]
33.5/0.16	8.6/1.00	400	24
33.5/0.16	8.6/1.00	500	24
33.5/0.16	8.6/1.00	700	48

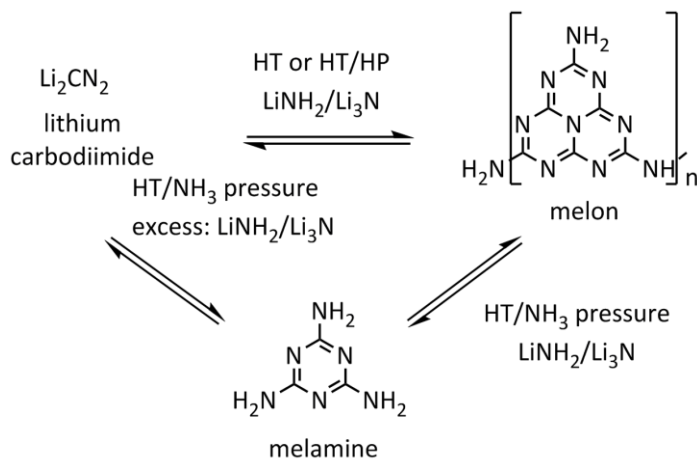
### High-pressure reactions

Decomposition reactions of melon  $[C_6N_7(NH_2)(NH)]_n$  under high-pressure and high-temperature were investigated by employing the multianvil technique in a Walker-type module (Voggenreiter, Mainleus) combined with a 1000 t press.<sup>[14]</sup>

The starting material was subjected to a temperature of 600 °C at 7.7 GPa for 120 min.

### 5.1.4. Conclusion

In this section the reverse reactions of condensation processes of the polymeric C/N/H material melon were investigated as illustrated in Scheme 3. Decomposition of melon was conducted by deprotonation reactions with bases and a variety of reaction conditions.



**Scheme 3.** Thermally induced reactions of melon.

Based on the synthesis pathway of melon the reversibility was conducted in two different parts. The first step of synthesis is the addition reaction of dihydrogen cyanamide and dicyandiamide to melamine. The decomposition of melon into these non cyclic initial compounds was achieved by thermal or high pressure reactions with bases. The second reaction part for the synthesis of melon is the condensation of melamine under release of ammonia.

To investigate decompositions to higher condensed materials like melamine ammonothermal reactions were conducted using autoclaves. It could be shown that ammonia as solvent acts against the complete decomposition so that the triazine core remains intact. An excess of bases led to decomposition to carbodiimide which is the most stable compound of this group of materials.

Therefore the reverse reaction of melon to carbodiimide and triazine based materials with suitable reaction conditions could be demonstrated. It could be shown that ammonia pressure plays a significant role for the decomposition of melon to the cyclic material melamine.

These deeper insights into reaction properties led to a better understanding of possible synthesis routes of new networked materials. Further plans will be focused on potentially less stable intermediate phases.

### 5.1.5. Bibliography

- [1] E. Kroke, M. Schwarz, *Coord. Chem. Rev.* **2004**, 248, 493.
- [2] G. Goglio, D. Foy, G. Demazeau, *Mater. Sci. Eng. R* **2008**, 58, 195.
- [3] J. Wagler, N. E. A. El-Gamel, E. Kroke, *Z. Naturforsch.* **2006**, 61b, 975.
- [4] A. Sattler, W. Schnick, *Z. Anorg. Allg. Chem.* **2006**, 632, 1518.
- [5] E. Horvath-Bordon, E. Kroke, I. Svoboda, H. Fueß, R. Riedel, S. Neeraj, A. K. Cheetham, *Dalton Trans.* **2004**, 3900.
- [6] E. Horvath-Bordon, E. Kroke, I. Svoboda, H. Fuess, R. Riedel, *New J. Chem.* **2005**, 29, 693.
- [7] A. Sattler, W. Schnick, *Eur. J. Inorg. Chem.* **2009**, 4972.
- [8] S. J. Makowski, W. Schnick, *Z. Anorg. Allg. Chem.* **2009**, 635, 2197.
- [9] E. Irran, B. Jürgens, W. Schnick, *Solid State Sciences* **2002**, 4, 1305.
- [10] U. Berger, W. Schnick, *J. Alloys Comp.* **1994**, 206, 179.
- [11] B. V. Lotsch, M. Döblinger, J. Sehnert, L. Seyfarth, J. Senker, O. Oeckler, W. Schnick, *Chem. Eur. J.* **2007**, 13, 4969.
- [12] E. Wirnhier, M. Döblinger, D. Gunzelmann, J. Senker, B. V. Lotsch, W. Schnick, *Chem. Eur. J.* **2011**, 17, 3213.
- [13] M. Döblinger, B. V. Lotsch, J. Wack, J. Thun, J. Senker, W. Schnick, *Chem. Commun.* **2009**, 1541.
- [14] a) N. Kawai, S. Endo, *Rev. Sci. Instrum.* **1970**, 41, 1178; b) D. Walker, M. A. Carpenter, C. M. Hitch, *Am. Mineral.* **1990**, 75, 1020; c) D. Walker, *Am. Mineral.* 1991, 76, 1092; d) D. C. Rubie, *Phase Transitions* **1999**, 68, 431; e) H. Huppertz, *Z. Kristallogr.* **2004**, 219, 33.

## 6. Discussion and Outlook

In this thesis the information on polymerization processes of carbon nitrides has been enlarged. Initially, the knowledge of *s*-triazine and *s*-heptazine based precursors could be extended through investigations of different synthesis strategies including heteroatom incorporation. New intermediate *s*-triazine-based phases as well as *s*-heptazine precursors with interesting structural properties like intermolecular interactions could be characterized.

In addition, reaction types which do not belong to classical inorganic methods were elaborated and it could be demonstrated that the combination of organic and inorganic chemistry leads to new materials which exhibit promising properties. In particular, organic cross coupling reactions generated new alkyne-functionalized triazines. Through appropriate thermal and metathesis reactions first condensed products were obtained. This projects are still ongoing and new polymers are expected.

Thermal polymerization processes have also been kept in mind and their reversibility was studied in detail. Decomposition reactions of melon have been worked out and intermediate phases could be identified. Thus, decomposition establishes new insights into reaction steps and significant work remains to be done.

### 6.1. Intermediate Phases and Salt-like Precursors for Carbon Nitrides

The quest for  $C_3N_4$  whose postulated hardness exceeds even that of diamond led to an increasing interest in carbon nitride chemistry.<sup>[1-3]</sup>  $C_3N_4$  can be described as final deamination product of a series of carbon nitride precursors.<sup>[4,5]</sup> Most stable compounds – even the first polymeric material melon – have already been

described in the early 19<sup>th</sup> century.<sup>[6-12]</sup> Thermal treatment of precursors like cyanamides, urea or thiocyanates led to *s*-triazine and *s*-heptazine-based materials like melamine, melam or melem. Recent works are dealing with further precursors like tricyanomelones or cyameluric salt-like compounds.<sup>[13-16]</sup>

In this study synthesis of new *s*-triazine- and *s*-heptazine-based precursors could be elaborated. Crystals of an alkaline-earth tricyanomelone and alkaline-earth cyamelurate were obtained by metathesis in aqueous solution with subsequent slow evaporation. Both structures exhibit crystal water molecules while first divalent Zn<sup>2+</sup>- and Ca<sup>2+</sup>- cyamelurates characterized by *Sattler* et al. embedded ammonia molecules due to synthesis in aqueous solution of ammonia.<sup>[16]</sup> Hydrogen bridges, van-der-Waals interactions as well as different coordination sites lead to numerous possible structure variations of such compounds. A previously unknown tilted zig-zag arrangement stabilized by hydrogen bridges was elucidated in strontium-cyamelurate tetrahydrate.

Beside their suitability as a precursor material, the large structural variety make these compounds interesting. Side-group carrying molecules are of interest for coordination compounds. One example to be mentioned is supramolecular arrangement of triazine based materials with heterocycles.<sup>[15]</sup> Due to the side chains tricyanomelones and cyamelurates are furthermore suitable for metal coordination. Further metathesis reactions with Eu<sup>2+</sup>-derivatives in order to obtain luminescence properties was not successful until now and are a demanding task for future research. Also the intended use as precursor for new polymeric carbon nitrides or as coordination compound could not be demonstrated so far.

Additionally, novel intermediate phases were identified by pyrolysis or thermal treatment of carbon nitride materials with foreign atoms. The formation of protonated melamium and melaminium adduct phases with embedded ammonium chloride or thiocyanate ions have provided an explanation for the basicity of melamin which is more basic than melem. The formation of melam can thus be promoted by Brønsted acids. Due to semiconducting properties carbon nitride type materials are suitable for photocatalytic water splitting. Chemical doping by

introduction of sulfur<sup>[17,18]</sup> is proposed to tune catalytic properties and is therefore a further major aim in carbon nitride chemistry. However the exchange of nitrogen with atoms in nitrides was unsuccessful so far and must be actively pursued.

## 6.2. Alkyne-triazines on the Way to New Triazine-based Networks

In this project new types of precursors exhibit new approaches for CN chemistry. First part is focused on functionalization of *s*-triazine based materials with alkynes. Herein organic cross coupling reactions yielded two new alkyne-triazines with interesting molecular structures. Triazines with residual organic side groups are built up of layer-like assemblies stabilized through hydrogen-bridges. Additionally, electronic constitution leads to van-der-Waals interactions and influences innermolecular stabilizations of alkyne-triazines. Comprehensive studies using organic syntheses might enable access to a great variety of new functionalized triazines with interesting structural properties. But it needs to be considered that organic reactions are frequently hindered due to electron poor aromatic carbon nitrides like triazines.

Through corresponding side groups of alkyne-triazines applications as building blocks for covalent organic frameworks are possible. It can also be assumed that

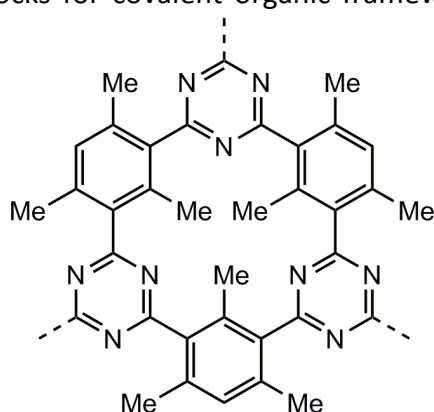


**Figure 1.** Tentative polymerization product of alkyne-triazines.

functional side groups and nitrogen atoms represent coordination sites and supramolecular networks with suitable ligands are possible.

Also new polymeric compounds are achievable from alkyne-triazines. A first disordered triazine-based polymer (poly-TPT) connected with mesitylene units as linkers could be prepared by thermal treatment.

However this is a tentative description of the polymer due to its disordered and amorphous assembly. Yielding of defined crystalline polymers are rather unlikely.

Such type of polymers with narrow pore size distributions are of great interest for e.g. catalytic applications. Just recently, carbon nitride type polymers like PTI<sup>[19]</sup> or melon<sup>[20]</sup> have already been discussed for photocatalytic water splitting<sup>[21]</sup> and the high surface and porosity properties of poly-TPT makes it an interesting compound for applications in material science.

Additionally, hydrogen-free polymers available through novel suitable reaction schemes differing from thermal treatment are conceivable. Therefore extended polymers of triazine rings connected by acetylene groups pretty similar to graphyne<sup>[22]</sup> were focused on (see Figure 1).

First attempts by alkyne metathesis of alkyne-triazines with a variation of catalysts were successful but there still lies plenty of work ahead. An alkylidene catalyst with a new silanol ligand has proved to be extremely promising. Catalysts for alkyne-

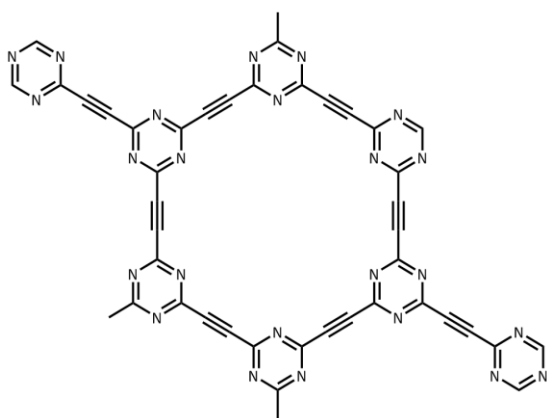


**Figure 1.** Possible polymerization product of alkyne-triazines by alkyne-metathesis.

metathesis are continuously improving and might provide access to more extended polymers. Up to now only a linear oligomer could be synthesized. Probably an extended polymer cannot be established due to steric hindrance between of the alkyne units of the triazine and the catalysts.

Therefore functionalized triazine-based compounds such as alkynyl-phenyl-triazines or heptazine-based alkynes have to be considered as new reactants for metathesis reactions and corresponding reactions are in progress. Thereby a further major challenge is caused by the catalysts which are extremely susceptible to water and oxygen and has to be handled under inert atmosphere with dried and degassed solvents.

To summarize, it has been shown that organic syntheses have the potential to yield new monomeric and even polymeric compounds. Certainly, new organic syntheses and different polymerisation routes without deammonation are capable of forming new networked materials. Therefore, the combination of inorganic and organic chemistry is a possible pathway to establish new compounds with interesting properties.

### **6.3. Investigations into the Polymerization Process of Carbon Nitrides**

Polymerisation processes of carbon nitrides have been extensively debated over the last decades due to interest in networked compounds and corresponding intermediate phases. However, reversibility of condensation of higher condensed materials has never been examined. Especially, the quest for melem oligomers demonstrates that reaction pathways are not fully understood yet and much remains to be done. Therefore this study is dealing with decomposition of melon.

Decomposition reactions were initiated by deprotonation with bases. Additionally, a variety of reaction parameters played a significant role. Thermal treatment or the use of unusual solvents best accessible by using autoclaves were necessary. The pressure in autoclave reactions much higher than in ampoules and probably decomposition proceeds faster. Due to utilization of ammonia as solvent, the condensation terminates at the lowest condensation product melamine. High pressure reactions using the multianvil press played a significant role in this thesis. Thereby extreme conditions permit complete decomposition of ring-shaped molecules.

A detailed description of different reaction steps could be carved out and a stepwise decomposition of melon into stable compounds could be observed. Nevertheless, the major aim of elucidation of new intermediate phases or oligomeric compounds could not be carved out and it is still not known whether this problem can be avoided or not. Future plans include reversibility reactions on PHI<sup>[23]</sup>

and PTI<sup>[19]</sup> because it is not completely proved if melem exists as intermediate phase in the formation of PTI. By means of decomposition reactions it could be clarified whether the triazine-based PTI is formed from *s*-triazines or *s*-heptazines.

In summary, suitable reaction conditions for decomposition could be figured out. Further reactions could clarify unsolved questions in polymerisation processes and additionally new oligomeric compounds could be achievable. Another important issue is an investigation of further reaction methods which are capable to initiate decomposition.

**Bibliography**

- [1] a) A. Y. Liu, M. L. Cohen, *Science* **1989**, *245*, 841; b) A. Y. Liu, M. L. Cohen, *Phys. Rev. B* **1990**, *41*, 10727, c) A. Y. Liu, R. M. Wentzcovitch, *Phys. Rev. B* **1994**, *50*, 10362.
- [2] D. M. Teter, R. J. Hemley, *Science* **1996**, *271*, 53.
- [3] C.-M. Sung, M. Sung, *Mater. Chem. Phys.* **1996**, *43*, 1.
- [4] E. Kroke, M. Schwarz, *Coord. Chem. Rev.* **2004**, *248*, 493.
- [5] G. Goglio, D. Foy, G. Demazeau, *Mater. Sci. Eng. R* **2008**, *58*, 195.
- [6] J. Liebig, *Ann. Chem. Pharm.* **1834**, *10*, 1.
- [7] J. Liebig, *Ann. Chem. Pharm.* **1844**, *50*, 337.
- [8] J. Liebig, *Ann. Chem. Pharm.* **1845**, *53*, 330.
- [9] J. Liebig, *Ann. Chem. Pharm.* **1847**, *61*, 262.
- [10] J. Liebig, *Ann. Chem. Pharm.* **1855**, *95*, 257.
- [11] L. Gmelin, *Ann. Pharm.* **1835**, *15*, 252.
- [12] W. Henneberg, *Ann. Chem. Pharm.* **1850**, *73*, 228.
- [13] A. Sattler, W. Schnick, *Eur. J. Inorg. Chem.* **2009**, 4972.
- [14] S. J. Makowski, W. Schnick, *Z. Anorg. Allg. Chem.* **2009**, *635*, 2197.
- [15] S. J. Makowski, D. Gunzelmann, J. Senker, W. Schnick, *Z. Anorg. Allg. Chem.* **2009**, *635*, 2434.
- [16] A. Sattler, M. R. Budde, W. Schnick, *Z. Anorg. Allg. Chem.* **2009**, *635*, 1933.
- [17] G. Liu, P. Niu, C. H. Sun, S. C. Smith, Z. G. Chen, G. X. Lu, H. M. Cheng, *J. Am. Chem. Soc.* **2010**, *132*, 11642.
- [18] Y. Zhang, T. Mori, J. Ye, M. Antonietti, *J. Am. Chem. Soc.* **2010**, *132*, 6294.
- [19] E. Wirnhier, M. Döblinger, D. Gunzelmann, J. Senker, B. V. Lotsch, W. Schnick, *Chem. Eur. J.* **2011**, *17*, 3213.

- [20] B. V. Lotsch, M. Döblinger, J. Sehnert, L. Seyfarth, J. Senker, O. Oeckler, W. Schnick, *Chem. Eur. J.* **2007**, *13*, 4969.
- [21] K. Schwinghammer, B. Tuffy, M.B. Mesch, E. Wirnhier, C. Martineau, F. Taulelle, W. Schnick, J. Senker, B.V. Lotsch, *Angew. Chem.* **2013**, *125*, 2495.  
*Angew. Chem. Int. Ed.* **2013**, *52*, 2435.
- [22] A. T. Balaban, C. C. Rentia, E. Ciupitu, *Rev. Roum. Chim.* **1968**, *13*, 231.
- [23] M. Döblinger, B. V. Lotsch, J. Wack, J. Thun, J. Senker, W. Schnick, *Chem. Commun.* **2009**, 1541.

## 7. Appendix

### 7.1. Supporting Information

#### 7.1.1. Formation of Melamium Adducts by Pyrolysis of Melamine/ $\text{NH}_4\text{Cl}$ Mixtures

##### Section 2.

**Table 1.** Bond lengths of  $[\text{C}_6\text{N}_{11}\text{H}_{10}]\text{Cl} \cdot 0.5 \text{NH}_4\text{Cl}$  (1) in Å.

N12	H21	0.79(2)
N12	H23	0.82(2)
N12	H22	0.82(2)
N12	H24	0.81(2)
N10	C5	1.321(2)
N10	H4	0.92(3)
N10	H5	0.83(4)
N9	C4	1.328(2)
N9	H6	0.88(3)
N9	H7	0.83(4)
N5	C2	1.314(2)
N5	C6	1.367(2)
N7	C5	1.326(2)
N7	C6	1.350(2)
N1	C2	1.360(2)
N1	C1	1.386(2)
N1	H1	0.90(3)
N6	C4	1.340(2)
N6	C3	1.346(2)
N8	C3	1.331(2)
N8	H9	0.82(4)
N8	H8	0.85(4)
N11	C6	1.315(2)
N11	H3	0.85(3)
N11	H2	0.91(3)
N4	C2	1.353(2)
N4	C5	1.367(2)
N4	H10	0.87(3)
N2	C1	1.331(2)
N2	C3	1.349(2)
N3	C1	1.328(2)
N3	C4	1.363(2)

**Table 2.** Angles in  $[\text{C}_6\text{N}_{11}\text{H}_{10}]\text{Cl} \cdot 0.5 \text{NH}_4\text{Cl}$  (**1**) in  $^\circ$ .

H21	N12	H23	111(3)	C2	N4	C5	118.79(16)
H21	N12	H22	110(3)	C2	N4	H10	120.9(18)
H23	N12	H22	107(3)	C5	N4	H10	119.2(19)
H21	N12	H24	112(3)	C1	N2	C3	113.91(14)
H23	N12	H24	108(2)	N10	C5	N7	121.25(17)
H22	N12	H24	108(3)	N10	C5	N4	117.65(17)
C5	N10	H4	121.8(18)	N7	C5	N4	121.09(15)
C5	N10	H5	122(2)	N11	C6	N7	118.23(17)
H4	N10	H5	116(3)	N11	C6	N5	115.83(15)
C4	N9	H6	120(2)	N7	C6	N5	125.94(16)
C4	N9	H7	117(2)	C1	N3	C4	113.66(15)
H6	N9	H7	123(3)	N3	C1	N2	127.56(17)
C2	N5	C6	114.51(15)	N3	C1	N1	119.00(15)
C5	N7	C6	115.89(15)	N2	C1	N1	113.44(15)
C2	N1	C1	128.08(15)	N8	C3	N6	117.61(16)
C2	N1	H1	113.3(18)	N8	C3	N2	117.57(15)
C1	N1	H1	118.4(18)	N6	C3	N2	124.82(16)
C4	N6	C3	115.41(16)	N5	C2	N4	123.08(16)
C3	N8	H9	125(2)	N5	C2	N1	117.81(15)
C3	N8	H8	122(2)	N4	C2	N1	119.10(16)
H9	N8	H8	112(3)	N9	C4	N6	118.76(17)
C6	N11	H3	124(2)	N9	C4	N3	116.62(16)
C6	N11	H2	119(2)	N6	C4	N3	124.62(15)
H3	N11	H2	116(3)				

**Section 3. Melamium adducts by pyrolysis of thiourea****Table 3.** Bond lengths of  $[\text{C}_6\text{N}_{11}\text{H}_{10}]\text{SCN} \cdot 2 \text{C}_3\text{N}_3(\text{NH}_2)_3$  (**2**) in Å.

N12	H21	0.79(2)
N12	H23	0.82(2)
N12	H22	0.82(2)
N12	H24	0.81(2)
N10	C5	1.321(2)
N10	H4	0.92(3)
N10	H5	0.83(4)
N9	C4	1.328(2)
N9	H6	0.88(3)
N9	H7	0.83(4)
N5	C2	1.314(2)
N5	C6	1.367(2)
N7	C5	1.326(2)
N7	C6	1.350(2)
N1	C2	1.360(2)
N1	C1	1.386(2)
N1	H1	0.90(3)
N6	C4	1.340(2)
N6	C3	1.346(2)
N8	C3	1.331(2)
N8	H9	0.82(4)
N8	H8	0.85(4)
N11	C6	1.315(2)
N11	H3	0.85(3)
N11	H2	0.91(3)
N4	C2	1.353(2)
N4	C5	1.367(2)
N4	H10	0.87(3)
N2	C1	1.331(2)
N2	C3	1.349(2)
N3	C1	1.328(2)
N3	C4	1.363(2)

**Table 4.** Angles in  $[\text{C}_6\text{N}_{11}\text{H}_{10}]\text{SCN} \cdot 2 \text{C}_3\text{N}_3(\text{NH}_2)_3$  (**2**) in °.

N4	C1	N2	118.0(2)	N21	C21	N29	118.6(2)
N4	C1	N3	117.0(2)	N21	C21	N23	124.89(19)
N2	C1	N3	125.00(19)	N29	C21	N23	116.5(2)
N5	C2	N1	118.0(2)	N28	C22	N22	118.6(2)
N5	C2	N2	116.3(2)	N28	C22	N21	116.8(2)
N1	C2	N2	125.7(2)	N22	C22	N21	124.57(19)
N6	C3	N3	118.2(2)	N22	C23	N23	126.3(2)
N6	C3	N1	116.7(2)	N22	C23	N24	115.31(18)
N3	C3	N1	125.1(2)	N23	C23	N24	118.36(19)
C2	N1	C3	114.68(18)	N26	C24	N25	123.3(2)
C2	N2	C1	114.57(19)	N26	C24	N24	119.16(18)
C3	N3	C1	114.94(18)	N25	C24	N24	117.58(19)
C1	N4	H4A	116.0(19)	N211	C25	N27	120.7(2)
C1	N4	H4B	113.3(16)	N211	C25	N25	118.4(2)
H4A	N4	H4B	129(3)	N27	C25	N25	120.92(19)
C2	N5	H5A	118.3(19)	N210	C26	N27	116.77(19)
C2	N5	H5B	122.2(16)	N210	C26	N26	117.48(19)
H5A	N5	H5B	120(3)	N27	C26	N26	125.74(19)
C3	N6	H6A	115.8(18)	C21	N21	C22	115.30(18)
C3	N6	H6B	121.8(17)	C23	N22	C22	114.41(18)
H6A	N6	H6B	122(3)	C23	N23	C21	114.49(18)
N14	C11	N11	117.6(2)	C24	N24	C23	127.35(19)
N14	C11	N13	116.6(2)	C24	N24	H24	114.3(16)
N11	C11	N13	125.7(2)	C23	N24	H24	118.0(16)
N15	C12	N11	117.2(2)	C24	N25	C25	119.24(19)
N15	C12	N12	117.6(2)	C24	N25	H25	116.4(15)
N11	C12	N12	125.1(2)	C25	N25	H25	124.3(15)
N13	C13	N12	126.7(2)	C24	N26	C26	114.54(18)
N13	C13	N16	117.6(2)	C25	N27	C26	116.19(18)
N12	C13	N16	115.7(2)	C22	N28	H28A	116.2(18)
C12	N11	C11	114.94(18)	C22	N28	H28B	121.4(15)
C13	N12	C12	114.03(18)	H28A	N28	H28B	122(2)
C13	N13	C11	113.44(19)	C21	N29	H29A	114.2(16)
C11	N14	H14A	119.0(17)	C21	N29	H29B	121.1(18)
C11	N14	H14B	122.3(15)	H29A	N29	H29B	124(2)
H14A	N14	H14B	119(2)	C26	N210	H21C	117.3(16)
C12	N15	H15A	116.7(16)	C26	N210	H21D	116.0(15)
C12	N15	H15B	117.4(18)	H21C	N210	H21D	126(2)
H15A	N15	H15B	126(29)	C25	N211	H21A	118.1(15)
C13	N16	H16A	113.4(18)	C25	N211	H21B	115.7(18)
C13	N16	H16B	112.5(17)	H21A	N211	H21B	126(2)
H16A	N16	H16B	119(3)	N31	C31	S1	178.3

**Table 5.** Bond lengths of  $[\text{C}_3\text{N}_6\text{H}_7]\text{SCN} \cdot 2 \text{C}_3\text{N}_3(\text{NH}_2)_3$  (**3**) in Å.

N9-C6	1.345(3)
N9-C5	1.345(3)
C6-N7	1.335(3)
C6-N10	1.340(3)
N8-C5	1.341(3)
N8-C4	1.342(3)
N7-C4	1.348(3)
C5-N12	1.334(3)
N10-H8	0.87(4)
N10-H7	0.87(3)
N12-H12	0.89(4)
N12-H11	0.87(4)
N11-C4	1.340(3)
N11-H9	0.88(4)
N11-H10	0.80(4)
N14-C7	1.318(4)
N14-C8	1.353(3)
N13-C7	1.356(4)
N13-C9	1.371(3)
N13-H19	0.89(4)
N15-C9	1.324(4)
N15-C8	1.351(3)
N17-C7	1.326(4)
N17-H15	0.95(5)
N17-H16	0.96(5)
N16-C9	1.312(4)
N16-H14	0.86(4)
N16-H13	0.90(4)

N18-C8	1.315(4)
N18-H18	0.75(4)
N18-H17	0.83(4)
N2-C2	1.340(3)
N2-C1	1.340(3)
N3-C3	1.344(3)
N3-C2	1.348(3)
N1-C3	1.338(3)
N1-C1	1.350(3)
C2-N6	1.327(4)
N6-H6	0.80(4)
N6-H5	0.79(4)
C1-N5	1.329(3)
N5-H3	0.86(3)
N5-H4	0.97(5)
N4-C3	1.349(3)
N4-H1	0.83(3)
N4-H2	0.80(4)
S1-C10	1.620(4)
N19-C10	1.153(5)

---

**Table 6.** Angles in  $[\text{C}_3\text{N}_6\text{H}_7]\text{SCN} \cdot 2 \text{C}_3\text{N}_3(\text{NH}_2)_3$  (**3**) in °.

---

C6-N9-C5	114.5(2)
N7-C6-N10	117.7(2)
N7-C6-N9	125.7(2)
N10-C6-N9	116.6(2)
C5-N8-C4	114.7(2)
C6-N7-C4	114.5(2)
N12-C5-N8	116.6(2)
N12-C5-N9	118.0(2)
N8-C5-N9	125.3(2)
C6-N10-H8	116(2)
C6-N10-H7	119(2)
H8-N10-H7	123(3)
C5-N12-H12	118(2)
C5-N12-H11	117(2)
H12-N12-H11	126(3)
C4-N11-H9	114(2)
C4-N11-H10	115(3)
H9-N11-H10	124(3)
N11-C4-N8	118.0(2)
N11-C4-N7	116.7(2)
N8-C4-N7	125.3(2)
C7-N14-C8	115.8(2)
C7-N13-C9	119.1(2)
C7-N13-H19	118(2)
C9-N13-H19	123(2)
C9-N15-C8	116.7(2)
C7-N17-H15	125(3)
C7-N17-H16	121(3)
H15-N17-H16	114(4)
C9-N16-H14	122(3)
C9-N16-H13	122(2)
H14-N16-H13	115(3)
C8-N18-H18	117(3)

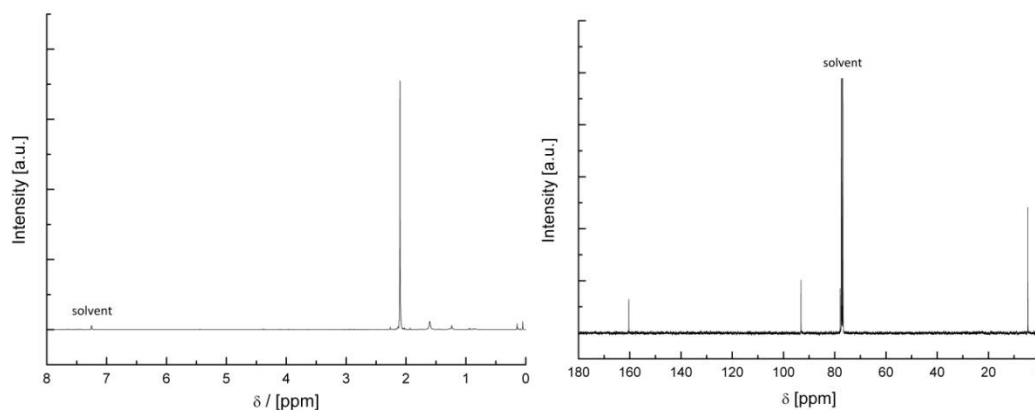
C8-N18-H17	124(3)
H18-N18-H17	118(4)
N14-C7-N17	120.9(3)
N14-C7-N13	122.3(2)
N17-C7-N13	116.8(3)
N18-C8-N15	118.3(3)
N18-C8-N14	116.4(2)
N15-C8-N14	125.3(2)
N16-C9-N15	120.5(3)
N16-C9-N13	118.7(3)
N15-C9-N13	120.8(2)
C2-N2-C1	114.9(2)
C3-N3-C2	114.4(2)
C3-N1-C1	114.0(2)
N6-C2-N2	117.4(2)
N6-C2-N3	117.4(2)
N2-C2-N3	125.1(2)
C2-N6-H6	118(3)
C2-N6-H5	115(3)
H6-N6-H5	127(4)
N5-C1-N2	118.1(2)
N5-C1-N1	116.4(2)
N2-C1-N1	125.5(2)
C1-N5-H3	116(2)
C1-N5-H4	117(3)
H3-N5-H4	127(3)
C3-N4-H1	114(2)
C3-N4-H2	112(2)
H1-N4-H2	131(3)
N1-C3-N3	126.0(2)
N1-C3-N4	117.7(2)
N3-C3-N4	116.3(2)
N19-C10-S1	179.0(4)

---

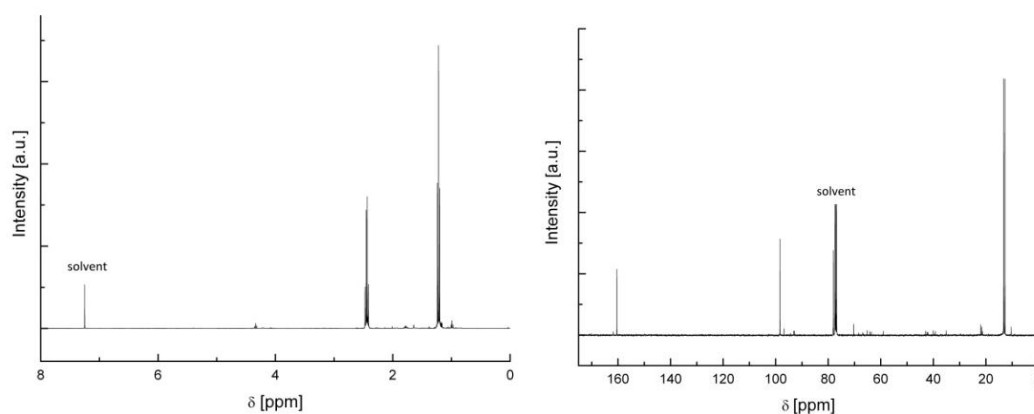
## 7.1.2. Synthesis of Novel Triazine-based Materials by Functionalization with Alkynes

### Section 2.

NMR investigations on tris(1-propynyl)-1,3,5-triazine (**1**) and tris(1-butynyl)-1,3,5-triazine (**2**)



**S 1.**  $^1\text{H}$  (left) and  $^{13}\text{C}$  (right) spectra of  $\text{C}_3\text{N}_3(\text{C}_3\text{H}_3)_3$  (**1**).

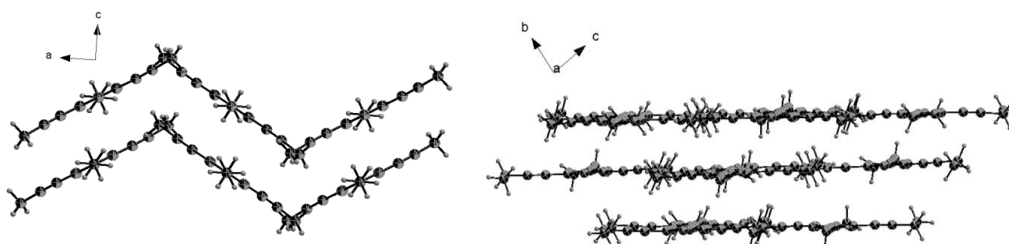


**S 2.**  $^1\text{H}$  (left) and  $^{13}\text{C}$  (right) spectra of  $\text{C}_3\text{N}_3(\text{C}_4\text{H}_5)_3$  (**2**).

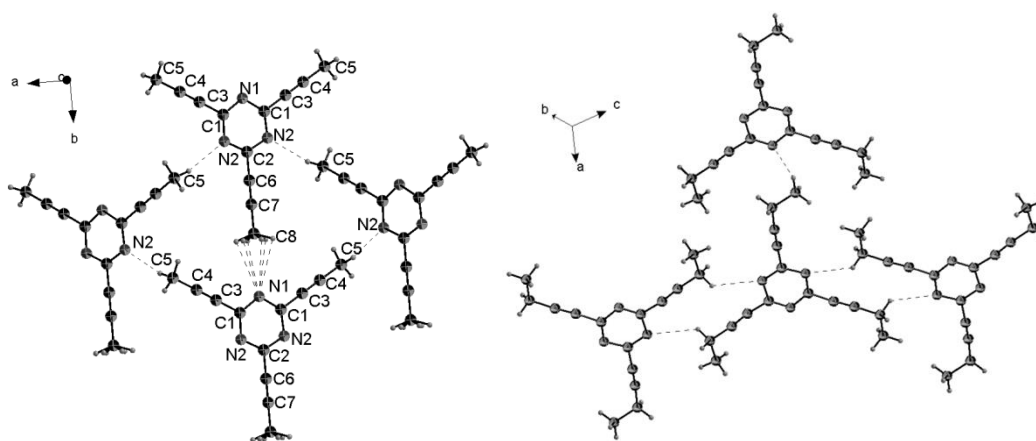
$^{13}\text{C}$ - and  $^1\text{H}$ -NMR investigations of  $\text{C}_3\text{N}_3(\text{C}_3\text{H}_3)_3$  (**1**) and  $\text{C}_3\text{N}_3(\text{C}_4\text{H}_5)_3$  (**2**) are well in line with the expectations for both compounds. The  $^1\text{H}$  spectrum of (**1**) (see Figure S 1) shows one singlet signal at  $\delta = 2.1$  ppm for the  $\text{CH}_3$ -group. Two peaks are found for (**2**) (see Figure S 2). One triplet signal at  $\delta = 1.2$  ppm corresponds to  $\text{CH}_3$ -groups of the butyn-1-yle fragment. The signal for the  $\text{CH}_2$ -groups could be observed at  $\delta = 2.4$  ppm. The  $^{13}\text{C}$  NMR spectra of (**1**) (see Figure S 1) and (**2**) (see Figure S 2)

show three signals, respectively. For (1) the peak at  $\delta = 3$  ppm corresponds to the  $\text{CH}_3$ -group. The signals for the alkyne group and the triazine core could be found at  $\delta = 93$  ppm and  $\delta = 160$  ppm. Peaks for  $\text{CH}_2$ - and  $\text{CH}_3$ -groups of (2) could be found at  $\delta = 11$  ppm. The signal at  $\delta = 98$  ppm corresponds to the atoms of the alkyne groups. The signal at 160 ppm is assigned to the triazine carbon.

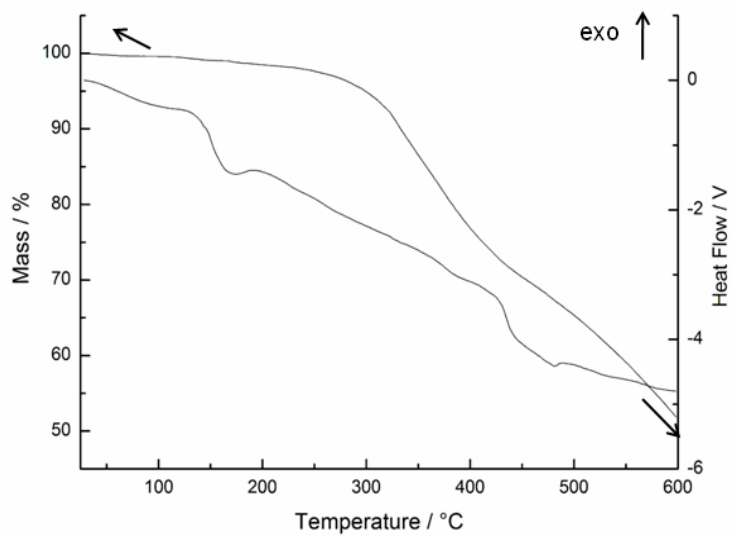
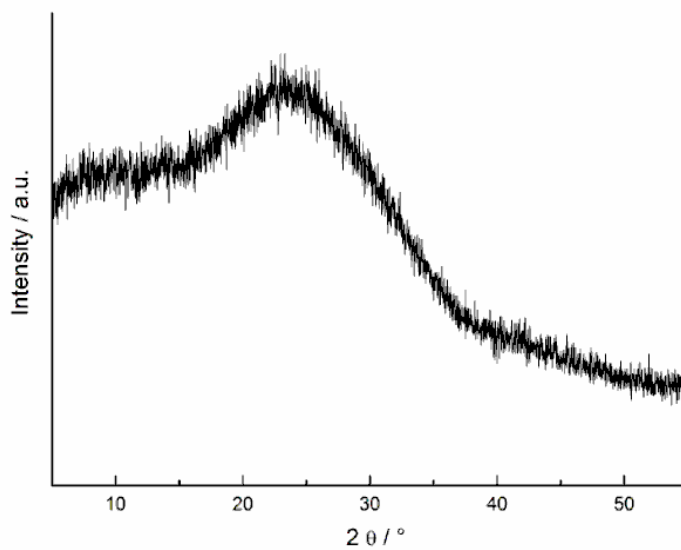
### Structural features of (1) and (2)

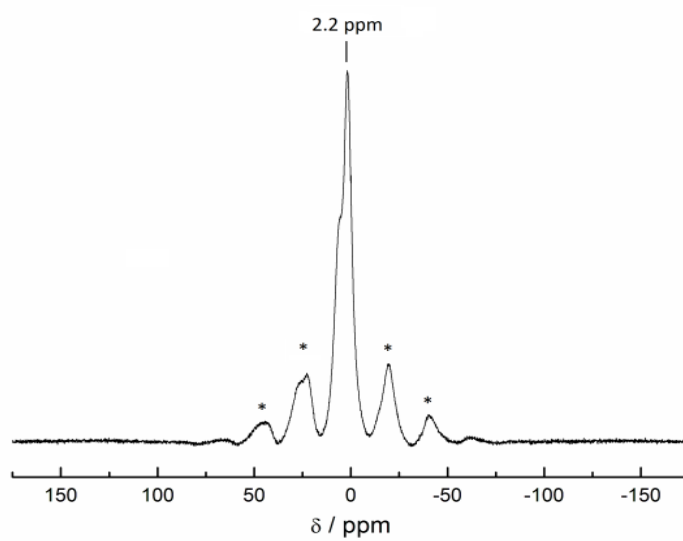


**S 3.** Zig-zag strands of  $\text{C}_3\text{N}_3(\text{C}_3\text{H}_3)_3$  (1), view along the  $b$  axis and the layer arrangement of  $\text{C}_3\text{N}_3(\text{C}_4\text{H}_5)_3$  (2) along  $a$ .

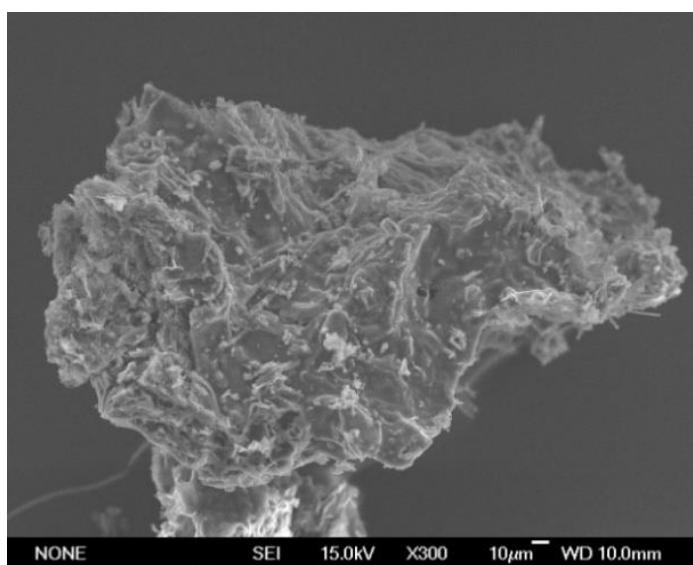


**S 4.** Hydrogen bonding motifs of  $\text{C}_3\text{N}_3(\text{C}_3\text{H}_3)_3$  (1) and  $\text{C}_3\text{N}_3(\text{C}_4\text{H}_5)_3$  (2).

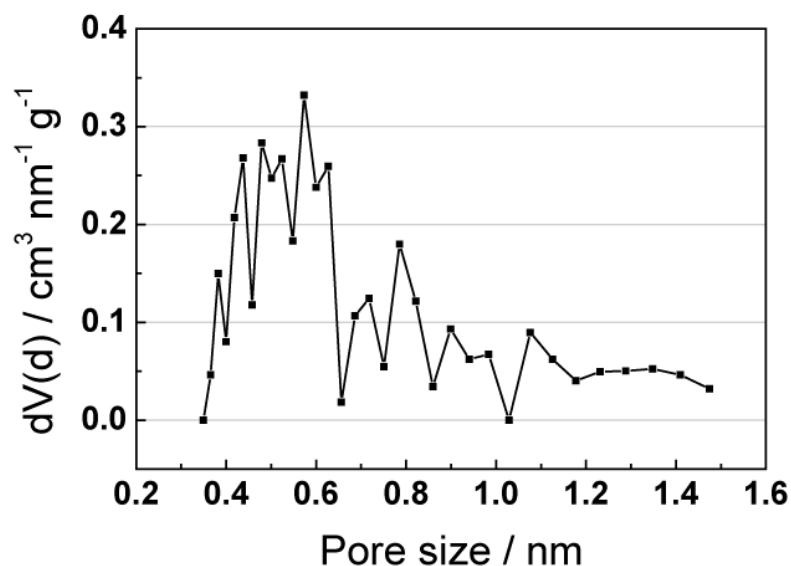
**Thermal measurements of (2)****S 5.** DTA and TG curves of  $C_3N_3(C_4H_5)_3$  (2).**Investigations of the polymerization product (poly-TPT)****S 6.** Powder diffraction measurement of poly-TPT.



S 7.  $^1\text{H}$  MAS solid-state NMR spectrum for the polymerization product. Rotational sidebands are labeled with \*.



S 8. SEM image of poly-TPT.

**CO<sub>2</sub> physisorption measurements of poly-TPT**

S 9. Pore size distribution derived from a Monte-Carlo fit of the CO<sub>2</sub> isotherm at 273 K.

**Section 4. Experimental Part**

**Structure determination:** Single-crystal XRD data of (1) and (2) were recorded on a Bruker Venture D8 diffractometer using Mo-K $\alpha$  radiation ( $\lambda = 71.073$  pm). The frames were integrated with Bruker SAINT software package using a narrow-frame algorithm. All data were corrected for absorption effects using the multi-scan method (SADABS). The crystal structures were solved and refined by direct methods using SHELXS-97. Crystallographic data are summarized in Tables 1 and 2. Molecular graphics were designed with diamond version 3.2i. CCDC 997458 (1) and CCDC 997459 (2) contain the supplementary crystallographic data for this manuscript. These data can be obtained from The Cambridge Crystallographic Data Centre via [www.ccdc.cam.ac.uk/data\\_request/cif](http://www.ccdc.cam.ac.uk/data_request/cif).

**FTIR spectra:** Fourier-transformed infra-red spectra were recorded on a Spectrum BX II FTIR spectrometer (Perkin Elmer) in reflection geometry. The spectrometer is equipped with a DuraSampler diamond ATR (attenuated total reflectance) unit. All spectra were corrected for ATR specific effects, and a baseline correction was applied.

**Thermoanalytical measurements:** DTA-TG measurements were performed with a Setaram Thermoanalyzer TG-DTA92. The measurements were conducted in a helium inert atmosphere employing alumina crucibles. The sample was heated from room temperature to 600 °C with a rate of 5 °C min<sup>-1</sup>.

**Mass spectrometry:** Mass spectrometric data were obtained with a JEOL MStation JMS 700 spectrometer (HRMS; ESI<sup>+</sup>, DEI).

**Elemental analyses:** Elemental analyses for C, N and H were recorded with the elemental analyzer systems Vario Micro and Vario El (Elementar Analysensysteme GmbH).

**NMR spectroscopy:** Liquid <sup>1</sup>H and <sup>13</sup>C-NMR data were recorded using different NMR spectrometers (Jeol Eclipse 270 and Jeol Eclipse 400). The spectra were measured in CDCl<sub>3</sub>. The chemical shifts  $\delta$  are quoted in units of ppm to the relative external standard TMS, Me<sub>4</sub>Si.

CP-MAS solid-state NMR spectra were recorded on a DSX 500 Advance Bruker FT-NMR spectrometer with an external magnetic field of 11.4 T. All spectra were recorded with 4.0 mm ZrO<sub>2</sub> rotors. Rotation frequencies were 10 kHz for all measurements.

For the <sup>13</sup>C MAS cross polarization {1H} solid-state NMR spectrum the recycle delay is 1 s and the contact time 5000  $\mu$ s.

**Powder diffractometry:** X-ray diffraction patterns were recorded on a Stoe STADI P diffractometer. Measurements were conducted using monochromatic Cu-K $\alpha$ 1 radiation at room temperature.

**Electron microscopy:** Electron microscopy was conducted on a JEOL JSM 6500 F scanning electron microscope (SEM) equipped with a field emission gun with a maximum acceleration voltage of 30 kV. The sample was prepared on adhesive conductive carbon pads and it was sputtered with a conductive carbon film. The chemical composition was determined by EDX spectroscopy on Oxford Instruments, model 7418.

**Sorption:** Carbon dioxide adsorption/desorption isotherms were run at 273 K with an Autosorb-iQ surface analyzer (Quantachrome Instruments, USA). Samples were outgassed in vacuum ( $10^{-7}$  mbar) at 150 °C for 12 h to remove all guests. Pore-size distributions were determined using the calculation model for CO<sub>2</sub> at 273 K on carbon (Monte-Carlo model) of the ASiQwin software (v3.01) from Quantachrome.

## 7.2. CCDC Numbers

Corresponding crystallographic data were deposited with the Cambridge Crystallographic Data Centre (CCDC, [http://www.ccdc.cam.ac.uk/data\\_request/cif](http://www.ccdc.cam.ac.uk/data_request/cif); 12 Union Road, Cambridge CB2 1EZ, UK (Fax: +44-1223-336-033; or E-Mail: [deposit@ccdc.cam.ac.uk](mailto:deposit@ccdc.cam.ac.uk)) and are available on quoting the respective CCDC depository numbers.

$C_6N_{11}H_{10}Cl \cdot 0.5 NH_4Cl$	CCDC 821352
$C_6N_{11}H_{10}SCN \cdot 2 C_3N_3(NH_2)_3$	CCDC 8221353
$HC_3N_3(NH_2)_3SCN \cdot 2 C_3N_3(NH_2)_3$	CCDC 821354
$C_{12}N_{14}O_{14}Sr$	CCDC 929678
$C_9H_{15}N_{13}O_7Sr$	CCDC 929677
$C_{12}H_9N_3$	CCDC 997458
$C_{15}H_{15}N_3$	CCDC 997459

### 7.3. List of Publications

#### Formation of Melamium Adducts by Pyrolysis of Thiourea or Melamine/ $\text{NH}_4\text{Cl}$

##### Mixtures

N. E. Braml, A. Sattler and W. Schnick

*Chem. Eur. J.* **2012**, *18*, 1811.

In this contribution, writing the main part of the manuscript and screening of literature were done by Nicole Braml and Dr. Andreas Sattler. Syntheses were carried out by Nicole Braml. Structure determinations and image preparation based on single-crystal data were done by Dr. Andreas Sattler and Nicole Braml. Interpretation of NMR data were carried out by Nicole Braml. This publication presents an essential completion of Dr. Andreas Sattlers and Dr. Barbara Jürgens previous works to this topic (B. Jürgens, Doctoral thesis, University of Munich 2007; A. Sattler, Doctoral thesis, University of Munich, 2010). Supervision of the research project was carried out by Wolfgang Schnick.

#### New Heptazine Based Materials with a Divalent Cation – $\text{Sr}[\text{HC}_6\text{N}_7\text{O}_3] \cdot 4 \text{H}_2\text{O}$ and $\text{Sr}[\text{HC}_6\text{N}_7(\text{NCN})_3] \cdot 7 \text{H}_2\text{O}$

N. E. Braml and W. Schnick

*Z. Anorg. Allg. Chem.* **2013**, *639*, 275.

In this part, writing the the manuscript and screening of literature were done by Nicole Braml. Structure determination based on single-crystal and powder XRD data and Rietveld refinement, image preparation and interpretation of FTIR- and DTA/TG–data were performed by Nicole Braml. Supervision of this research project was carried out by Prof. Wolfgang Schnick.

### **Synthesis of Novel Triazine-based Materials by Functionalization with Alkynes**

Nicole E. Braml, Linus Stegbauer, Bettina V. Lotsch and Wolfgang Schnick  
*Chem. Eur. J.* **2015**, *21*, 7866.

In this contribution, writing the main part of the manuscript, screening of literature, image preparation and structure determination based on single-crystal data were carried out by Nicole Braml. Sample syntheses were done by Nicole Braml and synthesis optimization was performed by Linus Stegbauer and Nicole Braml. Interpretation of NMR, powder XRD, FTIR- and DTA/TG-data were done by Nicole Braml and Linus Stegbauer. Sorption measurements and interpretation were done by Linus Stegbauer. Supervision of this research project was carried out by Prof. Wolfgang Schnick and Prof. Bettina Lotsch.

### **Polymerisation of Tris(1-proynyl)-1,3,5-triazine by Alkyne-metathesis**

To be published

For this part screening of literature and image preparation were done by Nicole Braml. Syntheseses of catalysts was carried out by Sebastian Zech and Sebastian Schaubach (Max-Planck-Institut für Kohleforschung Mülheim a. d. Ruhr). Metathesis reactions were done by Linus Stegbauer, Nicole Braml and Sebastian Schaubach at Max-Planck-Institut für Kohleforschung (Mülheim a. d. Ruhr). IR-spectroscopy and mass spectrometry date were interpreted by Nicole Braml, Linus Stegbauer and Sebastian Schaubach. Supervision of this research project was carried out by Prof. Wolfgang Schnick and Prof. Bettina Lotsch.

### **Investigations into the Polymerization Process of Carbon Nitrides**

To be published

Within this article, screening of literature were done by Nicole Braml. Sample syntheses and synthesis optimization were done by Annabelle Blum and Nicole Braml. Supervision of the research project was carried out by Wolfgang Schnick.

***Contributions to Conferences***

**Funktionalisierte Triazine als Bausteine für C/N-Netzwerke (oral presentation)**

Obergurgl-Seminar on Solid State Chemistry 2014, Obergurgl, Austria

N. E. Braml and W. Schnick

**Funktionalisierte Triazine als Bausteine für C/N-Netzwerke (oral presentation)**

Hirschegg-Seminar on Solid State Chemistry 2014, Hirschegg, Austria

N. E. Braml and W. Schnick

## 7.4. List of Abbreviations

2D / 3D	two-dimensional / three-dimensional
Å	Ångström
a.u.	arbitrary units
calcd.	calculated
CCDC	Crystallographic Data Centre
CN	carbon nitride
CP	cross polarization
CSD	Cambridge Structural Database
DTA	differential thermal analysis
EA	elemental analysis
e.g.	<i>exempli gratia</i> , for example
et al.	<i>et alii</i> , and others
FT	Fourier transformation
g-C <sub>3</sub> N <sub>4</sub>	graphitic C <sub>3</sub> N <sub>4</sub>
GOF / GooF	goodness of fit
h	hour
ICP-AES	inductively coupled plasma – atomic emission spectroscopy
IPDS	imaging plate diffraction system
IR	infrared
M	molar
MAS	magic angle spinning
NMR	nuclear magnetic resonance
no.	number
poly-TPT	poly-tris(1-propynyl)-1,3,5-triazine
PTI/LiCl	poly(triazine imide) with LiCl intercalation
TG	thermogravimetry
XRD	X-ray diffraction
Z	formula units per unit cell